Multislice CT of the symptomatic carotid artery

Annet Waaijer

ISBN: 9039343055

Cover: Photograph by Ellen van der Spek & Gabe Sonke, Namibië, Windhoek.
The Banded-legged Golden Orb-web Spider (Nephilia senegalensis)
Lay-out: Roy Sanders
Printed by: Gildeprint drukkerijen BV, Enschede, The Netherlands

Multislice CT of the symptomatic carotid artery

Multislice CT van de symptomatische arteria carotis

(met een samenvatting in het Nederlands)

Proefschrift

ter verkrijging van de graad van doctor aan de Universiteit Utrecht op gezag van de rector magnificus prof. dr. W.H. Gispen, ingevolge het besluit van het college voor promoties in het openbaar te verdedigen op donderdag 26 oktober 2006 des middags te 2.30 uur

door Annet Waaijer

geboren op 11-7-1976 te De Bilt, Nederland

Promotor: Prof. dr. M. Prokop

Co-promotor: Dr. M.S. van Leeuwen

Department of Radiology
University Medical Centre Utrecht
The Netherlands

Financial support by the Netherlands Heart Foundation for the publication of this thesis is gratefully acknowledged.
Financial support was also provided by: the Rontgen Stichting Utrecht, Terumo BV, Guerbet BV, Schering BV, Cordis, Johnson & Johnson Company and Philips Medical Systems.

Aan mijn vader

Contents

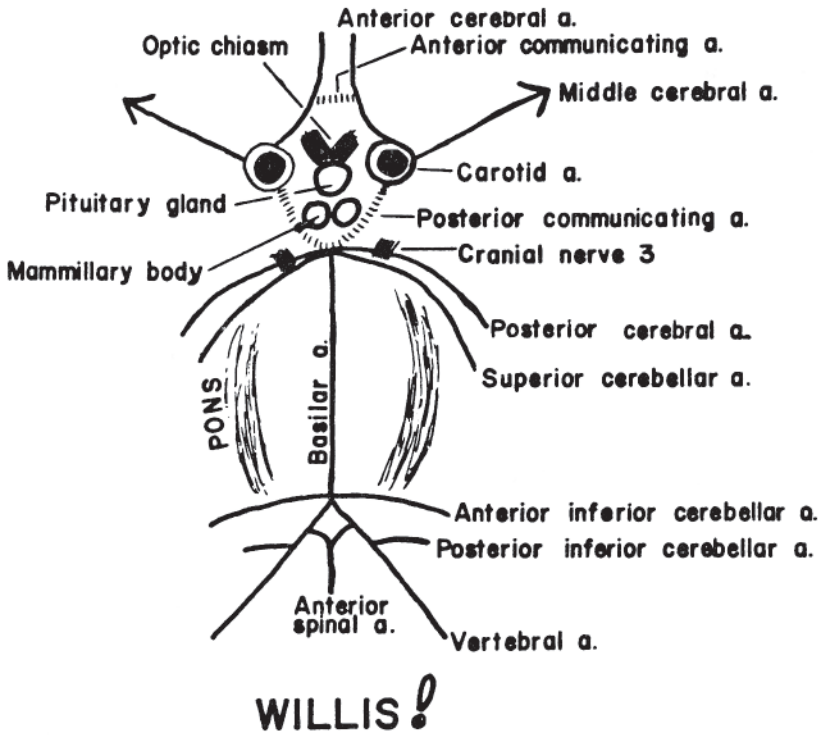

A ferocious spider lives in the brain. His name is Willis! Note (Fig) that he has a nose, angry eyebrows, two suckers, eyes that look outward, a crew cut, antennae, a fuzzy beard, 8 legs, a belly that according to your point of view, is either thin (basilar artery) or fat (the pons, which lies from one end of the basilar artery to the other), two feelers on his rear legs, and male genitalia.

(uit: Clinical Neuroanatomy Made Ridiculously Simple, by Stephen Goldberg, 3rd edition March 2005, MedMaster Inc.)

List of Abbreviations

ACA = Anterior Cerebral Artery
AcomA = Anterior Communicating Artery
AIF = Arterial Input Function
BG = Basal Ganglia
CAS = Carotid Artery Stenosis
CBF = Cerebral Blood Flow
CBV = Cerebral Blood Volume
CEA = Carotid Endarterectomy
CoW = Circle of Willis
CPR = Curved Planar Reformation
CT = Computed Tomography
CTA = Computed Tomograhic Angiography
CTV = Computed Tomograhic Venography
CTDI = CT Dose Index
DSA = Digital Subtraction Angiography
DUS = Duplex Ultrasound
ECA = External Carotid Artery
ECST = European Carotid Surgery Trial
HU = Hounsfield Unit
ICA = Internal Carotid Artery
ICSS = International Carotid Stenting Study
kVp = peak kilo Voltage (tube voltage)
mAs = milliAmperage – second (tube current)
MCA = Middle Cerebral Artery
MIP = Maximum Intensity Projection
MPR = Multi Planar Reformation
MRA = Magnetic Resonance Angiography
MRI = Magnetic Resonance Imaging
MTT = Mean Transit Time
NASCET = North American Symptomatic Carotid Endarterectomy Trial
NCCT = Non-Contrast enhanced CT
NNT = Number Needed to Treat
PCA = Posterior Cerebral Artery
PET = Positron Emission Tomography

PcomA = Posterior Communicating Artery
ROI = Region Of Interest
SAH = SubArachnoid Hemorrhage
SDD = Standard Deviation of Differences
SNR = Signal-tot-Noise Ratio
SPECT = Single Photon Emission Computed Tomography
TCD = Trans Cranial Doppler
TIA = Transient Ischemic Attack
UMCU = University Medical Centre Utrecht
VOF = Venous Output Function

General introduction

Chapter One

A Waaijer, TH Lo, LJ Kappelle, FL Moll, WPThM Mali. Nieuwe inzichten in behandelmogelijkheden voor patiënten met een symptomatische carotis stenose. Ned Tijdschr Geneeskd. 2005; 149:1261-6

Introduction

In the Netherlands the incidence of stroke and transient ischemic attack (TIA) is 180/100.000 persons/year. Treatment in patients with non-disabling stroke focuses mainly on secondary, preventive measurements which largely consists of medical therapy[1]. In 20-30% of these patients a substantial stenosis of the internal carotid artery (ICA) is found. This stenosis is caused by atherosclerotic plaque formation. Symptoms are thought to be the result of cerebral embolism by formation of thrombi at the plaque, and by the luminal obstruction which causes reduced blood flow to the brain. These patients are therefore called "patients with a symptomatic carotid artery stenosis".

Indications for treatment

Two large trials (NASCET (North American Symptomatic Carotid Endarterectomy Trial) and ECST (European Carotid Surgery Trial)) have shown that surgical intervention by means of carotid endarterectomy (CEA) is effective in the reduction of recurrent symptoms in patients with symptomatic carotid artery stenosis[2,3]. Surgery removes the atherosclerotic plaque and re-establishes the lumen. Recently data from both studies were combined and this analysis showed an absolute risk reduction after surgery of 16% if the degree of stenosis was 70-99% and of 4.6% if the degree of stenosis was 50-69%. In case of a lesser degree of stenosis no benefit was shown[4].

New treatment options

In the nineties a new way of treatment for carotid stenosis was introduced: endovascular treatment. In the beginning this consisted of balloon angioplasty only, while later this was replaced by primary stenting, so-called carotid artery stenting. Therefore, a balloon is inflated at the site of the stenosis where it stretches the vessel wall. After that, a stent is left within the vessel at the site of the previous stenosis to keep the lumen open (*Figure1a-b*). Local anaesthesia only is required at the site of the injection and most patients can leave the hospital after one day. Although this endovascular treatment is increasingly being used, there are no large randomised controlled trials that have shown equal effect of stenting compared to CEA and data of long-term results are lacking.

The ICSS

The effectiveness of carotid stenting is thus not yet clear. Therefore, the International Carotid Stenting Study (ICSS) has been designed, in which the UMCU participates[5]. This study randomizes patients with symptomatic carotid stenosis for either CEA or stenting. Practically, this means that about 70% of the 120 patients that yearly come to the UMCU are suited to participate in the ICSS trial. Randomization follows soon after the first consult to the neurologist, and the patient is followed for 5 years after treatment. The final results are expected to take another 4 years to be completed.

Figure 1

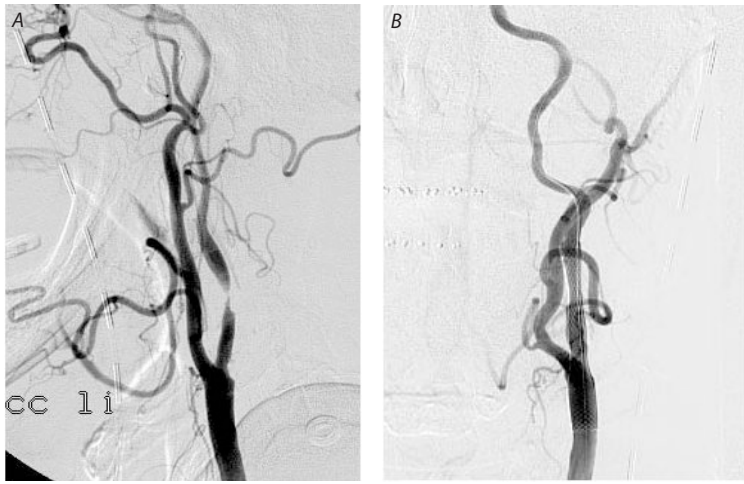

ICA stenosis before stent placement *ICA after stent placement*

Patient selection

As stated above, indication for treatment is based on the degree of stenosis. Measurement of carotid stenosis was primarily based on intra arterial digital subtraction angiography (DSA), but this is an invasive technique and carries a risk of serious complications. Therefore it has gradually been replaced by less invasive techniques like duplex ultrasound (DUS), magnetic resonance angiography (MRA) and computed tomography angiography (CTA). Usually duplex is used for screening and when the degree of stenosis is 50% or more this is an indication for further diagnostics. Large studies have shown that a combination of DUS and MRA results in good accuracy if both tests are in agreement, and DSA is only performed in cases of disagreement[6]. Data on the accuracy of CTA are more sparse and indicate that this technique also has a good accuracy for detection of >70% stenosis, but performs less in case of 50-69% stenosis[7]. However, the introduction of multislice technique has gained renewed interest in the use of CTA because these new scanners have better resolution which make them competitive with MRA.

Risk of complications

Intended to prevent subsequent cerebrovascular events, both surgery and stenting itself carry a risk of stroke or TIA during or shortly after the procedure. Although the efficacy of CEA in patients with symptomatic internal carotid artery stenosis ≥70% is beyond doubt, six patients have to undergo surgery to prevent one stroke. Surgery may also be considered for patients with ≥50% stenosis, but in these patients the number needed to treat to prevent one stroke is more than three times as high[4]. To improve the selection of patients for treatment, better understanding of the risk factors for stroke in these patients is required.

Although it is generally accepted that the majority of TIA's and ischemic strokes result from thrombosis and thrombo-embolism[8], it has been suggested that severe cerebral hemodynamic compromise is also associated with an increased risk of stroke and TIA[9-11]. Two factors have been focus of study to gain more insight in the cerebral hemodynamics in patients with carotid disease and search for a relation with recurrent symptoms.
The first one is the presence of collateral supply. Collateral supply can be provided by the ophthalmic artery, leptomeningeal arteries and by the contralateral carotid or vertebrobasilar system via the arterial circle of Willis. Adequate collateral supply via the circle of Willis is associated with a reduced risk of recurrent stroke[12], smaller infarct size[13], and a reduced occurrence of ischemia during clamping of the carotid artery[14]. However, it is common that one or more of these segments are not present, thereby preventing collateral supply. Assessment of the patency of the circle has mainly been performed with autopsy studies or with imaging techniques like digital subtraction angiography (DSA), duplex ultrasound (DUS) or magnetic resonance angiography (MRA).
The second focus of studies on cerebral hemodynamics is measurement of cerebral perfusion. Patients with symptomatic carotid artery stenosis and ipsilateral reduced cerebral perfusion are at higher risk of disabling stroke than patients with normal cerebral perfusion[9]. Also, impaired cerebral perfusion is associated with watershed infarctions[15] and improvement of cerebral perfusion after carotid revascularization is associated with improvement in cognitive function[16, 17]. Measurement of cerebral perfusion can be performed with single photon emission computed tomography (SPECT), positron emission tomography (PET) or different MRI techniques.
However, both assessment of collateralization and measurement of cerebral perfusion can be also be performed using multislice CT (MSCT). On the contrary to the previous techniques, CT is a widely available technique that allows quick assessment of both the carotid arteries, the intracranial vasculature as well as brain perfusion.

The aim of this thesis was to gain more insight in pathophysiology and treatment effects in patients with symptomatic carotid stenosis. Participation in the ICSS trial offered us the possibility to evaluate the carotid stenosis, collateralization and brain perfusion in patients with symptomatic carotid artery stenosis using multislice CT technique. This thesis describes the findings in the first 100 included patients.

First, in Chapter 2, the technique and possibilities of neurovascular MSCT are outlined. In Chapter 3, potential techniques for optimization and dose reduction for scanning the circle of Willis are discussed. The presence of collateral supply by the circle of Willis is described in Chapter 4 and compared to patients without cerebrovascular disease. In Chapter 5, different methods to assess the severity of stenosis using CTA are evaluated and compared to DSA. In Chapter 6 the reproducibility of brain perfusion measurements is studied.
In Chapter 7, we describe the use of CT perfusion to see whether we could reveal differences in treatment response in terms of cerebral perfusion based on the pre-treatment perfusion data.

Table 1 *Advantages and disadvantages of surgery and stent placement*

CEA	**STENT PLACEMENT**
Advantages	**Advantages**
Long experience	Short stay in hospital
Lasting result: 5-10% re-stenosis, mainly asymptomatic	No general anaesthesia
Brain "protected" against trombo-embolic particles by clamping	No wound in the neck
	Stenosis on most locations accessible
Disadvantages	**Disadvantages**
Risks related to general anaesthesia (i.e. myocardial infarction)	Long-term results not known
Incision in the neck (risk for hematoma and infection)	Re-stenosis up to 14% has been reported, mainly asymptomatic
Risk of cranial nerve damage	Risk of trombo-embolic particles during the procedure

References

1. Kappelle LJ, Frijns CJM Behandeling van patiënten met een TIA of een herseninfarct. Ned Tijdschr Geneeskd. 2002;146:1678-81.
2. NASCET collaborators. Beneficial effect of carotid endarterectomy in symptomatic patients with high grade carotid stenosis. N Engl J Med 1991;325:445-53.
3. ECST collaborators. Randomised trial of endarterectomy for recently symptomatic carotid stenosis: final results of the MRC European Carotid Surgery trial. Lancet 1998;351:1379-87.
4. Rothwell PM, Eliasziw M, Gutnikov SA, Fox AJ, Taylor DW, Mayberg MR et al. Analysis of poooled data from the randomised controlled trials of endarterectomy for symptomatic carotid stenosis. Lancet 2003;361:107-16.
5. CAVATAS investigators. Endovasculair versus surgical treatment in patients with carotid stenosis in the Carotid and Vertebral Transluminal Angioplasty Study (CAVATAS): a randomised trial. Lancet 2001;357:1729-37.
6. Nederkoorn PJ, van der Graaf Y, Hunink MG. Duplex ultrasound and magnetic resonance angiography compared with digital subtraction angiography in carotid artery stenosis: a systematic review. Stroke. 2003;34:1324-3.
7. Wardlaw JM, Chappell FM, Best JJ, Wartolowska K, Berry E; NHS Research and Development Health Technology Assessment Carotid Stenosis Imaging Group. Non-invasive imaging compared with intra-arterial angiography in the diagnosis of symptomatic carotid stenosis: a meta-analysis. Lancet. 2006;367:1503-12.
8. Barnett HJ. Hemodynamic cerebral ischemia. An appeal for systematic data gathering prior to a new EC/IC trial. Stroke 1997;28:1857-60
9. Blaser T, Hofmann K, Buerger T, Effenberger O, Wallesch CW, Goertler M. Risk of stroke, transient ischemic attack, and vessel occlusion before endarterectomy in patients with symptomatic severe carotid stenosis. Stroke 2002;33:1057-62
10. Caplan LR, Hennerici M. Impaired clearance of emboli (washout) is an important link between hypoperfusion, embolism, and ischemic stroke. Arch Neurol 1998;55:1475-82
11. Markus H, Cullinane M. Severely impaired cerebrovascular reactivity predicts stroke and TIA risk in patients with carotid artery stenosis and occlusion. Brain 2001;124:457-467
12. Henderson RD, Eliasziw M, Fox AJ, Rothwell PM, Barnett HJ. Angiographically defined collateral circulation and risk of stroke in patients with severe carotid artery stenosis. North American Symptomatic Carotid Endarterectomy Trial [NASCET] Group. Stroke 2000; 31:128-32.
13. Rodda RA. The arterial patterns associated with internal carotid disease and cerebral infarcts. Stroke. 1986; 17:69-75.
14. Rutgers DR, Blankensteijn JD, van der Grond J. Preoperative MRA flow quantification in CEA patients: flow differences between patients who develop cerebral ischemia and patients who do not develop cerebral ischemia during cross-clamping of the carotid artery. Stroke 2000; 31:3021-8.
15. Ringelstein EB, Weiller C, Weckesser M, Weckesser S. Cerebral vasomotor reactivity is significantly reduced in low-flow as compared to thromboembolic infarctions: the key role of the circle of Willis. J Neurol Sci 1994 ;121:103-9
16. Kishikawa K, Kamouchi M, Okada Y, Inoue T, Ibayashi S, Iida M. Effects of carotid endarterectomy on cerebral blood flow and neuropsychological test performance in patients with high-grade carotid stenosis. J Neurol Sci 2003;213:19-24
17. Moftakhar R, Turk AS, Niemann DB et al. Effects of carotid or vertebrobasilar stent placement on cerebral perfusion and cognition. AJNR 2005;26:1772-8
18. Paciaroni M, Eliasziw M, Kappelle LJ, Finan JW, Barnett HJ. Medical complications associated with carotid endartectomy. North American Symptomatic Carotid Endarterectomy Trial (NASCET). Stroke 1999;30:1759-63.
19. McCrory DC, Goldstein LB, Samsa GP, Oddone EZ, Landsman PB, Moore W et al. Predicting complications of carotid endarterectomy. Stroke 1993;24:1285-91.
20. Rothwell PM, Slattery J, Warlow C. Clinical and angiographic predictors of stroke and death from carotid endarterectomy: systematic review. BMJ 1997;315:1571-7.
21. Barr JD, Connors JJ 3rd, Sacks D, Wojak JC, Becker GJ, Cardella JF et al; American Society of Interventional and Therapeutic Neuroradiology; American Society of Neuroradiology; Society of Interventional Radiology. Quality improvement guidelines for the performance of cervical carotid angioplasty and stent placement. J Vasc Interv Radiol 2003;14:S321-35.

Technique and application of multislice Neurovascular CT

Chapter Two

A Waaijer, IC van der Schaaf, BK Velthuis, M Prokop. 40 slice Neuro-CT Angiography. Diagnostic Imaging Europe, December 2005/ January 2006

Introduction

CT angiography (CTA) is a vascular imaging technique using spiral CT during the passage of a bolus of intravenously administered contrast material. However, for imaging of the carotid arteries it has always played a secondary role. This is because duplex ultrasound (DUS) technique and digital subtraction angiography (DSA) for long time have been the best available methods. Ultrasound was and is the first line method of choice for screening, since it is not dependent on the use of contrast material and does not encompass radiation risk. DSA has the highest resolution but requires intra-arterial injection and therefore carries a certain risk for complications. Several MRA techniques have been proposed and ultimately studies showed that a combination of DUS and MRA can largely replace the use of DSA, the latter being only required in case of discrepancy between noninvasive tests[1].

With the advent of multislice CT, the situation has changed in favor of CTA: spatial resolution along the patient axis (z-axis) is substantially improved and compares favorably with current standard MRA techniques[2-4]. Multislice CTA can cover the whole range from the aortic arch to the intracranial circulation with a high spatial resolution in less than 15 seconds. CTA visualizes the whole vessel wall, is able to display calcium and may also be able to differentiate various plaque types. Further, multislice CT has the possibility of perfusion imaging. Since it is a widely available technique, it is increasingly assuming a role in stroke imaging. The combination of non-contrast enhanced CT (NCCT), CT Perfusion (CTP) and CTA results in a complete work-up in patients with ischemic brain disease[5,6].

Scan Protocol

For most indications scanning consists of a sequence of NCCT, CTP and CTA. NCCT is required to show an intracerebral hemorrhage, extensive infarct, or hemorrhagic transformation of an infarct. If no abnormality is seen on the NCCT, CTP may be able to elucidate early signs of ischemia, though many ongoing studies are still evaluating the meaning of absolute perfusion data (this will be discussed later on). As a final step, CTA is able to show most of the underlying vascular pathology (see *Figure 1* an d *Table 1*).

NCCT

The NCCT can be performed using spiral scan techniques or by using the axial scan mode. If an axial mode is used, the eye lenses can be kept outside the scan field by tilting the gantry. Using thin sections for scanning (16x0.75 or 40x0.625mm) and reconstructing thicker ones (5mm) results in a good signal-to-noise ratio. Thin sections (0.9mm) can retrospectively be reconstructed if deemed necessary by the radiologist. From these thin axial sections, 5mm thick coronal or sagittal sections can be reconstructed, and provide additional information about the skull base or the regions close to the vertex.

A spiral scan is an alternative in uncooperative patients because the scan takes only a few seconds and motion can be reduced to a minimum if the patient can be persuaded to lie still during this time. The additional advantage is that thin sections are immediately available and can be used to assure optimized symmetric positioning of axial

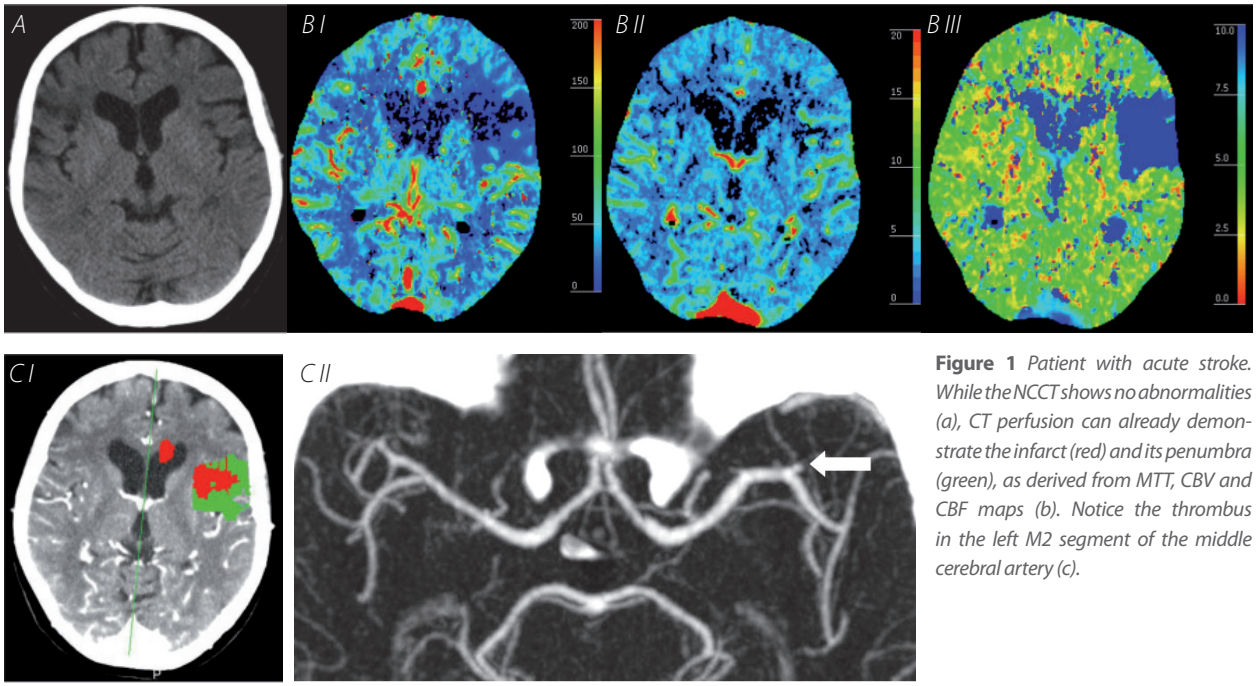

Figure 1 *Patient with acute stroke. While the NCCT shows no abnormalities (a), CT perfusion can already demonstrate the infarct (red) and its penumbra (green), as derived from MTT, CBV and CBF maps (b). Notice the thrombus in the left M2 segment of the middle cerebral artery (c).*

Table 1 *Indications for scanprotocol*

	NCCT	CTP	CTA
Acute:			
Subarachnoid hemorrhage (SAH)	+	(+)	+
Sinus thrombosis	+	(+)	+
Stroke/transient ischemic attack (TIA)	+	+	+
Carotid/vertebral dissection	+	+	+
Subacute:			
Follow-up of patients with SAH	+	+	+
Chronic:			
Positive family history of intracerebral aneurysms	-	-	+
Carotid artery stenosis and dissection	(+)	+	+
Follow-up after stent placement	-	+	+

\+ *indicated; (+) can be considered; - not indicated*

slices and provide additional 3D information about location and extent of bleeding or infarcts. The disadvantage is that the eye lenses are always included in the scan field, even if they are deliberately kept outside the scan range displayed on the scanner console. The reason is the so-called over-ranging: before and after the reconstructed scan range the scanner requires additional data for interpolation. This is approximately one additional rotation which makes it impossible to exclude the lenses from the exposed range (which is longer than the reconstructed scan range displayed on the scanner console).

Perfusion Imaging

In contrast to most techniques, CT perfusion imaging can assess functional parameters of the brain. During the scan, a contrast bolus is injected and is measured on the CT images as increase in enhancement. By means of dynamic scan technique, that means acquisition of multiple images at the same time during the passage of this contrast bolus, information about the cerebral blood volume (CBV), mean transit time (MTT) and cerebral blood flow (CBF) is achieved. A mathematical technique, the deconvolution method, is applied to assess absolute values for CBV, MTT and CBF [7,8].

CTP is preferably performed immediately after the NCCT since a non-enhanced base line is required for calculation of perfusion values. The time to peak enhancement of the CTP can then be used to serve as a "testbolus" for the CTA. Use of the lowest possible kilovoltage (kVp) results in optimal contrast-noise ratio, which is of major importance for calculation of perfusion maps[9]. Next, it is important to avoid inclusion of the eye lenses and thus on the scanogram exact determination of scan angulation is required. The 40 slice CT offers the possibility of scanning in the recently introduced "jog-mode" which doubles the covered volume, thereby almost covering the whole brain (2x4 cm). However, a disadvantage is that the posterior fossa cannot be included in one session.

For dose restriction, dynamic perfusion images can be acquired each two or even three seconds in stead of each second[10]. This does not influence perfusion parameters significantly and substantial dose reduction can be achieved. Thirty images are usually sufficient to cover the whole bolus and thus for calculation of perfusion data. It is essential to reduce patient head movement to a minimum since otherwise calculation of perfusion values becomes impossible. To ensure this, small cushions on both sides can be used to fixate the patients head.

The reconstructed slice thickness should be restricted since thicker slabs suffer seriously from partial volume effect thereby influencing perfusion values[11].

CTA; extra and intracranial

Although not essential, a delay of about five minutes between CTP and CTA is recommended to reduce venous over-projection from the contrast used for the CTP. In the mean time, perfusion images can be reconstructed. *Table 2-4* show the advised scan protocols.

Data Acquisition

For CTA of the circle of Willis conventionally 120 kVp was used in combination with 160-200 mAs. However, the use of lower kVp (80-90) has suggested to be advantageous since it results in a better contrast-to-noise ratio at equal or lower total dose (see also Chapter 3)[12]. Arterial enhancement will be brighter and despite increased noise it leads to better depiction of vascular structures, especially in the presence of subarachnoid hemorrhage. However, for the carotids 120 kVp is advised since the shoulder region causes too much noise at lower kVp. The introduction of dose modulation (DOM) and the adaptive filters is helpful in this case.
The scan direction is caudo-cranial for imaging of the circle of Willis but can be more useful in cranio-caudal direction when imaging the carotid arteries, since this results in less venous over-projection and scattering at the level of the subclavian artery. For optimum z-axis resolution, the thinnest possible collimation should be used that can still cover the desired scan range. A pitch of 1 or just below 1 (dependent on the scanner manufacture) will be sufficient. A lower pitch (0.3 – 0.6) can be used in cases of clipped cerebral aneurysms to reduce the clip artifact[13]. Increased kVp (140) in combination with higher concentration of contrast (370mg I/ml) also helps to reduce clip artifact.

Contrast Injection

Contrast injection is critical for CTA procedures. It is important to obtain a sufficiently high degree of vascular opacification throughout the imaging volume and to display the vessel of interest with as few artifacts as possible. The very short scan duration using the 40-slice (or more) scanner makes it no longer necessary to achieve a "plateau-phase" of contrast enhancement.
The focus is now mainly on individual determination of scan delay which is mandatory with these short scan times. If as little venous enhancement as possible is the goal, the CTP should be used as a testbolus or bolustracking techniques can be applied. If the venous structures are also of interest an additional waiting time of 4-8 s should be considered (see *Table 2*).
To reduce high contrast artifacts in the injection veins and to increase the potential enhancement, use of a saline flush is another important factor for both CTA and CTP[14, 15].

Image Review

Image review is primarily based on curved planar reformations (CPR) in coronal and sagittal direction (*Figure 2a*,*b*). X-ray technicians can reconstruct such CPR but it is important that they are precisely centered in order not to create artifactual stenoses. Vessel tracking may help to automatically track the vessel course but it usually fails for the petrous segment of the carotid arteries. CPR should follow the vessels from the aortic arch to the intracranial portion of the internal carotid artery, to one of the branches of the external carotid artery, and to the vertebral arteries on either side. Thus, a total of 3 vessels on each side x 2 projections = 12 images have to be reviewed. Evaluation thus becomes quite easy and time-efficient.

Table 2 *Suggested scan parameters for intracerebral CTA*

Scan parameters	16-slice	40/64-slice
Collimation (mm)	16x0.75	40/64x0.625
Slice thickness (mm)	1.0	0.67
Slice increment (mm)	0.5	0.33
Pitch	1.0	0.77
Rotation time (s)	0.42	0.5
kVp / mAs	90 / 330	120 / 245
Scan time (s) for 200 mm	12-14	6
Scan range	C1 to 3 cm under vertex	C1 to 3 cm under vertex
Scan direction	↑	↑
Contrast volume (ml)	70	60/50
Flow rate (ml/s)	5	5
Saline flush / flow rate	40/5	40/30 / 5
Scan delay	time to peak enhancement (TTP) on CTP	

Axial sections should be reviewed if there is a suspected abnormality to double-check the findings of CPR and to determine the eccentricity of a lesion. Thin-slab MIPs (ca. 10mm wide) are good for obtaining and overview of the carotid bifurcation (*Figure 2c*). Volume-rendered images can be used for complex anatomic situations and for presentation of findings to the referring physicians (*Figure 2d*). Both, MIP and VRT, however, suffer from superimposing structures, especially vascular wall calcifications.
For the intracranial portions of the circulation, thin- and thick-slab MIP of the circle of Willis are well suited (*Figure 3*). Shaded surface displays and virtual angioscopy play no clinical role for evaluation of the carotid arteries. Both techniques are extremely dependent on correct choice of threshold in order not to over- or underestimate stenoses[16-18]. Virtual angioscopy in particular fails in regions of calcified plaques (despite the fact that images look impressive).

Application in ischemic brain disease

Acute Ischemia (Stroke)

Stroke is the third leading cause of mortality in western countries and accounts for a high morbidity. For a long time only conservative treatment was available, but recently thrombolytic therapy has shown to be successful in 15-20% of the patients. However, it contains a certain risk for complications and adequate imaging is essential[19]. In patients with acute stroke, NCCT is followed by CTP and CTA in a stepwise procedure to make a diagnosis and optimize treatment planning[5,6].

Figure 2 *Example of a patient with severe atherosclerotic disease of the left carotid artery. CPR can nicely visualize the whole carotid and bifurcation in sagittal and coronal plane, while MIP images suffers from superimposing calcifications.*

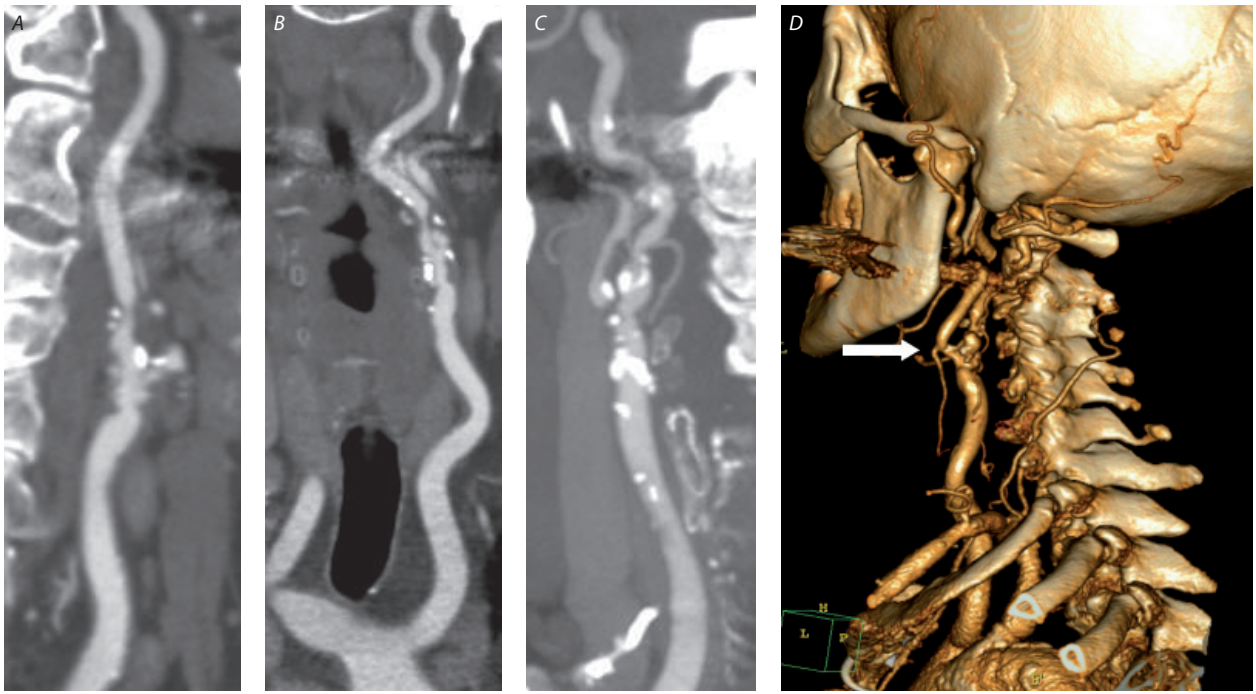

Sagittal *Coronal* *MIP* *3D vol*

Figure 3 *Three dimensional reconstruction of intracranial aneurysm and volume rendering of incomplete circle of Willis.*

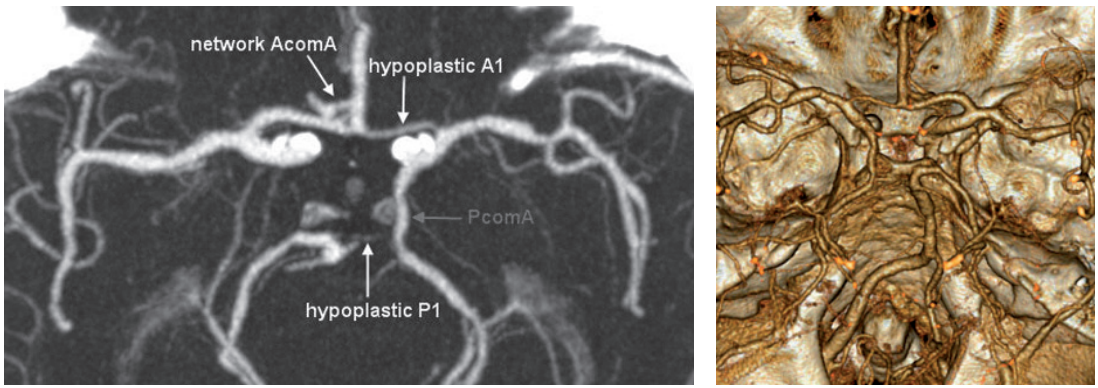

If NCCT shows extensive infarction or intra-parenchymal bleeding, no further scans are required. If little or no abnormalities are seen, perfusion imaging may reveal early ischemia and potentially salvageable tissue (penumbra). To define the status of the brain tissue usually Cerebral Blood Volume (CBV), Cerebral Blood Flow (CBF) and Mean Transit Time (MTT) are used. When absolute CBV is <2 ml/100 g or CBF <20 ml/100 g/min, reperfusion is not likely to save this brain tissue anymore. Most manufactures present this on the image viewer as definite infarct location (red) or penumbra (green). The benefit of thrombolytic therapy has been proven if treatment can be started within 3 hours after the onset of symptoms. However, extension of this time-window may be acquired if the perfusion scan shows a large penumbra (ischemic but viable tissue) (*Figure 1a-c*)[20,21].
High resolution and shorter scan duration makes scanning of intracranial and extracranial vessels possible within 10 seconds. This may eventually result in more rapid instigation of preventive treatment. Since for both CTA and CTP a certain contrast amount must be used, each option for reduction should be incorporated in the protocol. Although contrast is used for both CTA and CTP, the total amount can be kept within reasonable limits with the fast CTA available with a multislice CT.

Chronic Ischemia (Carotid Artery Stenosis)

Carotid artery stenosis (CAS) is a common complication of atherosclerosis. Ultrasound is the preferred technique to screen patients after stroke or TIA to search for carotid stenosis in the non-acute phase. If stenosis of >50% is present, further imaging is required to determine the exact degree of stenosis, presence of tandem stenosis and eventually completeness of the circle of Willis. Imaging carotid plaque can provide additional information about plaque composition. This is important since it is known that the stroke risk is also increased in patients with ulcerated plaques that facilitate formation of thromboemboli[22]. Lipid plaques have been reported to have a density below 50 HU, fibrous plaques have densities between 50 HU and 150 HU, and calcified plaques have the highest densities (over 150 HU, often more than 1000 HU)[23-24]. Small plaques, however, are susceptible to partial volume effects. Calcified plaques make evaluation of stenosis difficult unless transverse sections or curved planar reformations are generated and a wide window setting is used. Studies determining whether fatty plaques or calcified plaques influence the outcome of carotid artery stent placement are ongoing. In the follow-up after stent placement CTA demonstrates new plaques outside the stent as well as 'intima' proliferation and in-stent re-stenosis (*Figure 4*).

Sinus thrombosis and Dissection

Sinus thrombosis has a wide spectrum of presenting symptoms and can occur spontaneously or as a complication of several diseases. NCCT is often the first imaging modality requested and CT venography (CTV) can easily be performed in the same session. NCCT may reveal a dense vessel sign or a hemorrhagic infarct due to venous congestion, but often shows no abnormalities. CTP can replace the usual bolus timing and can reveal brain tissue at risk in an early stage (*Figure 5a-c*). Unlike for CTA, no waiting period between CTP and CTV is necessary as venous enhancement is desirable. A 4 to 8 second longer start delay (4 – 8 seconds) should be used.
Viewing the scan volume in three planes in MPR mode is the most easy way of detecting sinus thrombosis.

Figure 4 *Example of carotid artery stent one year after implantation. Neo-intima hyperplasia can be visualized on the axial images as well as on the coronal images.*

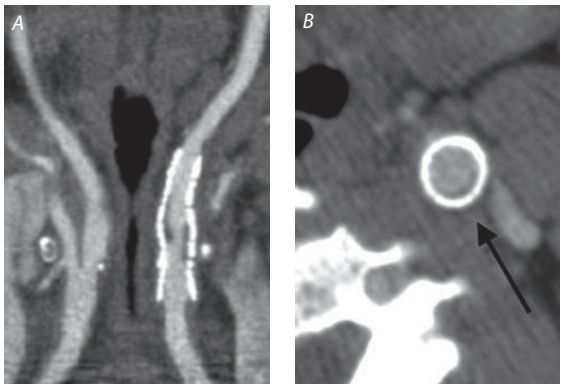

Additional CPR can show the thrombus throughout the sagittal sinus. X-ray technicians can reconstruct such CPR but it is important that they are precisely centered in order not to create artifactual thrombus or lumen (*Figure 5d*).
CT venograms are comparable to MR venography for detecting sinus thrombosis with the added advantage of easy availability, less chance of motion artifact, and better monitoring possibilities.

Internal carotid artery dissections occur in young or middle-aged patients and are a major cause for stroke (5–20%) in the young population. In spontaneous (nontraumatic) dissections, there is either no precipitating factor or they can occur after trivial trauma such as rapid head turning or during normal sporting activity. Stroke is often delayed for days to weeks when the dissection remains extra cranial. Anticoagulation therapy is usually effective, and 85% of patients with minor symptoms do well. Only 5% of patients suffer severe strokes.
The most common extra cranial dissection site is the internal carotid, a few cm beyond the bifurcation. Carotid dissection may present as a smooth, long stenotic segment that may extend intracranial („string" sign, *Figure 6a-c*). Usually the false channel is thrombosed and may appear hyperdense with a crescent shape. A thin rim of enhancing vasa vasorum may be seen around the intramural hematoma. If the false channel is perfused, diagnosis is easy with CTA[25]. High resolution is essential for optimal display of such a false channel and since it often occurs in the young, use of the dose modulation is obligatory.

Traumatic dissection presents similar to nontraumatic dissections, but more frequently involves the common carotid artery and results more often in complete occlusion. Patients with traumatic dissection present more often with cerebral ischemia, and response to therapy is less satisfactory. Comparison with the contralateral side is crucial for diagnosis. If necessary, CTA of the carotids in such trauma patients can be combined in one session with scanning of chest and abdomen.

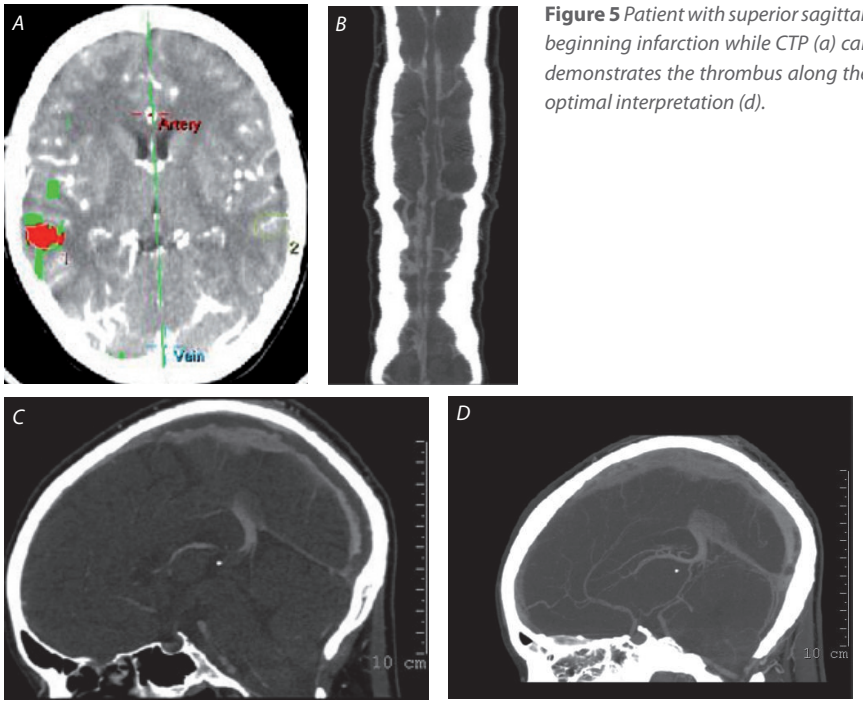

Figure 5 *Patient with superior sagittal sinus thrombosis. NCCT shows sign of possible beginning infarction while CTP (a) can already show the region of infarct. Thin CPR demonstrates the thrombus along the vessel course (b,c), while thick MPR hampers optimal interpretation (d).*

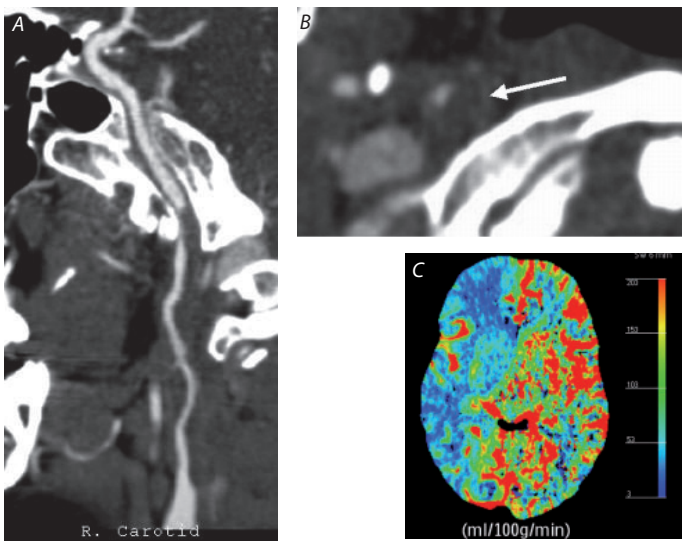

Figure 6 *Young girl suffering from carotid artery dissection. CPR (a) can show the irregular course of the carotid artery and the axial images visualize the thin rim of enhancing false lumen (b). There is a trombus in the osseous part of the carotid. Perfusion imaging shows decreased CBF but no infarct (c).*

Artifacts and Pitfalls

Artifacts may arise from ***dental implants*** but only gold can produce artifacts large enough to cause 'blind spots' on CPR. They can be reduced by placing the patient's head in such a way that the line of the teeth runs as closely parallel to the scan plane as possible.

Swallowing may cause irregularities and undulation of vascular contour as well as of the vessel itself. Rarely, the affected segment cannot be evaluated.

CPR may simulate stenoses if not centered properly. If in doubt, the corresponding axial section will bring the solution.

Carotid stents and calcified plaques may cause 'blooming' artifacts that let them appear wider than they really are. Wide window settings help differentiate between real stenoses and pseudostenoses due to blooming effects.

Pulsation may cause undulations of the vessel contours close to the aortic arch (proximal left carotid or brachiocephalic artery) but also may cause under- or overestimation of stenoses in the region of carotid kinking or coiling.

Highly concentrated contrast material in the left brachiocephalic vein can cause significant streak artifacts that obscure adjacent structures. A saline flush and a craniocaudal scanning direction that captures the injected veins at the end of the scan may reduce these artifacts.

Partial volume effects are less important for the carotids than for other regions in the body because of the perpendicular orientation of the vessels relative to the axial CT sections. Partial volume effects, however, may disturb the evaluation of small plaques and stenoses in horizontally oriented portions of the carotids (kinking or coiling, petrous segment).

Conclusion

Multislice CT has become a competitive technique for evaluation of the intra- and extra cranial arteries. The high spatial resolution, larger coverage and reduced amount of required contrast material makes this tool excellent for many acute and sub acute situations by using CT angiography as well as CT perfusion. It remains important to focus on options for dose reduction and optimization of image reviewing.

Table 3 *Suggested scan parameters for carotid CTA*

Scan parameters	16-slice	40/64-slice
Collimation (mm)	16x0.75	40/64x0.625
Slice thickness (mm)	1.0	0.9
Slice increment (mm)	0.5	0.4
Pitch	0.851	0.77
Rotation time (s)	0.42	0.42
kVp / mAs	120 / 180	120 / 180
Scan time (s) for 200 mm	13-15	8-12 / 6-8
Scan range:	origin ACC to 3 cm under vertex	aortic arch to 3 cm under vertex
Scan direction:	↓	↓
Contrast volume	80	70 / 50
Flow rate	5	5
Saline flush / flow rate	40 /5	40/30 / 5
Scan delay D	time to peak enhancement (TTP) on CTP	
	If TTP >25 sec → D = TTP + 2 sec !	

Table 4 *Scan parameters for CT perfusion (CAS & CoW)*

Scan parameters	16-slice	40/64-slice
Collimation (mm)	8x3.0	32x1.25/64x0.625
Cycletime	1 sec	2 sec
kVp / mAs	90 / 150	80 / 150
Slice Thickness (mm)	6.0 (4 slabs)	5.0 (8 slabs)
CTDIvol	40x8.9	30x5.6/30x5.3
FOV	200	200
Contrast volume	40	40
Flow rate	5	5
Saline flush / flow rate	40 / 5	40 /5
Scan delay	5 sec is sufficient for non-enhanced baseline	

References

1. Nederkoorn PJ, van der Graaf Y, Hunink MG. Duplex ultrasound and magnetic resonance angiography compared with digital subtraction angiography in carotid artery stenosis: a systematic review. Stroke. 2003; 34:1324-32.
2. Prokop M. Multislice CT angiography. Eur J Radiol 2000;36: 86–96.
3. Ohnesorge B, Flohr T, Schaller S, et al. Principles and applications of multi-slice CT. Der Radiologe 1999;39:923–931.
4. Lell M, Wildberger JE, Heuschmid M, et al. CT-angiography of the carotid artery: first results with a novel 16-slice spiral-CT scanner. RöFo Fortschr Röntgenstr 2002;174:1165-1169.
5. Klotz E, Konig M. Perfusion measurements of the brain: using dynamic CT for the quantitative assessment of cerebral ischemia in acute stroke. Eur J Radiol. 1999;30:170-84.
6. Smith WS, Roberts HC, Chuang NA, Ong KC, Lee TJ, Johnston SC, Dillon WP. Safety and feasibility of a CT protocol for acute stroke: combined CT, CT angiography, and CT perfusion imaging in 53 consecutive patients AJNR 2003;24:688-90.
7. Wintermark M, Maeder P, Thiran JP, Schnyder P, Meuli R. Quantitative assessment of regional cerebral blood flows by perfusion CT studies at low injection rates: a critical review of the underlying theoretical models. Eur Radiol. 2001;11:1220-30.
8. Nabavi DG, Cenic A, Dool J et al. Quantitative assessment of cerebral hemodynamics using CT: stability, accuracy, and precision studies in dogs. J Comput Assist Tomogr 1999;23:506-15.
9. Wintermark M, Maeder P, Verdun FR, Thiran JP, Valley JF, Schnyder P, Meuli R. Using 80 kVp versus 120 kVp in perfusion CT measurement of regional cerebral blood flow. AJNR 2000;21:1881-4.
10. Wintermark M, Smith WS, Ko NU, Quist M, Schnyder P, Dillon WP. Dynamic perfusion CT: optimizing the temporal resolution and contrast volume for calculation of perfusion CT parameters in stroke patients. AJNR 2004;25:720-9.
11. van der Schaaf I, Vonken EJ, Waaijer A, Velthuis B, Quist M, van Osch T. Influence of partial volume on venous output and arterial input function. AJNR 2006;27:46-50.
12. Bahner ML, Bengel A, Brix G, Zuna I, Kauczor HU, Delorme S. Improved vascular opacification in cerebral computed tomography angiography with 80 kVp. Invest Radiol. 2005;40:229-34.
13. van der Schaaf I, van Leeuwen M, Vlassenbroek A, Velthuis B. Minimizing clip artifacts in multi CT angiography of clipped patients. AJNR 2006;27:60-6.
14. Cademartiri F, Lugt A v/d, Luccichenti G. Parameters affecting bolus geometry in CTA: A review. J Comp Ass Tomography 2002;26:598-607.
15. Fleischman D, Hittmar K. Mathematical analysis of arterial enhancement and optimization of bolus geometry for CT angiography using the discrete fourier transform. J Comp Ass Tomography 1999; 23:474-484.
16. Dix JE, Evans AJ, Kallmes DF, Sobel AH, Phillips CD. Accuracy and precision of CT angiography in a model of carotid artery bifurcation stenosis. AJNR 1997;18:409-15.
17. Takahashi M, Ashtari M, Papp Z, et al. CT angiography of carotid bifurcation: artifacts and pitfalls in shaded-surface display. AJR 1997;168: 813–817.
18. Liu Y, Hopper KD, Mauger DT, Addis KA. CT angiographic measurement of the carotid artery: optimizing visualization by manipulating window and level settings and contrast material attenuation. Radiology 2000;217: 494–500
19. Schellinger PD, Fiebach JB, Hacke W. Imaging-based decision making in thrombolytic therapy for ischemic stroke: present status. Stroke 2003;34:575-83.
20. Hacke W, Albers G, Al-Rawi Y, Bogousslavsky J, Davalos A, Eliasziw M, Fischer M, Furlan A, Kaste M, Lees KR, Soehngen M, Warach S; DIAS Study Group. The Desmoteplase in Acute Ischemic Stroke Trial (DIAS): a phase II MRI-based 9-hour window acute stroke thrombolysis trial with intravenous desmoteplase. Stroke 2005;36:66-73.
21. Schramm P, Schellinger PD, Klotz E, Kallenberg K, Fiebach JB, Kulkens S, Heiland S, Knauth M, Sartor K. Comparison of perfusion computed tomography and computed tomography angiography source images with perfusion-weighted imaging and diffusion-weighted imaging in patients with acute stroke of less than 6 hours' duration. Stroke 2004;35:1652-8.

22. Eliasziw M, Streifler JY, Fox AJ et al. Significance of plaque ulceration in symptomatic patients with high grade carotid stenosis. NASCET. Stroke 1994; 25:304-308.
23. Estez JM, Quist WC, Gefro FW. Noninvasive characterisation of plaque morphology using helical computed tomography. J cardiovasc Surg 1998;39:527-34.
24. Oliver TB, Lammie A, Wright AR. Atherosclerotic plaque at the carotid bifurcation: CTA appearance with histopathologic correlation. AJNR 1999; 20:897-901.
25. Leclerc X, Godefroy O, Salhi A, et al. Helical CT for the diagnosis of extracranial internal carotid artery dissection. Stroke 1996;27:461–466.

Dose Reduction and Image Quality: Reducing kVp and Increasing mAs Settings for CT Angiography of the Circle of Willis

Chapter Three

A Waaijer, MS van Leeuwen, BK Velthuis, CJG Bakker, GAP de Kort, M Prokop. Dose Reduction and Image Quality: Reducing kVp and Increasing mAs Settings for CT Angiography of the Circle of Willis. Accepted for Radiology

Abstract

Purpose

To prospectively assess the effect of lower kVp and varying mAs_{eff} on image quality for CT Angiography (CTA) of the circle of Willis (CoW).

Materials and Methods

The study was performed with institutional review board approval and written informed consent was given by all patients or their family members. We determined signal-to-noise ratios (SNR) in a head phantom for various mAs_{eff} settings at 90, 120 and 140kVp. In a clinical study, we included patients referred for CTA of the CoW because of acute subarachnoid hemorrhage (n=20) or family history of cerebral aneurysms (n=20). In each group of referrals, 10 patients were scanned with 120kVp/200mAs_{eff} (CT dose index, CTD_{vol}=27.2mGy) and 10 with 90kVp/330mAs_{eff} ($CTDI_{vol}$= 20.6mGy). CT numbers were measured in the carotid T-junction and compared with a t-test. Using a five-point scale, two radiologists subjectively scored arterial enhancement, visualization of small arterial detail, image noise, venous contamination and interference of subarachnoid blood. Statistical analysis was performed using the Mann Whitney U test.

Results

In the phantom, SNR^2 was proportional to mAs_{eff} and $CTDI_{vol}$. At identical mAs_{eff}, SNR^2 was substantially lower at 90kVp compared to 120 and 140kVp. However, at identical $CTDI_{vol}$, the use of 90kVp resulted in 45-52% increase of SNR^2 compared to 120kVp. In patients, mean CT attenuation in the carotid T-junction was higher with 90kVp (340HU) than with 120kVp (252HU, $p<0.001$). Despite a 30% lower dose at 90kVp, arterial enhancement and visualization of small arterial detail yielded significantly higher scores than at 120kVp (4.0 versus 3.2, and 3.6 versus 3.1, respectively; $p<0.005$).

Conclusion

In head phantoms the use of a lower tube voltage substantially improves SNR at equal radiation dose. For CTA of the circle of Willis this fact translates into superior image quality for 90kVp compared to 120kVp even if patient dose is reduced by approximately 30%.

Introduction

Computed Tomography Angiography (CTA) of the circle of Willis (CoW) is a well-established minimally invasive diagnostic procedure for detecting cerebral aneurysms[1-4]. In patients with subarachnoid hemorrhage (SAH), CTA can be acquired immediately after the non-contrast scan to facilitate prompt treatment planning[5-7]. As aneurysms and their supplying vessels are small, arterial contrast enhancement needs to be optimized by using appropriate contrast injection and scan parameters.

There is a trend towards increasing scan dose with thin-section multislice CT compared to single slice CT[8]. Evaluation of potential options for dose reduction is therefore important and has become the focus of research[9-12].

X-ray absorption of iodine increases substantially at low effective beam energy as long as the effective energy remains above the k-edge of iodine (33 keV)[13]. By lowering tube voltage below the 120-140kVp typically used in diagnostic CT, the arterial enhancement increases substantially at constant intravascular iodine concentration. This increased intra-arterial 'signal' should provide a means for dose reduction without influencing signal-to-noise (SNR) ratios. However, decreasing the tube voltage without changing mAs settings may not be sufficient for this goal: at Lower kVp settings the dose decreases rapidly if the mAs settings are not adapted. This will result in a substantially increased image noise, which may or may not be compensated for by the increase in arterial enhancement ('signal')[14]. Despite various phantom studies on the subject of low-kVp scanning, the relation between SNR and dose for different tube voltages in clinical patients is not well established[15,16].

Two recent studies on the use of lower tube voltage for CTA of the circle of Willis in a clinical setting, led to contradictory results. Ertl-Wagner found that higher kVp resulted in better image quality, whilst Bahner showed benefit with Lower kVp[17,18].

The purpose of our study was therefore to prospectively assess the effect of lower kVp and varying mAs_{eff} on image quality for CT Angiography (CTA) of the circle of Willis (CoW). For this purpose we first studied the effect of Lower kVp and varying mAs_{eff} settings on contrast enhancement and SNR in a head phantom. We then performed a clinical study to prospectively assess the effect of Lowering kVp while adapting mAs settings on image quality of CT Angiography (CTA) of the circle of Willis (CoW).

Materials and Methods

As a first step, we performed a phantom study to establish the iodine attenuation curve for our scanner at 90, 120, and 140kVp to quantify the increase in enhancement at lower tube voltage. Next, this phantom was scanned at 90, 120 and 140kVp, while varying mAs_{eff} and kVp independently. Subsequently two groups of patients undergoing CTA for aneurysm detection were included in a clinical study to compare image quality at 90 and 120kVp.

Scanner

All experiments and clinical studies were performed on a 16-slice scanner (MX 8000 IDT, Philips, Cleveland, OH) with 16x0.75mm collimation at a rotation time of 0.75s. A slightly smoothing filter (B filter) was used in combination with a 512x512 matrix. Scans were reconstructed with a slice thickness of 1.0 mm and a reconstruction increment of 0.5 mm. To assure consistent image quality, calibration of the scanner was performed every week.

Phantom Study

We used a proprietary cylindrical polymethylmethacrylate (PMMA) head phantom with a diameter of 185mm. In the center of the phantom a tube of 25mm diameter filled with contrast material could be inserted.

Iodine Attenuation Curve, Statistical Analysis

We prepared thirteen different iodine concentrations (0, 0.5, 0.75, 1.0, 1.5, 2, 4, 6, 7.5, 12, 25, 30 and 50mg I/ml) by diluting contrast material (Ultravist, 300mg I/ml; Schering, Berlin, Germany) with distilled water. All contrast material solutions were prepared just prior to scanning in order to prevent settling of the contrast solution. We used tube voltage settings of 90kVp, 120kVp and 140kVp and chose the effective mAs settings so that the head CT dose index ($CTDI_{vol}$) was as close as possible to 27.2mGy for all three protocols. This was achieved by using 450mAs_{eff} at 90kVp, 200 mAs_{eff} at 120kVp and 135mAs_{eff} at 140kVp with a pitch of 0.3 and a FOV of 200mm.
Attenuation was measured by one observer (AW) by drawing a region of interest (ROI) of approximately 100mm^2 in the middle of the tube. Mean CT value (expressed in Hounsfield Units; HU) for that ROI was plotted against the iodine concentration. Data were analyzed using linear regression analysis and by determining the Pearson correlation coefficients.

Variation of kVp and mAs Settings

Next, we chose the contrast concentration that best resembled the enhancement seen in clinical patients to perform SNR measurements (12 mg/ml iodine, enhancement approximately 250 to 420HU, depending on thekVp setting). Scans of the phantom were performed at three tube voltages, 90, 120 and 140kVp, combined with nine mAs settings each varying from 25-370mAs_{eff}.

Dose Measurements

In order to be able to estimate patient dose at the variouskVp and mAs_{eff} settings, we recorded the numbers for $CTDI_{vol}$ indicated on the scanner interface and compared them to our own measurements in a standard 160mm CTDI head phantom. In order to be able to relate SNR to local dose, we also performed dose measurements in the central hole of the 185mm head phantom that we used for SNR calculations.
All dose measurements were performed by two observers (AW and MP) with a 10cm pencil ionization chamber (Solidose 400, RTI Electronics, Sweden). Each measurement was repeated 10 times and readings were averaged.
For the standard 160mm CTDI phantom, a weighted average of the measurements in the four peripheral and the central position was used to calculate the weighted CTDI, which, in a static setup, is identical to $CTDI_{vol}$[19]. Linear regression analysis was used to determine a calibration factor for our scanner that transformed mAs_{eff} into $CTDI_{vol}$ for the three kVp settings.
Local dose in the 185mm PMMA phantom was measured in the central hole ($CTDI_{local}$). Again we performed linear regression analysis to determine a calibration factor that transformed mAs_{eff} into $CTDI_{local}$ values for the three kVp settings

Signal-to-Noise Measurements, Statistical Analysis

For each scan of the 185mm PMMA phantom containing the contrast solutions, we determined mean CT value (signal) and standard deviation (image noise) by placing an ROI of approximately $100mm^2$ in the center of the tube. Measurements were performed by one observer (AW) at five equidistant levels along the z-axis to correct for variations in noise over the phantom. SNR was calculated by dividing the CT value in the tube by its standard deviation. Because CT numbers are normalized to water (0 HU), the CT number of a contrast-enhanced structure actually corresponds to the contrast between this structure and water. The SNR used in the above definition therefore can also be interpreted as a contrast-to-noise ratio (CNR) in which contrast is defined as the difference in CT numbers between the contrast-enhanced structure and water.
In theory, $noise^2$ (σ^2) and dose in CT are inversely related ($\sigma^2 \propto 1/dose$)[20]. Dose as given by the CTDI is proportional to the mAs_{eff} setting, and therefore SNR^2 can be expected to show a linear relation also with mAs_{eff} and CTDI[13]. Because of this linear relationship we used SNR^2 to quantify the differences in SNR between the three kVp settings. Both the relation between SNR^2 and mAs_{eff}, and SNR^2 and CTDI (measured $CTDI_{vol}$ and $CTDI_{local}$), were established for the three different tube voltages, using linear regression analysis, and by determining Pearson's correlation coefficient.

Clinical Study

Patients

We included 40 patients who were referred to us for CTA of the circle of Willis because of SAH or screening in patients with a positive family history for intracranial aneurysms. In each of these groups we recruited 20 consecutive patients between October 2003 and March 2004. In the both groups of referrals, the first 10 patients

were consecutively scanned with 120kVp and the next 10 with 90kVp.
Poor-quality CTAs due to patient movement or failure of contrast injection were excluded from the study. Mean age of the patients was 61 year (SD 12.9, range 22-85); there were 17 men and 23 women. The study was performed with institutional review board approval. Informed consent was obtained from all patients or their family members.

Scan Protocol

We chose our standard scanning parameters for the circle of Willis according to the recommendations of the manufacturer. Consequently, we used 16x0.75mm collimation with a pitch of 1.0, a rotation time of 0.75s and exposure settings of 120kVp and 200mAs$_{eff}$, resulting in a CTDI$_{vol}$ of 27.2mGy. The scan volume in patients extended from the posterior arch of C1 to the vertex of the brain. Scans were reconstructed with a slice thickness of 1.0 mm and a reconstruction increment of 0.5mm, with FOV of 160mm.
At 90kVp we chose the same scan and reconstruction parameters, except for the effective mAs settings. The mAs settings were to result in a CT dose index that was as close as possible to that at 120kVp. However, because at a pitch of 1.0 the maximum tube current available on the scanner only allowed for 330 mAs$_{eff}$ (and not 450mAs$_{eff}$. as would have been theoretically required), the resultant CTDI$_{vol}$ was 20.6mGy and thus 33% lower than at 120kVp.
Contrast (Ultravist 300, 300mg I/ml; Schering, Berlin, Germany), was injected during 17 seconds (50ml at 5ml/s and 20ml at 3ml/s), followed by a saline chaser of 30ml injected at 3 ml/sec. A test bolus was applied to determine the individual scan delay.

Image Assessment, Statistical Analysis

Attenuation was measured in the internal carotid artery at the T-junction by drawing a ROI of 2.5-3.5mm^2 just within the vessel lumen by one observer (AW, 1 year full-time experience in head CTA, under supervision of MvL). Mean CT value (HU) and standard deviation were noted. Attenuation of the brain parenchyma was noted by placing a ROI of 250mm^2 within the center of one occipital lobe, avoiding vascular structures. CT values were rounded off to the nearest number. SNR was calculated by dividing the mean enhancement at the internal carotid T-junction (signal) by the standard deviation in the brain parenchyma (noise). Two radiologists (BV, GK) who had more than 5 years experience with evaluating the circle of Willis (>300 CTA exams per year), independently performed subjective rating of image quality on a five-point scale in which the center of the scale (rating = 3) corresponded to the quality expected from a standard CTA of the circle of Willis. One point signified that image quality was non-diagnostic, two points sub-standard, three standard, four better than standard and five excellent. The two observers also independently scored the following image quality parameters: arterial enhancement, visibility of small arterial detail (based on depiction of small arteries, such as the ophthalmic, anterior choroid, anterior and posterior communicating and superior cerebellar arteries), interference of venous structures (venous contamination) and noise. A lowering of kVp may also increase venous enhancement. We therefore also evaluated the influence of interference of venous structures on image quality. In patients with SAH, we also evaluated interference of subarachnoid blood, which was defined as the visibility of vascular detail in regions where there was perivascular hemorrhage present. Observers were blinded to whether the scan was performed with 120kVp or 90kVp. They were free to choose window and level settings as they deemed appropriate.

For evaluation of subjective scoring the Wilcoxon Signed ranks-test was applied to analyze the differences between 90 and 120kVp for both observers. For further analysis we pooled data from both observers and both clinical indications, except for the evaluation of subjective scores for interference of subarachnoid blood, in which only SAH patients were included. The Mann-Whitney-U test for two independent samples was used to analyze differences in arterial attenuation as well as SNR, and subjective scoring between 90 and 120kVp scans. P-values <0.05 were considered statistically significant.

Results

Iodine Attenuation Curve - Phantom

We found a linear relationship between iodine concentration and attenuation for all tube voltages (*Figure 1*). The Pearson correlation coefficients varied between r > 0.9999 for 90kVp and r = 0.999 for 120 and 140kVp (p<0.001) (*Figure 1*). Attenuation at 90kVp was 43% higher (33 HU/mg I) than at 120kVp (23 HU/ mg I) and 74% higher than at 140kVp (19 HU/mg I).

Figure 1 *CT value as function of iodine concentration.*

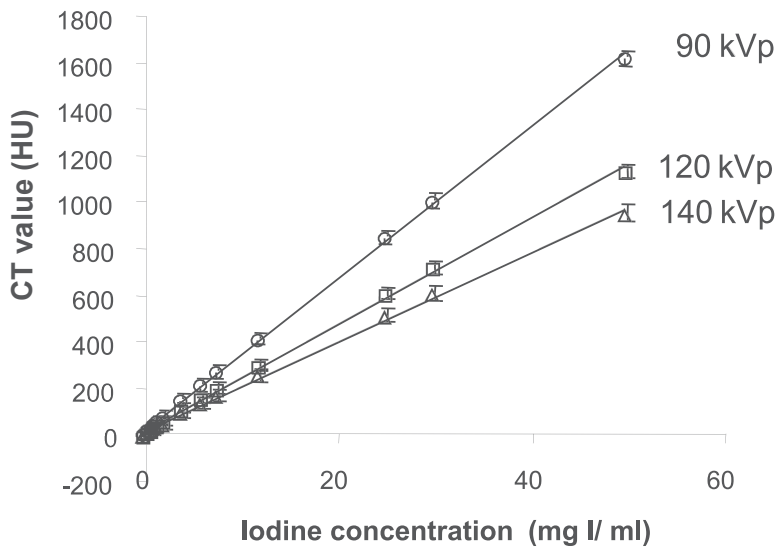

The linear relationship for three different tube voltage was as follows:
90 kVp: y = 32.5x + 13.3 (r = 1.000)
120 kVp: y = 22.8x + 13.4 (r = 0.999)
140 kVp: y = 19.1x + 12.0 (r = 0.999)

Dose Measurements – Phantom

The calibration factors to transfer mAs_{eff} into the $CTDI_{vol}$ provided on the scanner interface, the measured $CTDI_{vol}$ and the local dose ($CTDI_{local}$) are given in *Table 1*. The CTDI values displayed on the scanner interface overestimated the measured $CTDI_{vol}$ on average by 12%. The local dose in the center of our contrast phantom was on average 31% (between 29 and 33%) lower than the dose displayed on the scanner interface. Dose per mAs was always lowest at 90kVp and increased substantially at higher kVp.

Table 1 *Calibration factors to transfer mAs_{eff} into the $CTDI_{vol}$ provided on the scanner interface, the measured $CTDI_{vol}$ and the local dose ($CTDI_{local}$)*

Dose (CTDI)	Interface	Measured (160mm)	Local (185mm)
90kVp	0.069	0.061	0.047
120kVp	0.150	0.134	0.105
140kVp	0.219	0.190	0.156

Signal-to-Noise Ratios – Phantom

As theoretically expected, $(noise)^2$ was inversely proportional to mAs ($\sigma^2 \propto 1/dose$). At equal mAs, the lowest noise was seen at 140kVp and the highest noise at 90kVp (*Figure 2**a***). SNR^2 was proportional to mAs_{eff} as well as proportional to local and volume CTDI with Pearson correlation coefficients between 0.996 and 1.000 ($p<0.001$). At identical mAs, SNR^2 at 120 and 140kVp were almost identical but SNR^2 was substantially lower at 90kVp (*Figure 2b*). However, at identical $CTDI_{vol}$ and $CTDI_{local}$, the use of 90kVp resulted in a 45% to 52% increase of SNR^2 compared to 120kVp and 102% to 115% compared to 140kVp (*Figure 2c and d*).

Signal-to-Noise Ratios – Patients

We paid special attention in the phantom study to the dose level used in our clinical study to assess whether the PMMA measurements were comparable to the patients' heads. Based on the linear regression analysis we calculated the SNR that was expected for the phantom when using the clinical exposure settings of 120kVp and 200 mAs_{eff} ($CTDI_{vol}$ = 27.2mGy) and 90kVp and 330 mAs_{eff} ($CTDI_{vol}$ = 20.6mGy). The calculated SNR for 120kVp and 200 mAs_{eff} was 19.3, while we measured an SNR of 19.8 in our clinical scans (standard error 1.5). The calculated SNR for 90kVp and 330 mAs_{eff} was 20.4, while we measured 21.6 in clinical scans (standard error 1.4), indicating a small underestimation of SNR using a PMMA phantom in comparison to clinical patients.

Figure 2a-d *Comparison of the relation between noise or signal-to-noise ratios and mAs_{eff} settings or patient dose for three different kVp settings, (a) relation between mAs_{eff} and noise, (b) relation between mAs_{eff} and SNR^2 and (c) relation between dose expressed as $CTDI_{vol}$ and SNR^2. SNR calculation was based on the mean enhancement in an ROI measured at the internal carotid T-junction (signal) divided by the standard deviation in the brain parenchyma (noise) as measured within the occipital lobe.*

A Relation between mAseff and noise

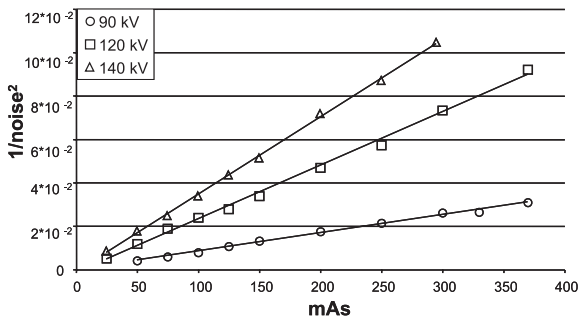

B Relation between mAs_{eff} and SNR^2

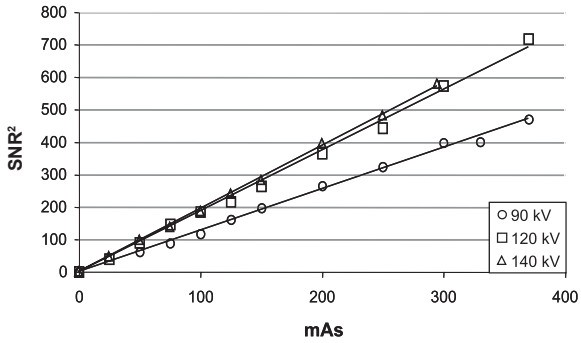

140 kVp $SNR^2 = 1.94 \times mAs_{eff}$ (r =1.000)
120 kVp $SNR^2 = 1.87 \times mAs_{eff}$ (r = 0.998)
90 kVp $SNR^2 = 1.27 \times mAs_{eff}$ (r = 0.998)

C Relation between dose expressed as $CTDI_{vol}$ and SNR^2

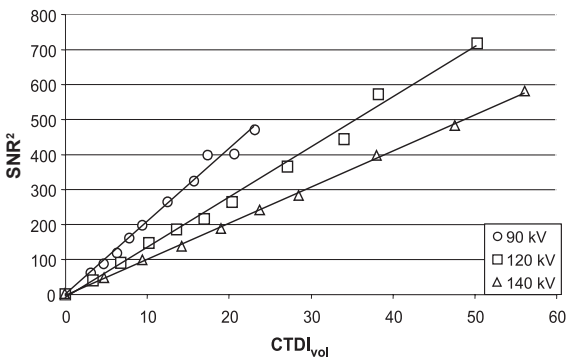

90 kVp $SNR^2 = 20.8 \times CTDI_{vol}$ (r = 0.999)
120 kVp $SNR^2 = 14.3 \times CTDI_{vol}$ (r = 0.993)
140 kVp $SNR^2 = 10.3 \times CTDI_{vol}$ (r =0.999)

D Relation between $CTDI_{local}$ as measured within the 185mm PMMA phantom and the SNR^2

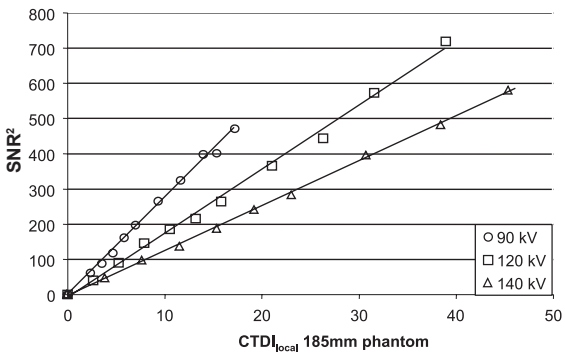

90 kVp $SNR^2 = 27.5 \times CTDI_{vol}$ (r = 0.996)
120 kVp $SNR^2 = 18.2 \times CTDI_{vol}$ (r = 0.997)
140 kVp $SNR^2 = 12.8 \times CTDI_{vol}$ (r =0.999)

Clinical Study

In the clinical scans mean CT value at the internal carotid T-junction was 340HU (range: 189-446) in 90kVp-scans and 253HU (range: 185-349) in 120kVp-scans, with a mean difference of 87HU (95%CI: 53-121; p<0.001). This indicates a 35% increase in arterial attenuation at 90kVp compared to 120kVp (*Figure 3*). Attenuation of the brain parenchyma was not significantly different at 90kVp (37 HU) compared to 120kVp (35 HU) (*Table 2*). The SNR at 120 (19.8) was not significantly different from 90kVp (21.6).

No significant inter-observer differences were seen in subjective rating of image quality criteria except for venous contamination, where observer B scored 0.3 points higher (p=0.016) (*Table 3*).

When analyzing pooled data from both observers and both clinical indications we found that scans acquired with 90kVp were rated significantly better than those acquired with 120kVp regarding arterial enhancement, visualization of small arterial detail and overall image quality (*Table 4*). The quality scores increased 3.2 to 4.0 for arterial enhancement (p<0.005), from 3.1 to 3.6 for visualization of small arterial detail (p<0.005) and from 3.1 to 3.6 for overall image quality (p<0.005). We found no significant difference between the 90 and 120kVp scans regarding the scores for interference of venous structures and noise. In patients with SAH, subarachnoid blood surrounding the vessels interfered significantly less (better vascular detail) at 90kVp (score 3.6) than at 120kVp (score 3.0, p<0.01) as illustrated in *Figure 4*.

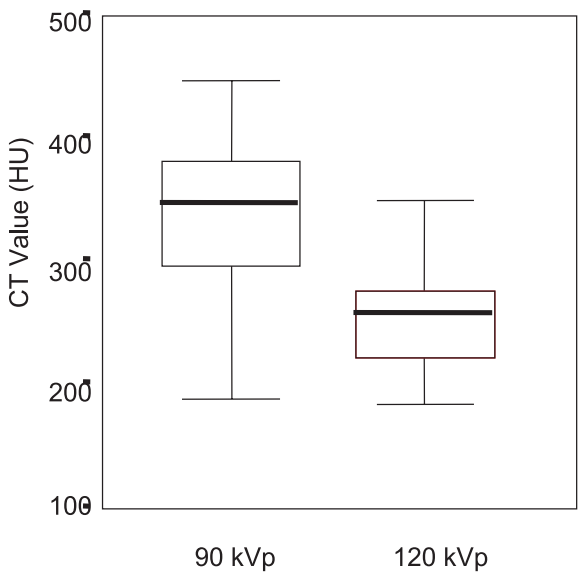

Figure 3 *Arterial attenuation for patient groups scanned with 90 and 120kVp*

Bars showing the range of values of arterial enhancement in 20 patients scanned with 90kVp (left) and 20 patients scanned with 120kVp (right). In the box are all values within the 25th and 75th percentile (interquartile range), the black line representing the median.

Table 2 *Mean CT numbers (± standard deviation) for all patients. CT numbers were measured by one observer (AW) in 40 clinical scans in the internal carotid artery (ICA) at the T-junction and expressed in absolute numbers (HU). Twenty patients were scanned at 120kVp and 20 patients were scanned at 90kVp. CT numbers of the brain parenchyma were measured in the center of one occipital lobe.*

	Mean CT number	Mean CT number	ICA T-junction	background
kVp	120	90	120	90
CT number (HU)	253 (± 46.3)	340 (± 60.1)*	35 (± 8.0)	37 (± 6.6) **
SNR	19.8	21.6†		

** p <0.001 ** p = 0.441 † Difference not statically significant*

Table 3 *Comparison of subjective scoring by observers A and B. Mean scores (± standard deviation) are provided for combined data from all 40 patients for each observer separately for 90 and 120 kVp.*

	90kVp		120kVp	
	Observer A	Observer B	Observer A	Observer B
Arterial enhancement†	4.0 (0.6)	4.0 (0.7)	3.1 (0.7)	3.3 (0.5)
Venous contamination	3.0 (0.6)	3.4 (0.5)*	3.0 (0.0)	3.1 (0.6)
Detail visibility†	3.6 (0.6)	3.6 (0.7)	3.0 (0.7)	3.2 (0.7)
Noise	3.0 (0.3)	3.0 (0.6)	3.0 (0.0)	3.1 (0.5)
Total†	3.6 (0.7)	3.6 (0.6)	3.0 (0.7)	3.1 (0.7)

Comparison of scores between observer A and B showed no significant differences except for venous contamination (*) at 90 kVp for which observer B gave significant higher scores than observer A (p=0.011).
† Both observer A en B scored the 90 kVp scans significantly higher than the 120 kVp scans.

Table 4 *Subjective scoring (pooled data of two observers) for all patients (n=40) expressed on a five-point scale.*

	All patients		
kVp/ mAs eff	**120/ 200**	**90/ 330**	**p-value**
Mean age (range)	61.7 (42-85)	59.8 (22-78)	0.648*
Arterial enhancement	3.2	4.0	<0.001†
Detail visibility	3.1	3.6	<0.001†
Noise	3.1	3.0	0.085†
Venous contamination	3.0	3.2	0.418†
Interference of SAH#	3.0	3.6	<0.001†
Overall score	3.1	3.6	<0.005†

** P-value according to Student's t-test*
† P-value according to Mann Whitney U test
 # Vascular detail visibility in presence of subarachnoid blood (only evaluated in the subgroup of patients with SAH)

Figure 4 *These images show non-contrast CT (a and c) and corresponding CTA (b and d) in two different SAH patients. The non-contrast CT has been performed with the same protocol, the CTA was performed with 120kVp in the patient in (b) and with 90kVp in the other patient in (d). Both CTA images are a 20mm thick slab-MIP with equal window width/level setting at 470/200, demonstrating that 90kVp resulted in increased visibility of vascular structures surrounded by subarachnoid blood.*
The patient in (a) and (b) had a right middle cerebral artery (MCA) aneurysm (black arrow) with a total score of 2 points for image quality by both observers. Interference of subarachnoid blood was scored with 2 points for observer A and 3 points for observer B.
The patient in (c) and (d) had a left MCA aneurysm (white arrow) with a total score of 5 points by observer A and 4 points by observer B. Interference of subarachnoid blood was scored with 5 points for observer A and 4 points for observer B.

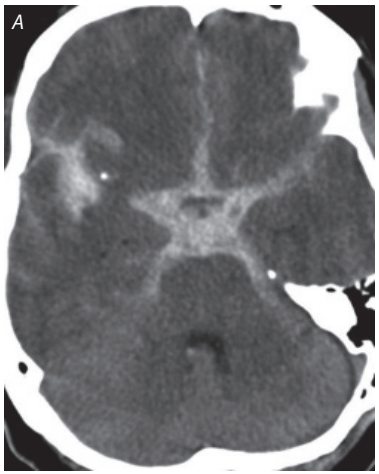

Patient I, Non-Contrast CT

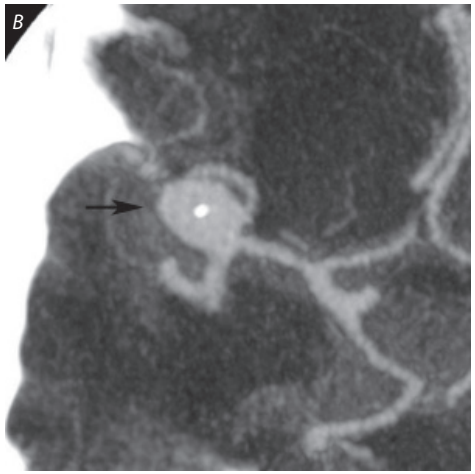

Patient I, CTA (120kVp/200 mAs_{eff})

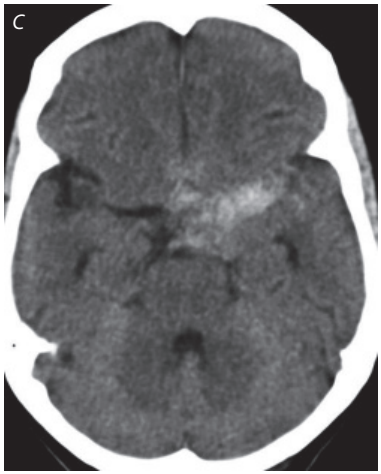

Patient II, Non-Contrast CT

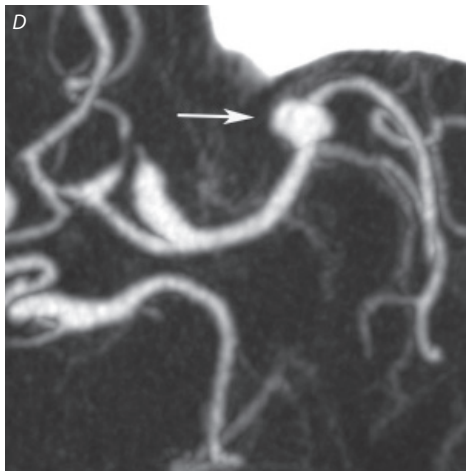

Patient II, CTA (90kVp/330 mAs_{eff})

Discussion

We demonstrated that, although SNR decreases for 90kVp at identical mAs setting, SNR improves substantially when identical dose levels ($CTDI_{vol}$ or $CTDI_{local}$) are used. For evaluation of CT angiography of the circle of Willis in clinical patients this fact translated into superior image quality for 90kVp compared to 120kVp even if patient dose was reduced by approximately 30%. Most improvement can be expected in patients with acute SAH, where the visibility of vascular detail improved in the presence of subarachnoid hemorrhage at 90kVp as compared to 120kVp.

Some reports have been published with regard to optimizing image quality in CT angiography of the brain by adapting tube voltage[17,18]. Whilst most articles advocate 120kVp for CTA of the brain[1-5], we found that enhancement was higher for CTA acquired with 90kVp and that experienced radiologists rated these scans better than 120kVp-scans, even though we had to use a reduced dose ($CTDI_{vol}$) of 20.6 mGy for 90kVp scans instead of the conventional 27.2 mGy for 120kVp. The improved subjective scores were found for vascular enhancement, visibility of small arterial detail and, in patients with SAH, interference of subarachnoid blood. This is concordance with the results of Bahner et al. who showed improved vascular opacification at lowkVp in patients with intracranial vascular malformations who had been scanned with 80kVp and 120kVp during follow-up of radiation therapy[18]. In this study, mAs_{eff} level was also adjusted at the lowestkVp, resulting in an even lower $CTDI_{vol}$ compared to our study (13.5 mGy at 80kVp compared to 21.9 mGy at 120kVp).

Our clinical results seem to be in conflict with the findings of Ertl-Wagner et al.[17], who reported better image quality of cerebral CTA at higher kVp. The principal difference with our study is that Ertl-Wagner and co-workers chose not to adapt effective mAs settings when reducing tube voltage, which lead to an almost four-fold increase in radiation dose at the highest kVp setting. This led to a substantial noise reduction, which can explain the observed improved image quality at higher kVp.

Our results are in accordance with our phantom study, in which we could demonstrate that the SNR was substantially less at 90kVp than at 120kVp if the mAs_{eff} settings were kept constant. However, when comparing the SNR at identical dose ($CTDI_{vol}$ or $CTDI_{local}$), we found substantially higher SNR at 90kVp compared to the SNR at 120 or 140kVp. In fact, SNR^2 at 90kVp was 45% to 52% higher than at 120kVp. We therefore believe that this difference in study design; i.e. varying kVp at constant mAs_{eff} (Ertl Wagner) versus varying kVp at constant radiation dose (our study) explains the seemingly contradictory results between the two studies.

In our clinical study we found no difference between 90 and 120kVp regarding subjective scoring of venous contamination or image noise. The lack of difference in noise score probably has to do with the fact that we allowed readers to adapt window settings to the arterial enhancement: On average, 90kVp scans had better enhancement and therefore would require wider window settings. Such wider window settings, on the other hand, reduce the subjective appreciation of image noise[21].

We choose to calculate the SNR instead of CNR since PMMA is dependent for its attenuation on thekVp and thus incorporation of background attenuation would strongly influence CNR ratios in the phantom study. Also, background attenuation in patients can widely vary between liquor density, brain tissue and hemorrhage, thus

influencing CNR. We therefore also used the SNR to compare the phantom study with the clinical study.
Our study had limitations. First, scanning protocols could not be compared intra-individually in the same patients as it was judged unethical to scan each patient with both 120 and 90kVp. Second, for optimum comparison the CTA scans at 90kVp should have been performed at the same dose ($CTDI_{vol}$) as with 120kVp but tube limitations prevented this. Our results do however imply that equal or better results can be obtained even with a dose reduction by approximately 30%. However, it should be realized that these results, and especially the dose-noise relationship, are specific for CT images and not for conventional x-ray images.
Third, we were unable to determine how much sensitivity and specificity for detection of aneurysms would increase with 90kVp because we did not have angiography as an independent standard of reference available in all patients. Finally we did not study the effect of lowkVp settings in the presence of metallic material (vascular clips or coils), which could cause stronger streak artifacts.

Conclusion

The use of a lower tube voltage substantially improves SNR if radiation dose is kept constant. For evaluation of the circle of Willis in clinical patients this translates into superior image quality for 90kVp compared to 120kVp even if patient dose is reduced by approximately 30%. For this reason, we recommend lowkVp scanning with properly adjusted mAs for CTA of the circle of Willis in patients with acute subarachnoid hemorrhage or for screening patients with a positive family history for intracranial aneurysms.

References

1. Kato Y, Katada K, Hayakawa M, et al. Can 3D-CTA surpass DSA in diagnosis of cerebral aneurysm? Acta Neurochir 2001; 143:245-250.
2. Velthuis BK, Rinkel GJ, Ramos LM, et al. Subarachnoid hemorrhage: aneurysm detection and preoperative evaluation with CT angiography. Radiology 1998; 208:423-430.
3. Villablanca JP, Jahan R, Hooshi P, et al. Detection and characterization of very small cerebral aneurysms by using 2D and 3D helical CT angiography. AJNR 2002; 23:1187-1198.
4. Wintermark M, Uske A, Chalaron M, et al. Multislice computerized tomography angiography in the evaluation of intracranial aneurysms: a comparison with intraarterial digital subtraction angiography. J Neurosurg 2003; 98:828-836.
5. Velthuis BK, van Leeuwen MS, Witkamp TD, Ramos LM, Berkelbach van der Sprenkel JW, Rinkel GJ. Computerized tomography angiography in patients with subarachnoid hemorrhage: from aneurysm detection to treatment without conventional angiography. J Neurosurg 1999; 91:761-767.
6. Verro P, Tanenbaum LN, Borden NM, Sen S, Eshkar N. CT angiography in acute ischemic stroke: preliminary results. Stroke. 2002; 33:276-8.
7. Ruigrok YM, Rinkel GJ, Buskens E, Velthuis BK, van Gijn J. Perimesencephalic hemorrhage and CT angiography: A decision analysis. Stroke 2000; 31:2976-2983.
8. Brix G, Nagel HD, Stamm G, Veit R, Lechel U, Griebel J, Galanski M. Radiation exposure in multi-slice versus single-slice spiral CT: results of a nationwide survey. Eur Radiol. 2003; 13:1979-91.
9. Wintermark M, Maeder P, Verdun FR, et al. Using 80kVp versus 120kVp in perfusion CT measurement of regional cerebral blood flow. AJNR 2000; 21:1881-1884.
10. Sigal-Cinqualbre AB, Hennequin R, Abada HT, Chen X, Paul JF. Low-kilovoltage multislice chest CT in adults: feasibility and effect on image quality and iodine dose. Radiology 2004; 231:169-174.
11. Cohnen M, Fischer H, Hamacher J, Lins E, Kotter R, Modder U. CT of the head by use of reduced current and kilovoltage: relationship between image quality and dose reduction. AJNR 2000; 21:1654-1660.
12. Mullins ME, Lev MH, Bove P et al. Comparison of image quality between conventional and low-dose nonenhanced head CT. AJNR 2004; 25:533-538.
13. Farr RF, Allisy-Roberts PJ. Radiation physics. In: WB Saunders. Physics for medical imaging. 1st ed. London, Elsevier Science Limited, 2002; 19-22.
14. Zonneveld FW. Principles of computed tomography. In: Urban & Schwarzenberg. Computed tomography of the temporal bone and orbit. 1st ed. Munich. 1987; 12-13.
15. Zatz LM. The effect of thekVp level on EMI values. Selective imaging of various materials with differentkVp settings. Radiology 1976; 119:683-688.
16. Keller MR, Kessler RM, Brooks RA, Kirkland LR. Optimum energy for performing CT iodinated constrast studies. Br J Radiol 1980; 53:576-579.
17. Ertl-Wagner BB, Hoffmann RT, Bruning R, Herrmann K, Snyder B, Blume JD, Reiser MF. Multislice CT angiography of the brain at various kilovoltage settings. Radiology 2004; 231:528-535.
18. Bahner ML, Bengel A, Brix G, Zuna I, Kauczor HU, Delorme S. Improved vascular opacification in cerebral computed tomography angiography with 80kVp. Invest Radiol 2005: 40;229-34.
19. DeMarco JJ, Cagnon CH, Cody DD, et al. A Monte Carlo based method to estimate radiation dose from multidetector CT (MDCT): cylindrical and anthropomorphic phantoms. Phys Med Biol 2005 ;50:3989-4004.
20. Prokop M. Image Analysis. In: Prokop M, Galanski M. Computed tomography of the body, 1st ed. Stuttgart, Germany, Georg Thieme Verlag, 2003; pg143.
21. Husstedt H, Prokop M, Becker H. Window width as a dosage-relevant factor in high-contrast structures in CT. Rofo 1998;168:139-43.

Anatomic variations in the circle of Willis in patients with symptomatic carotid artery stenosis assessed with multislice CT angiography

Chapter Four

A Waaijer, MS van Leeuwen, HB van der Worp, HJM Verhagen, WPThM Mali, BK Velthuis. Anatomic variations in the circle of Willis in patients with symptomatic carotid artery stenosis assessed with multislice CT angiography.
Accepted for Cerebrovascular Disease.

Abstract

Purpose

To assess the presence of anterior and posterior collateral pathways in the circle of Willis in patients with symptomatic carotid artery stenosis (SCAS) and to compare this to patients without carotid artery stenosis.

Materials & Methods

Multislice CT angiography (CTA) was performed in 91 patients and 91 control subjects. Using consensus reading, two observers evaluated the presence and diameter of the anterior communicating artery (AcomA), the A1 segments of the anterior cerebral arteries, the posterior communicating arteries (PcomA) and the P1 segments of the posterior cerebral arteries. Anterior or posterior pathways were assumed to be present if diameter of continuous arterial segments was > 1mm; both A1 segments and AcomA anterior, and ipsilateral P1 segment and PcomA posterior. Comparison between patients and controls was performed using the Chi square test.

Results

In patients we found significantly more hypoplastic (<1mm) or invisible A1 segments (16 and 14 versus 4 and 1 respectively ($p<0.01$)). The AcomA was invisible in 4 patients versus 1 control. An isolated compromised anterior pathway and a combined compromised anterior and posterior pathway occurred more frequently in patients as compared to controls; 9 vs 1% ($p<0.01$) and 26 vs 4% ($p<0.01$).

Conclusion

A compromised anterior collateral pathway, usually combined with a compromised posterior pathway, occurs more frequently in patients with SCAS as compared to controls which suggests a relation between symptomatic carotid stenosis and an incomplete circle of Willis.

Introduction

In patients with symptomatic carotid artery stenosis (SCAS), reduction of blood flow in the stenotic carotid artery requires a compensatory increase in flow via other pathways to maintain sufficient perfusion of the affected vascular territory. The circle of Willis serves as an important collateral pathway and may allow supply of blood from the contralateral carotid artery or the basilar artery to the territory of the stenotic internal carotid artery[1-3]. The potential to develop these anterior and posterior collateral pathways depends on the continuity of the anterior and postero-lateral parts of the circle of Willis, respectively. Collateral flow via the circle of Willis can be provided anteriorly via the right and left precommunicating anterior cerebral arteries (A1 segments) and the anterior communicating artery (AcomA), and posteriorly via the ipsilateral posterior communicating artery (PcomA) and precommunicating posterior cerebral artery (P1 segment). Discontinuity of the circle in patients with SCAS is associated with a higher risk of transient ischemic attack (TIA) and ischemic stroke[2]. Substantial individual differences in the anatomy of the circle of Willis of healthy subjects have been described[4]. Studies of the prevalence of discontinuity in the circle of Willis in patients with SCAS have reached conflicting results. Early autopsy studies showed that the prevalence of absent or hypoplastic segments was increased in stroke patients as compared to normal subjects[5-7], while more recent non-invasive imaging studies showed no difference or even a decreased prevalence of these variants in brains of patients with TIA or ischemic stroke due to carotid disease[8, 9]. Multislice CT angiography provides consistent detailed anatomical depiction of the intracranial arteries in a single acquisition. Since recent data on the prevalence of discontinuity of the circle of Willis in patients with symptomatic carotid disease are sparse and conflicting, we aimed to assess the prevalence of anatomical variants of the circle of Willis which may hamper collateral supply in patients with SCAS using multislice CTA and compared this to patients without carotid stenosis.

Materials and Methods

Study Population

Patients

All patients were participants of the International Carotid Stenting Study (ICSS), a randomized controlled trial to compare carotid endarterectomy (CEA) and stent placement (www.cavatas.com). Inclusion in the ICSS was based primarily on the presence of a carotid artery stenosis >50% and a recent history of ipsilateral TIA, amaurosis fugax, or non-disabling stroke. Between September 2003 and June 2005, 103 consecutive patients were prospectively evaluated for inclusion in the present CTA study. The only additional exclusion criterion was a contra-indication for CTA, such as renal failure or contrast allergy. All patients were scanned between 2 weeks to 1 day before treatment. The medical ethics committee of our hospital had given approval for this study and written informed consent was obtained from all patients.

Patients without carotid stenosis (Controls)

Controls were retrospectively collected from our data collection system. All patients that had a multislice CT angiography for either the carotid arteries or the circle of Willis between September 2003 and December 2005 were selected. Both protocols include a non-contrast CT of the brain as well as imaging of the intracranial arteries. Patients without suspicion of stroke or TIA and with negative findings on CTA (no intra- or extracranial stenosis, aneurysm, dissection, thrombus or intracranial vascular malformation) were included. This resulted in 16 patients suspected of dissection, 8 patients suspected of traumatic dissection, 18 patients suspected of glomus tumor or vascular malformation, 10 patients suspected of sinus trombosis, 16 patients with a non-aneurysmal perimesencephalic hemorrhage, 16 patients with acute headache, and 7 patients screened because of familiar prevalence of aneurysms. Mean age of the controls was 52 years (range 26-88) and there were 55 men and 36 women included.

CT Angiography

CT angiography was performed using a 16- or a 40-slice scanner (MX 8000 IDT, or Brilliance-40, Philips Medical Systems, Cleveland, OH). Patients were scanned in supine position with the head tilted so that the jaw was parallel to the gantry in order to minimize dental artefacts. The scan range started 3cm under the vertex and ended below the aortic arch. Either 16x0.75 or 40x0.625mm collimation was used with a pitch between 0.77 and 0.85 and a rotation time of 0.42s. Overlapping sections were reconstructed of 1.0mm slice thickness (16-slice) or 0.9mm thickness (40-slice) at a reconstruction interval of 0.5mm and a field of view of 160mm, using 120kVp and 180 mAs, resulting in a volume CT dose index ($CTDI_{vol}$) of 13.2mGy. A slightly smoothing filter was applied. Controls were scanned either with the same protocol (for possible dissection and glomus tumor) or with a smaller range from vertebral body level C2 upwards (for possible aneurysm or sinus thrombosis). The sinus thrombosis protocol used a 8 second longer delay to ensure both arterial and venous enhancement. Scan delay was determined from a 40ml bolus injection (Ultravist 300, Schering, Berlin, Germany) followed by a 40ml saline chaser at 5ml/sec. CT angiography was performed after injection of 80ml of contrast material followed by a saline chaser bolus of 50ml, both injected at 5ml/s. The resulting images were sent to a dedicated CT workstation (Extended Brilliance Workspace, Philips, Cleveland, OH) for further evaluation. This workstation allows for interactive scrolling through the data set and adaptation of the viewing plane. Visualization was started with a 6-8mm sliding maximum intensity projection (MIP) slab parallel to the anterior skull base, providing an overview of the circle of Willis. Slab thickness and orientation were interactively adjusted to obtain optimal visualization of vascular details and final decisions were made on thinnest section images.

Assessment of patency of the circle of Willis

Seven arterial sections of the circle of Willis were evaluated in each patient: two A1 segments, the anterior communicating artery (AcomA), two P1 segments and the two posterior communicating arteries (PcomAs). For each segment it was noted whether it was visible and if so, the diameter was assessed and compared with other arteries.

Scoring of the anterior pathway was performed as follows: A1 segments could be not visible, hypoplastic (<1 mm), or normal (>1 mm). Subsequently, each pair of A1 segments was graded as symmetric or asymmetric, noting the diameter of the smallest A1 segment as not visible, hypoplastic, or less than 2/3 in diameter compared to the contralateral side. The AcomA could be not visible or present.

For the posterior pathway, P1 segments were evaluated in relation to the ipsilateral PcomA since both segments need to be sufficiently developed to allow collateral supply from the basilar artery to the ipsilateral carotid. Size of the P1 segment is also important for potential leptomeningeal collateral flow from the basilar artery to the MCA territory. P1 segments and PcomAs could be not visible, hypoplastic (<1 mm), or normal (≥1 mm). The P1-PcomA relationship was described as follows: normal [adult] configuration (P1> PcomA), subdivided in normal caliber PcomA (≥1 mm), hypoplastic PcomA (<1 mm), and invisible PcomA; transitional configuration (P1 = PcomA); and fetal (embryonic or dominant PcomA) configuration (PcomA>P1) subdivided in absent P1, P1<1 mm or P1≥1 mm. Examples of the circle configuration are shown in *Figure 1*.

Figure 1

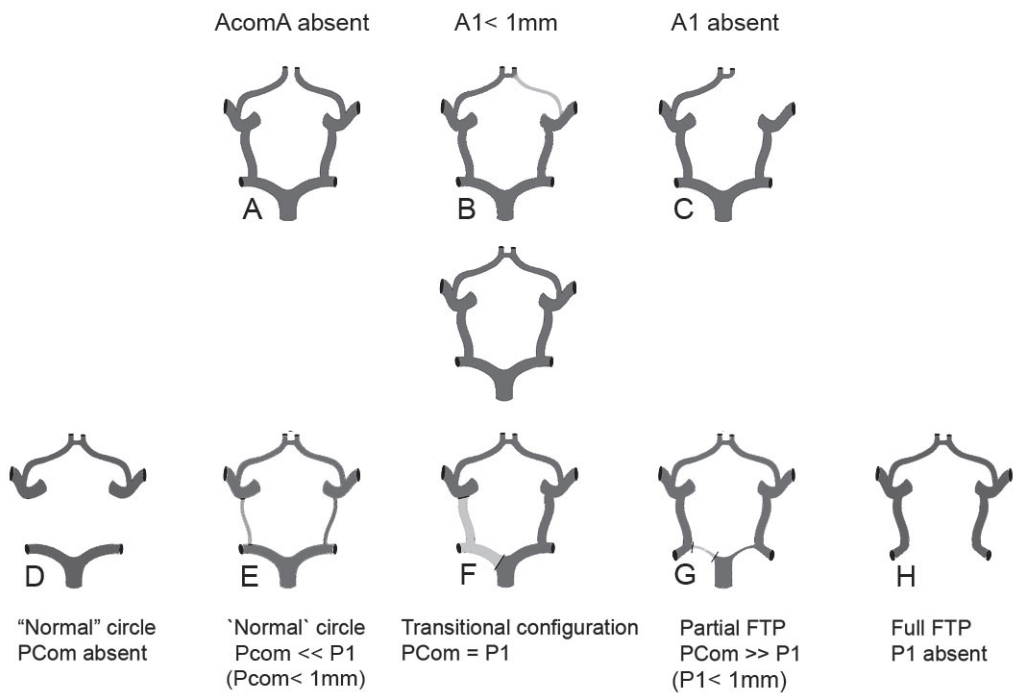

Examples of the circle of Willis. The middle circle represents the complete "normal" variant were all segments are > 1mm. The upper row shows the variations in the anterior part, while the lower row shows variations of the posterior part.

Analysis of the complete circle was performed with the aim to determine the collateral capacity for each circle in relation to the ipsilateral stenosis. Based on prior studies[4,10], a patent collateral pathway was assumed to require continuous arterial segments with diameters equal to or greater than 1 mm. We classified the circles into four types: 1) non-compromised collateral capacity: all anterior and ipsilateral posterior segments >1 mm; 2) compromised anterior pathway and non-compromised ipsilateral posterior pathway: one A1 <1 mm or invisible or invisible AcomA with all ipsilateral posterior segments ≥1 mm; 3) compromised posterior pathway and non-compromised anterior pathway: all anterior segments ≥1 mm, posterior ipsilateral PcomA or P1 segment <1 mm, and 4) both anterior and posterior compromised collateral pathways: one anterior segment <1 mm in combination with at least one posterior segment <1 mm. For the control group, the left P1 segment and the left PcomA were used as substitute for the ipsilateral side.

Data analysis

Studies were scored by two readers in consensus (A, B) and in case of doubt, consensus was reached after consultation of a third radiologist (C). The Chi square test was applied to calculate significance of differences between patients and controls, a p-value <0.05 was considered statistically significant (Statistical Software Package SPSS for Windows, version 12).

Results

Patients

Of the 103 patients included in the ICSS in our centre, nine patients were excluded for logistic reasons (lack of scan time (n=6) or elevated serum creatinine (n=3)). Consequently, CT angiography of the carotids and the intracranial vasculature was performed in the remaining 94 patients. Assessment of the circle of Willis failed in 3 patients due to movement artefacts or insufficient contrast enhancement. Consequently, 91 patients were included in the present study. Patient characteristics are shown in *Table 1*.

Anterior part of the circle

Table 2a shows the result of the analysis of the anterior part. In total, the anterior collateral pathway was compromised in 34 patients (36%) in whom the AcomA was invisible or one A1 segment was invisible or hypoplastic, compared to 6% in the control group (p<0.01).

Posterior part of the circle

In both patients and controls an adult configuration was most commonly observed (79% vs 85%, difference not significant), a fetal configuration was seen in 17% of patients and 14% controls (ns), while a transitional variant was only occasionally observed (4% vs 1%, ns). There were no significant differences in configuration between ipsilateral versus contralateral and right versus left side in patients and controls respectively.

Table 1 *Patient characteristics*

Age, years (mean ± SD (range))	67.5 ± 9.8 (43, 84)
Male: Female sex	60 : 31
Presenting event	
Amaurosis fugax	27 (30%)
TIA	49 (54%)
Ischemic stroke	40 (44%)
Carotid arteries	
Mean stenosis symptomatic side* (range)	82.6 ± 15.0% (45, 99)
Mean stenosis asymptomatic side* (range)	38.8 ± 30.0% (0, 100)
Left-sided symptomatic stenosis	38 (42%)
Contralateral stenosis >50%	16
Medical history	
Hypertension	49 (54%)
Diabetes mellitus	15 (16%)
Cardiac disease**	34 (37%)

** Measured on CTA.*

*** Including cardiac failure, previous coronary artery bypass graft, atrial fibrillation, or previous myocardial infarction.*

Table 2a *Anterior part of the circle*

	Patients		**Controls**	**p-value**
	(%) ipsilateral : contralateral			
AcomA (n=91)				
Not visible	4 (4)		1 (1)	n.s.
A1 (paired, n=91)				
Asymmetric	51 (56)		13 (14)	<0.01
smallest segment:				
Not visible	14 (15)	9 : 5	1 (1)	<0.01
Hypoplastic (<1 mm)	16 (17)	7 : 9	4 (4)	<0.01
<2 /3 contralateral	22 (24)	16 : 6	8 (9)	<0.01

In terms of compromise no significant difference was seen between the patients and controls; within the group of adult configuration the PcomA was >1 mm in 20% of patients and 21% of controls and in the group of fetal configurations the P1 was ≥1 mm in 54% and 56% respectively. The only difference with regard to the posterior circulation was finding that patients showed significantly more invisible segments, while controls showed more hypoplastic segments. Subdivision for the ipsilateral side is shown in *Table 2b*.

Table 2b *Posterior part of the circle (for each side, n=182) (%)*

Configuration	Patients		Controls		p-value
	ipsilateral:	contralateral		R:L	
Adult (P1 > PcomA)	144 (79)	155 (85)			ns
PcomA invisible	90 (63)	43 : 47	48 (31)	25 : 23	<0.01
PcomA <1 mm	25 (17)	12 : 13	75 (48)	38 : 37	<0.01
PcomA ≥1 mm	29 (20)	17 : 12	32 (21)	16 : 16	ns
Transitional (P1=PcomA)	8 (4)	6 : 2	2 (1)		=0.054
Fetal (PcomA > P1)	30 (17)		25 (14)		ns
P1 invisible	12(40)	6 : 6	3 (12)	1 : 2	<0.01
P1 <1 mm	1 (6)	1 : 0	8 (32)	4 : 4	<0.01
P1 ≥1 mm	17 (54)	7 : 10	14 (56)	8 : 6	ns

Table 2c *Complete circle analysis (%)*

	Patients	Controls	p-value
Anterior and posterior			
non-compromised collateral capacity	20 (22)	24 (26)	ns
Anterior compromised, posterior non-compromised	8 (9)	1 (1)	<0.01
Posterior compromised, anterior non-compromised			
PcomA or P1 non-visible	30 (33)	25 (27)	ns
PcomA or P1< 1mm	9 (10)	37 (40)	<0.01
Both anterior and posterior			
compromised collateral capacity	24 (26)	4 (4)	<0.01

For the analysis of collateral capacity the posterior circulation was assessed on the ipsilateral side. For analysis of the posterior circulation in the control group we used the left side.

Combined analysis

In the combined analysis a type 1, non-compromised circle of Willis configuration was found in 20 patients (22%) compared to 24 controls (26%, not significant difference) while type 4, compromised anterior and posterior pathway was present in 24 patients (26%) compared to only 4 controls (4%, p<0.01). Patients showed more isolated compromised anterior circulation (9 vs 1%, p<0.01) but less frequently an isolated compromised posterior circulation (39 vs 67%, p<0.01)(*Table 2c*). Examples are shown in *Figure 2a-d*

Figure 2

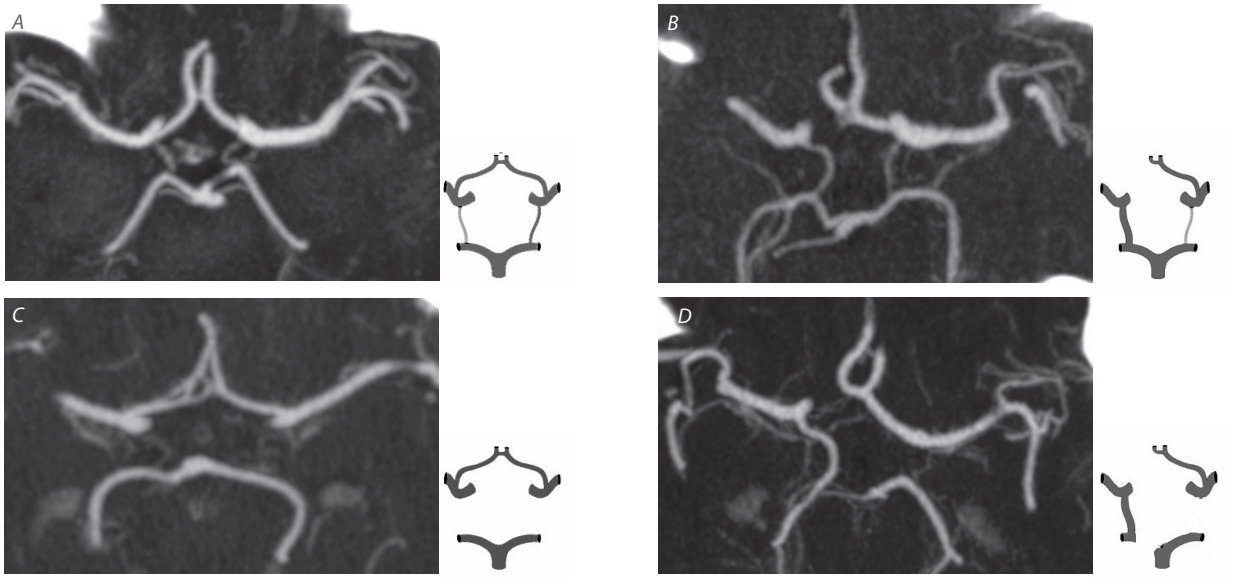

Thick slab MIP (10 mm) of the circle showing four different types of the circle of Willis, according to the presence of collateral capacity.
Figure a represents a "normal" circle. A patient from the control group is shown, where on both sides a small PcomA is visible in combination with a normal AcomA, comparable to image E from figure 1.
In b the right A1 segment is missing on the ipsilateral side in a patient with symptomatic stenosis, comparable to image C in figure 1, resulting in a compromised anterior pathway. On the contralateral side a hypoplastic PcomA is present as is shown in image E from figure 1.
In c both PcomA's are missing in a patient with symptomatic stenosis, comparable to image D in figure 1, resulting in compromised flow by the posterior pathway (and there is a web-like AcomA).
In d a patient with symptomatic stenosis is shown, where an absent A1 segment is present in combination with a fetal variant of the PcomA without a P1 segment on the ipsilateral side, a combination of image C and H from figure 1. This results in a complete compromise of ipsilateral collateral flow.

Discussion

The major finding of this study is that we saw a significant higher prevalence of hypoplastic or absent segments in the anterior part of the circle of Willis in patients with symptomatic carotid artery stenosis. A compromised anterior pathway occurred significantly more in patients (35%, isolated in 9% and combined with a compromised posterior pathway in 26%) compared to 1% and 4% in the controls respectively. To our knowledge this is the first study on circle of Willis morphology evaluating only patients with high grade symptomatic stenosis, i.e. the category of patients who have most benefit of treatment according to the North American Symptomatic Carotid Endarterectomy Trial and European Carotid Surgery Trial (NASCET and ECST). We used multislice CTA since this technique is increasingly being used in the evaluation of carotid artery stenosis as well as acute stroke, and may provide additional information when different treatment strategies like surgery or stent placement are considered.

Knowledge of the circle of Willis is of importance since the prevalence of adequate collateral supply via the circle of Willis is associated with a reduced risk of recurrent stroke[2], smaller infarct size[18], normal response to CO_2 reactivity tests[19], and a reduced occurrence of ischemia during clamping of the carotid artery[20]. Likewise, a significant difference in the prevalence of normal circles between patients with and without cerebral infarction has been shown at autopsy (22% versus 52%, respectively)[6]. In addition, asymmetry of the A1 segments (defined as "marked caliber difference") was significantly more frequent in patients with than without infarction (28 versus 14%), and cerebral infarction was most frequently seen when asymmetric A1 segments were present in combination with an ipsilateral fetal variant of the posterior circulation (93%), compared to the presence of a fetal variant only (30%). These findings indicate that a compromised collateral supply by the circle of Willis is associated with an increased occurrence of cerebral infarction.

In the present study, a cut-off at <1 mm for hypoplasia was chosen based on literature reports of autopsy studies and flow models, which indicate that significant flow reduction can be expected below this diameter[4,7,10,21]. A difference of 1/3 in diameter compared to the contralateral segment was chosen for "marked" asymmetry since this equals a cross-sectional area reduction of more than 50%, consistent with substantial impediment to blood flow[21].

Our finding of a high number of absent and hypoplastic segments in the anterior part of the circle, is in accordance with a recent study, comparing 21 patients with SCAS to patients with asymptomatic carotid stenosis and to healthy subjects, who found significantly larger diameters and more collateral flow in the anterior part of the circle in patients with asymptomatic carotid stenosis as compared to symptomatic patients[15].
Hypoplasia or absence of the A1 segment is uncommon. Autopsy studies revealed that hypoplastic A1 segments were present in 2 to 12% of normal brains[4,14], while absence was reported in only 2 to 4%[12,14]. Although part of the non-visualized A1 segments in our study will probably be hypoplastic segments, below the resolution

level of CT angiography, the prevalence of 15% non-visualized and 17% hypoplastic A1 segments in this study is high compared to the normal population. While the prevalence of any difference in diameter between both A1 segments may be as high as 78%[13], apparent asymmetry of visualized A1 segments was substantially more frequent in our study (56%) than in earlier studies of adult brains (10 to 21%)[13,14]. This finding may bear relevance to previous suggestions that the anterior pathway plays an important role in the prevention of cerebral infarction in the presence of carotid artery stenosis[15-17].

For the posterior circulation the most important anatomical variant is the presence of a fetal configuration, which, in the presence of a hypoplastic or absent P1 segment, precludes collateral supply from the basilar artery to the carotid territory. In patients with an adult configuration and an invisible or hypoplastic PcomA the collateral circulation will also be jeopardized, and this configuration is a risk factor for cerebral ischemia in patients with carotid artery occlusion[10]. In the current study, there was no significant difference in the number of fetal variant between patients and controls.

Although the prevalence of a compromised posterior pathway due to any invisible or hypoplastic PcomA segment was not significantly different between patients and controls, we did observe more absent PcomAs in the patient group and more hypoplastic segments in the control group. This was also true for the P1 segments that were more often not visualized in the patient group. Again, a substantial percentage of the non-visualized PcomAs in this study may be hypoplastic vessels, smaller than the resolution of the CTA-scanner, as in autopsy studies absence is found in only 0.6 to 2%[4,7,14]. One can hypothesize that hypoplastic vessels in control patients have the potential to fulfil a role if required and that patients have fewer functional posterior segments. Further studies on asymptomatic patients will be performed to see whether these patients indeed have more >1mm PcomAs that function as collateral.

Other recent articles report conflicting findings; in some studies a complete circle was more often present in patients as compared to controls[8,9] while others reported that the absence of collateral pathways in symptomatic patients was associated with increased risk of infarction[16,17] or that no difference in circle morphology between patients with symptomatic and asymptomatic carotid stenosis existed[22,23]. Part of this controversy may have been caused by grouping asymptomatic patients, carotid occlusions, and patients with bilateral disease. In our population a small group (18 patients) suffered from bilateral disease and no significant differences were seen if these patients were left out of the analysis. Also, time-of-flight magnetic resonance angiography (MRA)[24] may be less sensitive for the detection of small vessels since visualisation is based on the presence of flow, which may be marginal in small vessel segments.

Other imaging techniques, such as digital subtraction angiography, transcranial doppler, or 2D phase contrast or contrast-enhanced MRI, have also been used to evaluate the circle of Willis. Each of these techniques has its own disadvantages. Selective visualization of one artery may hinder a fair interpretation in DSA due to the injection pressure; absence of a temporal window hampers TCD use in approximately 25% of patients; and flow-based MRA techniques may not visualize non-functional but patent arterial segments. Multi-detector row CT scanning allows consistent imaging of intra-cerebral arteries together with the carotid and vertebral arteries and thereby represents an excellent tool for imaging the anatomy of circle of Willis[25].

Our study has some limitations. We only included patients with carotid stenosis who were eligible for carotid revascularization by CEA or stenting. In our center, patients with a severe disability due to large infarcts are generally not subjected to carotid desobstruction. This may have resulted in an underestimation of the number of patients with compromised collateral capacity. However, age, symptoms, and severity of stenosis of our patients were comparable to those included in large randomized trials of CEA[26]. In addition, we have not tested the reproducibility of measurements of diameters in the circle of Willis, but previous studies have shown that visualization and quantification of the segments of the circle can be reliably performed using CTA in comparison to DSA[27, 28].

To our knowledge this is the first study on patients with symptomatic carotid artery stenosis to assess anatomical variants in the circle of Willis using multislice CT angiography. Using a conventional definition of hypoplasia we found significantly more incompletely developed segments in the anterior pathway in our patients compared to control subjects. Often the posterior pathway was also compromised in these patients. These findings are in line with previous studies which indicate that a compromised collateral circulation via the circle of Willis may play an important role in the development of symptoms in patients with SCAS.

References

1. Powers WJ et al. The effect of hemodynamically significant carotid artery disease on the hemodynamic status of the cerebral circulation. Ann Int Med 1987; 106:27-35.
2. Henderson RD, Eliasziw M, Fox AJ, Rothwell PM, Barnett HJ. Angiographically defined collateral circulation and risk of stroke in patients with severe carotid artery stenosis. North American Symptomatic Carotid Endarterectomy Trial [NASCET] Group. Stroke 2000; 31:128-32.
3. Barnett HJ, Meldrum HE. Endarterectomy for carotid stenosis: new approaches in patient selection. Cerebrovasc Dis 2001; 11 Suppl 1:105-11.
4. Alpers BJ, Berry RG, Paddison RM. Anatomical studies of the circle of Willis in normal brain. AMA Arch Neurol Psychiatry 1959; 81:409-18.
5. Alpers BJ, Berry RG. Circle of Willis in cerebral vascular disorders. The anatomical structure. Arch Neurol 1963; 8:398-402.
6. Kameyama M, Okinaka SH. Collateral circulation of the brain with special reference to atherosclerosis of the major cervial and cerebral arteries. Neurology 1963; 13:279-86.
7. Battacharji SK, Hutchinson EC, McCall AJ. The Circle of Willis--the incidence of developmental abnormalities in normal and infarcted brains. Brain 1967; 90:747-58.
8. Hedera P, Bujdakova J, Traubner P, Pancak J. Stroke risk factors and development of collateral flow in carotid occlusive disease. Acta Neurol Scand. 1998; 98:182-6.
9. Hartkamp MJ, van der Grond J, van Everdingen KJ, Hillen B, Mali WPThM. Circle of Willis collateral flow investigated by magnetic resonance angiography. Stroke 1999; 30:2671-8.
10. Schomer DF, Marks MP, Steinberg GK, Johnstone IM, Boothroyd DB, Ross MR, Pelc NJ, Enzmann DR. The anatomy of the posterior communicating artery as a risk factor for ischemic cerebral infarction. N Engl J Med 1994; 330:1565-70.
11. Lazorthes G. Gouaze A. The Arterial Circle of the brain [circulus arteriosus cerebri]. Anatomica Clinicia 1, 1979; 241-257.
12. Lippert H, Pabst R. Arterial variations in man. Classification and frequency. J.F. Bergmann, Verlag Munchen. 1985; 92-93.
13. Van Overbeeke JJ. The development of the variations of the human basal cerebral arteries. An ontogenetic study. Thesis. University of Utrecht, Utrecht, The Netherlands, 1991.
14. Huber P, Krayenbuhl H. Cerebral angiography, 2nd ed. Stuttgart, Thieme-Stratton, 1982. [pg 85]
15. Hendrikse J, Eikelboom BC, van der Grond J.Magnetic resonance angiography of collateral compensation in asymptomatic and symptomatic internal carotid artery stenosis. J Vasc Surg 2002; 36:799-805.
16. Hoksbergen AW, Legemate DA, Csiba L, Csati G, Siro P, Fulesdi B. Absent collateral function of the circle of Willis as risk factor for ischemic stroke. Cerebrovasc Dis 2003; 16:191-8.
17. Miralles M, Dolz JL, Cotillas J, Aldoma J, Santiso MA, Gimenez A et al. The role of the circle of Willis in carotid occlusion: assessment with phase contrast MR angiography and transcranial duplex. Eur J Vasc Endovasc Surg 1995; 10:424-30.
18. Rodda RA. The arterial patterns associated with internal carotid disease and cerebral infarcts. Stroke. 1986; 17:69-75.
19. Norrving B, Nilsson B, Risberg J. rCBF in patients with carotid occlusion. Resting and hypercapnic flow related to collateral pattern. Stroke 1982; 13:155-62.
20. Rutgers DR, Blankensteijn JD, van der Grond J. Preoperative MRA flow quantification in CEA patients: flow differences between patients who develop cerebral ischemia and patients who do not develop cerebral ischemia during cross-clamping of the carotid artery. Stroke 2000; 31:3021-8.
21. Cassot F, Vergeur V, Bossuet P, Hillen B, Zagzoule M, Marc-Vergnes JP. Effects of anterior communicating artery diameter on cerebral hemodynamics in internal carotid artery disease. A model study. Circulation 1995; 92:3122-31.
22. Kluytmans M, van der Grond J, van Everdingen KJ, Klijn CJ, Kappelle LJ, Viergever MA. Cerebral hemodynamics in relation to patterns of collateral flow. Stroke 1999; 30:1432-9.

23. Lee JH, Choi CG, Kim do K, Kim GE, Lee HK, Suh DC. Relationship between circle of Willis morphology on 3D time-of-flight MR angiograms and transient ischemia during vascular clamping of the internal carotid artery during carotid endarterectomy. AJNR 2004; 25:558-64.
24. Krabbe-Hartkamp MJ, van der Grond J, de Leeuw FE, de Groot JC, Algra A, Hillen B et al. Circle of Willis: morphologic variation on three-dimensional time-of-flight MR angiograms. Radiology 1998; 207:103-11.
25. van der Lugt A, Buter TC, Govaere F, Siepman DA, Tanghe HL, Dippel DW. Accuracy of CT angiography in the assessment of a fetal origin of the posterior cerebral artery. Eur Radiol. 2004;14:1627-33.
26. NASCET collaborators. Beneficial effect of carotid endarterectomy in symptomatic patients with high grade carotid stenosis. N Engl J Med 1991; 325:445-53.
27. Wintermark M, Uske A, Chalaron M, Regli L, Maeder P, Meuli R et al. Multi-detector row computerized tomography angiography in the evaluation of intracranial aneurysms: a comparison with intraarterial digital subtraction angiography. J Neurosurg 2003; 98:828-36.
28. Velthuis BK, van Leeuwen MS, Witkamp TD, Ramos LM, Berkelbach van der Sprenkel JW, Rinkel GJ. Surgical anatomy of the cerebral arteries in patients with subarachnoid hemorrhage: comparison of computerized tomography angiography and digital subtraction angiography. J Neurosurg 2001; 95:206-12.

Grading of Carotid Artery Stenosis with Multislice CT Angiography: Visual Estimation or Measurements?

Chapter Five

A Waaijer, MS van Leeuwen, TH Lo, FJ Beek, J Kardux, WB Velthuis, M Prokop. Grading of Carotid Artery Stenosis with Multidetector CT Angiography: Visual Estimation or Measurements? In revision for Radiology

Abstract

Purpose:

To assess the optimum method for grading of carotid artery stenosis with CTA we compared visual estimation to caliper measurements in patients with carotid artery disease, and determined inter-observer variability as well as accuracy relative to DSA as the reference standard.

Materials & Methods:

We included 46 patients with symptomatic carotid stenosis in whom CTA and selective catheter angiography of 55 carotids were available. For stenosis quantification by CTA we compared visual estimation using 10% intervals (1) to caliper measurements using subjectively optimized wide window settings (2) or predefined contrast-dependent narrow window settings (3). Measurements were independently performed by two radiologists and two residents of varying experience with CTA. The average degree of stenosis obtained from independent measurements by two interventional radiologists on DSA served as standard of reference. To determine accuracy and inter-observer variability, we calculated Pearson correlation coefficients, performed a Bland-Altman analysis and calculated mean difference (bias) and standard deviation of differences (SDD).

Results:

Correlation between CTA and DSA was best for estimation, method 1 ($r=0.872$-0.919) and worst for method 3 ($r=0.702$-0.845) for all four observers ($p<0.05$). Compared to DSA, method 1 led to an overestimation (bias 7.3-9.4%) while method 3 led to underestimation of the degree of stenosis (bias -5.8 to–2.4%). For all observers the measurement variability (SDD) increased from method 1 to methods 2 or 3. Correlation between visual estimation and DSA measurements was not significantly different from the correlation between two experienced observers for DSA.

Conclusion:

For CTA of carotid arteries, stenosis grading based on visual estimation provides better correlation with grading by DSA and lower inter-observer variability compared to stenosis grading based on caliper measurements.

Introduction

Recent investigations have shown that the incidence of stroke and transient ischemic attacks is exceeding the incidence of coronary heart disease[1]. Both carotid endarterectomy and carotid artery stenting are performed to reduce the risk of recurrent stroke and transient ischemic attack[2,3]. Accurate measurements of the degree of stenosis are important because higher grades of carotid artery stenosis are associated with an increased risk of stroke. Moreover, the degree of stenosis together with stenosis-related symptoms will determine how much a patient might profit from carotid endarterectomy or stent placement[3,4]. Based on the results of the North American Symptomatic Endarterectomy Trial (NASCET), only discrimination between 50-69% and 70-99% stenosis was considered to be important. However, more recent studies made use of different cut-off values for patient selection, using stenosis degree of 50%, 60%, 70% and 80% dependent on the presence of symptoms and co-morbidity[2,4-6].

While stenosis grading was primarily based on intra-arterial digital subtraction angiography (DSA), this technique has gradually been replaced by less invasive techniques such as duplex ultrasound, magnetic resonance angiography (MRA) and computed tomographic angiography (CTA). With the introduction of multislice scanning, CTA has become faster, easier to use and has further gained in spatial resolution[7]. In addition CTA of the carotids and intracerebral arteries has been advocated as part of the workup of patients with acute stroke[8].

Stenosis grading on digital subtraction angiography (DSA) is most commonly based on the NASCET criteria[9]. Stenosis grading by cross-sectional techniques such as MRA or CTA can be based on visual estimation or caliper measurements either on the source data or on images that are processed to resemble angiographic projections, such as maximum intensity projections (MIP), multiplanar reformations (MPR) or curved planar reformations (CPR)[10-13]. Despite the good overview that these processed images can provide, axial images have been shown to be most accurate for CTA measurements[13-17].

Cross-sectional techniques, in general, suffer from a reduced spatial resolution compared to angiography. This is especially evident when trying to precisely define the borders of a vessel, in particular if this vessel is small or stenosed. Because of this lack of a well-defined border, placing calipers for digital measurements may be less precise than usually assumed. In an effort to avoid these blurred vessel edges and increase precision, contrast-dependent window settings have been suggested for CTA[18,19], but these have not been tested in clinical practice where very high degrees of stenosis and calcified stenoses are present. Because of the potential limitations of caliper measurements, we hypothesize that visual estimation may actually perform better than assumed.

To assess the optimum method for grading of carotid artery stenosis with CTA we compared visual estimation to caliper measurements in patients with carotid artery disease, and determined their inter-observer variability as well as their accuracy relative to DSA as the reference standard.

Materials and Methods

Study Population

Between September 2003 and August 2005 48 consecutive patients were included in this prospective diagnostic study. All patients had a more than 50% symptomatic carotid artery stenosis diagnosed by ultrasound eventually in combination with MRA, and had been scheduled for DSA and stent placement because of participation in the ICSS trial (www.cavatas.com, registered under number ISRCTN25337470). Carotid multislice CTA was performed within two weeks of DSA. We included all carotid arteries for further evaluation in which there were at least two DSA projections available for comparison. The ICSS trial and the CTA study were performed with institutional review board approval. All patients had given written informed consent before entering the study.
One patient was excluded because of renal failure and one patient had to be excluded because of a technical failure of contrast injection during CTA. In the remaining 46 patients, correlation of CTA with at least two diagnostic DSA series was available for 55 carotid arteries. The group of patients included 29 males and 17 females with a mean age of 68 years (range, 44 to 84 years). Symptoms were stroke in 23 patients, transient ischemic attack in 20 patients and amaurosis fugax in 14 patients. Eleven patients had two or more symptoms.

CT Angiography

CT angiography was performed using a 16-slice scanner (MX 8000 IDT, Philips Medical Systems, Cleveland, OH) in 37 patients, a 40-slice scanner in 8 patients and a 64-slice scanner in 3 patients (Brilliance-40 and Brilliance-64, Philips Medical Systems, Cleveland, OH). Patients were scanned in supine position with the head tilted so that the mandible was perpendicular to the table in order to minimize dental artifacts. The scan range started 3 cm under the vertex and ended just below the aortic arch. We used either 16x0.75 mm collimation or 40x0.625 mm or 64x0.625 mm collimation with a pitch between 0.77 and 0.85 (dependent on the scanner options) and a rotation time of 0.42 s. In order to keep the differences between scanners as small as possible we reconstructed overlapping sections of 1.0 mm slice thickness (16 slice) or 0.9 mm thickness (40 and 64 slice) at a reconstruction interval of 0.5 mm and a field of view of 160 mm. A slightly smoothing filter was applied (filter B) on all scanners. We employed 120 kVp tube voltage and 180 mAs (effective) with both scanners.
Scanning was performed after injection of 80 ml of contrast material (Ultravist 300, Schering, Berlin, Germany) at 5 ml/s followed by a saline chaser bolus of 50 ml injected at the same flow rate. The scan delay was determined from injection of a bolus of 40 ml contrast material that was used for a brain perfusion study.
The resulting images were sent to a dedicated CT workstation (Extended Brilliance Workspace, software version 2.2, Phillips Medical Systems, Cleveland, OH) for further evaluation.

Digital Subtraction Angiography

Intra-arterial DSA was performed on a Philips Integris V3000 angiographic unit (Philips Medical Systems, Best, The Netherlands). A 5F catheter was introduced using the Seldinger technique and was selectively positioned in one or both common carotid arteries. At least two projections (postero-anterior and lateral) were acquired from each

carotid artery. For patients undergoing stent placement, frequently only the symptomatic side was selectively catheterized to keep intervention times low. For each projection 6 ml of contrast material (Ultravist 300, Schering, Berlin, Germany) was injected at a flow rate of 3ml/s.

Grading of Carotid Stenosis

Two radiologists with a long experience in reading CTA studies, and two radiology residents (observer O3 at the end of his residency-period and observer O4 at the beginning of his residency period) were asked to determine the degree of carotid artery stenosis on CT angiography using three different methods (*Figure 1*). Every observer was blinded to clinical information. All evaluations were performed interactively on the CT workstation and were based on the NASCET criteria[9]: degree of stenosis = (1- minimal residual lumen diameter/distal lumen diameter) x100%.

Figure 1 *Comparison of DSA (a) and CTA (b-f) of a high grade carotid artery stenosis. On DSA two observers performed measurements with calipers according to the NASCET criteria. Visual estimation of the degree of stenosis on CTA (in 10% steps) was performed by four observers that interactively scrolled through multiplanar reformation adapted to the carotid anatomy (here: sagittal reconstruction (b)). Caliper measurements were performed on transverse sections perpendicular to the central lumen line of the internal carotid artery. The luminal diameter in the region of the stenosis (c,e) was related to a distal reference diameter (d,f). This was done using individually adapted wide window settings (here: W/L = 600/150) and using the predefined contrast-dependent window settings (here: W/L: 98/163). On DSA the two observers measured a 82 and 88% stenosis, respectively. Visual estimation on CTA yielded a degree of stenosis between 75 and 95%. Caliper measurements using a wide window setting resulted in 58-83% stenosis while caliper measurements with the predefined window setting resulted in 69-81% stenosis.*

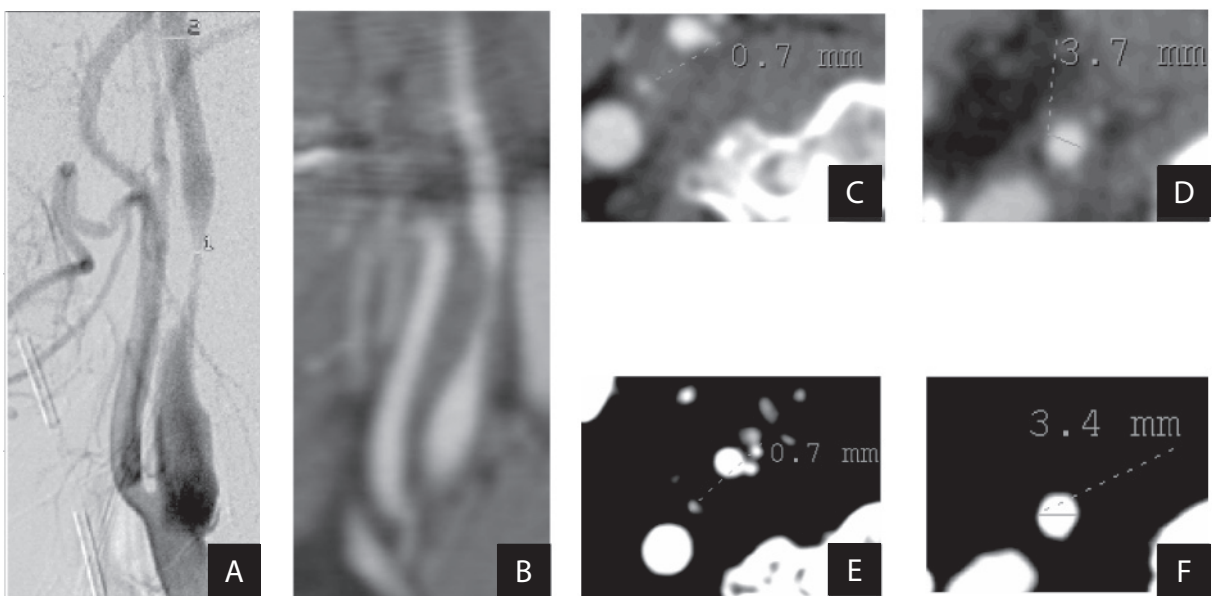

In case the observers did not consider it possible to grade the stenosis using a specific grading technique, they were asked to state the reason for it. For each method we determined the number of cases in which grading was not considered possible.

Method 1 was visual estimation (CTA_{VE}) of the degree of stenosis based on interactive reformations perpendicular and parallel to the internal carotid artery. Visual estimation was performed interactively on the CT workstation. This workstation allows for interactively scrolling through the data set in a cine-like display and adapting the view plane interactively so as to be perpendicular to the vessel axis or parallel to the carotid bifurcation. The observers were asked to adapt the window setting so that calcifications in the region of stenosis would not be rendered completely 'white' and the background soft tissue would not be rendered completely 'black', starting with a wide window typically at a width/level of 600/150. They were free to interactively adapt the sectional plane to optimally display the region of maximum stenosis as well as a distal reference segment. They were asked to assign the degree of luminal stenosis to one of the 11 following categories: 0-9%, 10-19%, …, 90-99%, 100% (= occlusion). For further analysis of visual estimation data, these categories were substituted by the median of each range, i.e. 5%, 15%, …, 95%, 100%.

The other two methods were based on measurements using the caliper function of the workstation on transverse cuts perpendicular on the central lumen line. This central lumen line was semi-automatically acquired using the "Advanced Vessel Analysis" program (Phillips Medical Systems, Cleveland, OH) on the CT workstation. Care was taken to manually adapt the central lumen line whenever necessary so that it avoided crossing calcified plaques. For determining the location of the stenotic segment and the distal reference segment for further measurements according to the NASCET criteria, the observers used interactive window settings as described for method 1. Each observer could freely define the level of the cut plane he deemed most appropriate for measuring the stenosis and the distal reference segment. All observers used equal magnification (4 cm display field of view on a 4-on-1 monitor subdivision).

Method 2 was based on caliper measurements using a wide window setting (CTA_{WW}) as described for method 1. This window setting could be individually adapted by the observer if deemed appropriate.

Method 3 was based on the predefined window settings (CTA_{PW}) proposed by Liu et al[16]. Using phantom experiments in which they varied luminal contrast, degree of stenosis and window/level settings, they suggested optimum window/level settings based on the luminal contrast enhancement in the carotid arteries. In their article eight categories of arterial enhancement were selected and appropriate narrow window settings are given for each category. Therefore, we determined the individual CT numbers by drawing a ROI of 10 mm^2 in the centre of the common carotid artery just proximal to the carotid bifurcation and determined from Liu's publication which preset window settings to use for measuring the diameter of the carotid artery at the level of the stenosis and in the distal reference segment. Two experienced interventional radiologists performed all diameter measurements on DSA images using calipers. They could choose image enlargement at the viewing workstation according their personal preference. They chose the projection with maximum stenosis and determined the degree of stenosis using the NASCET criteria[9]. If the degree of stenosis could not be measured due to severe distal collapse, the observers assigned a 95% degree of stenosis.

Statistical Analysis

The mean of the two stenosis measurements on DSA served as a reference standard for CTA. If the degree of stenosis could not be measured due to severe distal collapse, these measurements were excluded from analysis of caliper measurements on CTA (methods 2 and 3).

We assessed inter-observer variability for the two experienced interventional radiologists for DSA as well as for the two most experienced observers for CTA. For assessment of inter-observer variability, Pearson's correlation coefficient was calculated and a Bland-Altman analysis was applied[20]: we determined the mean difference between pairs of repeated stenosis gradings to assess bias and calculated the standard deviation of the differences (SDD) to assess variability. Upper and lower limits of agreement (LoA; 95% confidence interval for two repeated measurements) were calculated from the mean difference ±1.96 x SDD.

For determining the accuracy of the various CTA measures for each observer relative to the grading of carotid stenoses with DSA, we also calculated Pearson's correlation coefficient and used a normalized Bland-Altman analysis in which the mean of the two DSA measurements served as the standard of reference. We calculated the mean difference and SDD for each method and each observer relative to DSA measurements. For each observer, we tested the significance of difference between the various Pearson correlation coefficients (for correlation between each CTA grading technique and DSA measurements) using a Z-test[21]. For each observer separately, significance of differences between the SDDs of three methods was tested with Levene's test for homogeneity of variances (Statistical Software Package SPSS for Windows, version 12).

A Bland-Altman analysis of subgroups of stenoses (0-50%, 50-69% and 70-99%) was performed in order to determine whether the amount of over- or under-estimation of stenoses with CTA depended on the degree of stenosis. For this purpose, the mean of the 4 observers was set in relation to the mean of the two stenosis measurements on DSA. Bias and SDD were separately analyzed for the three groups of stenoses (0-50%, 50-69% and 70-99%).

Results

Standard of Reference

Stenosis grading with DSA revealed a mean degree of stenosis of 76% (range, 46% to 100%) on the symptomatic side (n=46) and 34% (range, 0% to 82%) on the asymptomatic side (n=9).

Carotid Enhancement

The mean common carotid enhancement on CTA was 343 HU (range 207 to 501 HU) with a standard deviation of 89 HU.

Carotid Evaluability

With DSA the exact degree of stenosis could not be measured in two cases because of severe narrowing of the distal lumen and extensive calcifications. In these cases a 95% stenosis was assigned.

All observers could use visual estimation (method 1) for grading every carotid artery included in the study. With method 2 (caliper measurements using a wide window setting), observer 1 could not assess the stenosis degree in 4 cases, observer 2 in 5, observer 3 in 3 and observer 4 in 7 cases. On average, this amounted to 12% of carotid arteries. Reasons given for non-evaluability were the presence of distal collapse (n = 8), calcifications (n = 5) or high-grade stenosis resulting in reduction of intra-luminal contrast enhancement (n =6). With method 3 (caliper measurements using a predefined window setting), the number of non-evaluable segments was 9, 12, 13 and 5 cases for observers 1-4, respectively (on average 24% of carotid arteries). For this method, the main reasons for non-evaluability were calcifications that could not be differentiated from lumen using the predefined window settings (n = 19), or because the stenosis was so severe that the stenotic lumen was not visualized using the predefined window settings (n = 8). Distal collapse was named as a reason in 12 cases. *Figures 2 and 3* provide examples for high-grade and calcified stenoses that could not be evaluated using the predefined window setting.

Figure 2 *Example of a high-grade stenosis that cannot be evaluated using the predefined window (W/L: 142/ 238) because the lumen is no longer visible at this window setting (b). Using the wide window setting an 81-92 % stenosis was measured by the four observers.*

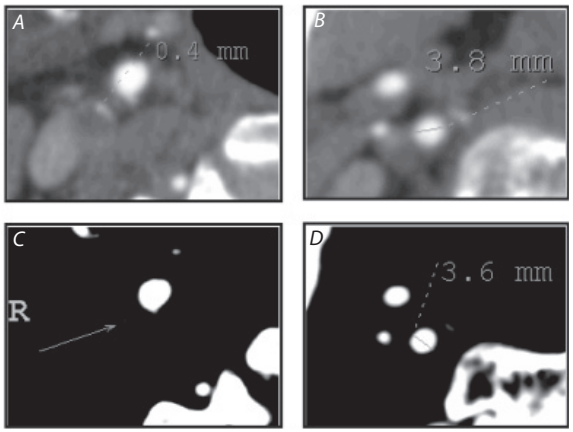

Figure 3 *Example of a calcified plaque that cannot be evaluated using the predefined window (W/L: 83/138) because lumen and plaque can no longer be discriminated (b). Using the wide window setting a 62-86% stenosis was measured by the four observers.*

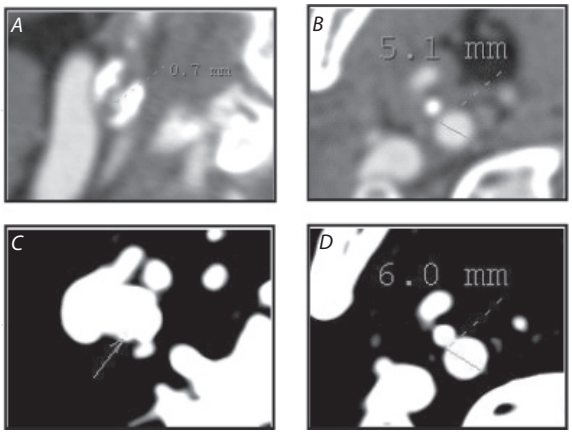

Inter-observer Variability

The correlation between the results of the first and the second observer for DSA as well as between the two most experienced observers for CTA is summarized in *Table 1*. A scatter plot for the DSA measurements is shown in *Figure 4*. We found higher inter-observer correlation for CTA using visual estimation or caliper measurements using predefined window settings than for DSA but this difference was not significant (p=0.2061 and p=0.4641 respectively). Inter-observer correlation for caliper measurements using wide window settings was significantly lower than with the other techniques (p=0.0031).

Results of the Bland-Altman analysis for inter-observer variability are also shown in *Table 1*. Variability for visual estimation on CTA was comparable to DSA with bias <5% and SDD between 10-11% (*Figure 5*). For caliper measurements however, variability was significantly higher with bias 5-10% and SDD between 13-16% (p<0.05).

Table 1 *Inter-observer variability for measurement of carotid artery stenosis by two experienced interventional radiologists on DSA in comparison to inter-observer variability for grading of carotid stenosis by the two most experienced observers (O1 and O2) using various CTA grading techniques.*

Pearson's correlation coefficient		**Bland-Altman Analysis**				
	r	**95% CI**	**Bias**	**SDD***	**LLoA**	**ULoA**
DSA	0.894	0.824-0.937	-4.8	11.6	-27.5	17.9
CTA_{VE}	0.922	0.869-0.954	-2.2	10.3	-22.4	18.0
CTA_{WW}	0.783**	0.645-0.710	9.3	13.4	-17.1	35.6
CTA_{PW}	0.925	0.865-0.959	5.9	15.8	-25.1	36.9

CI = confidence interval

Bias = mean difference between scores of first and second observers (% stenosis)

SDD = standard deviation of the difference (% stenosis)

LLoA / ULoA = lower / upper 95% level of agreement (% stenosis)

** SDD was significantly different between techniques (Levene's test for homogeneity of variances, p < 0.05)*

*** Inter-observer correlation with CTA_{WW} was significantly lower than with the other techniques*

Correlation of CTA Grading with DSA

Compared to DSA as the standard of reference, Pearson's correlation coefficients were highest for visual estimation (r = 0.919-0.872) and lowest for caliper measurements using predefined window settings (r = 0.846-0.702) (*Table 2*). The correlation between visual estimation and DSA measurements was significantly higher with visual estimation than at least one of the caliper-based methods (*Table 2*). *Figure 6* provides Bland Altman plots that demonstrate the correlation between visual estimation on CTA and DSA for the most experienced and least experienced observer.

Figure 4 *Scatter plot demonstrating the inter-observer correlation for measuring the degree of carotid artery stenosis on DSA.*

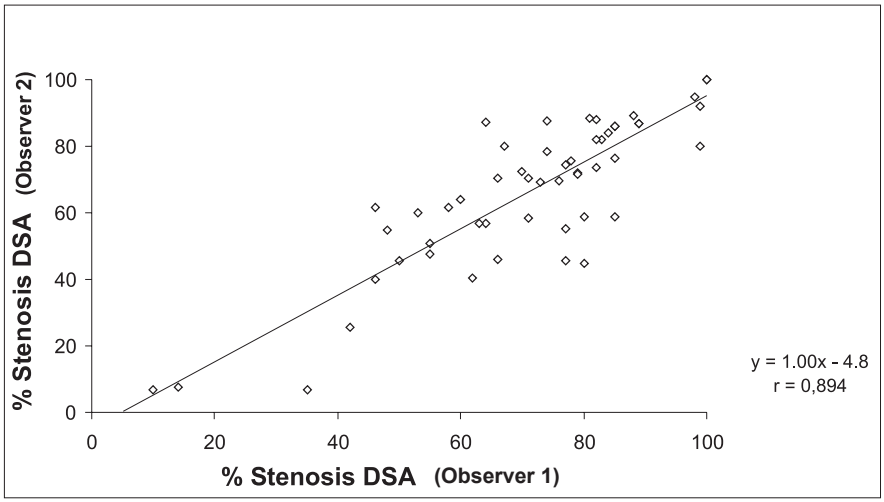

Table 2 *Individual correlation coefficients between CTA and DSA for the three measurement techniques. Correlation was significant for all observations (p<0.001). The mean of two DSA readings was used as standard of reference. The 95% confidence intervals are given in brackets.*

Pearson's Correlation Coefficient r for correlation with DSA				
CTA	**Observer 1**	**Observer 2**	**Observer 3**	**Observer 4**
Visual estimation	0.919	0.909	0.909	0.872
	(0.864-0.952)	(0.848-0.946)	(0.848-0.946)	(0.789-0.924)
Wide window	0.869	0.739	0.821	0.718
	(0.780-0.923)	(0.580-0.844)	(0.706-0.894)	(0.572-0.820)
Predefined window	0.830	0.846	0.813	0.702
	(0.711-0.930)	(0.732-0.914)	(0.676-0.896)	(0.527-0.820)

For observer 1 the correlation for CTA_{VE} was significantly better than for CTA_{PW} ($p<0.05$).
For observer 2 the correlation for CTA_{VE} was significantly better than for CTA_{WW} ($p<0.05$).
For observer 3 & 4 the correlation for CTA_{VE} was significantly better than for CTA_{PW} and CTA_{WW} ($p<0.05$).

Figure 5 *Scatter plot showing the correlation of visual estimation on CTA versus DSA, for O1(◊) and O4 (⁎). The mean of two DSA readings was used as standard of reference.*

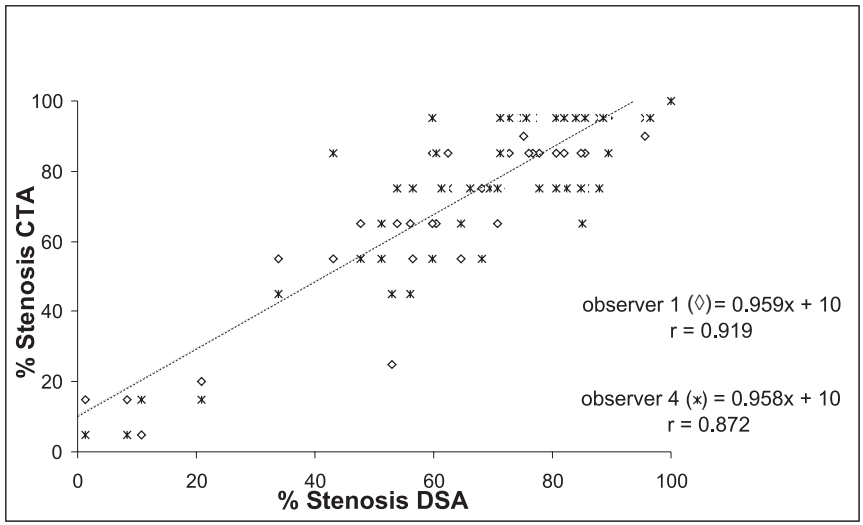

Bland-Altman Analysis of the Accuracy of CTA Grading relative to DSA

Compared to the mean of two readings on DSA as standard of reference, visual estimation on average resulted in a slight overestimation of stenoses (bias 7.3-9.4%), caliper measurements using wide window setting resulted in slight over- or underestimation (bias -1.0 to 10.1%), depending on the observer. Caliper measurements using the preset window settings resulted on average in a slight underestimation that varied from –5.8 to –2.4% (*Table 3*). The differences between the various techniques were not significant.

Variability between CT and DSA measurements was least for visual estimation (SDD 9.8 – 12.8%), followed by caliper measurements using wide window settings (SDD 11.8 – 17.8%). The largest variability between CT and DSA measurements was seen for method 3 (SDD 13.1 – 19.7%). For two of four observers (O1 and O3) visual estimation showed a statistically significantly higher accuracy (SDD) compared to the other techniques ($p<0.05$). While the more experienced observers tended to have a lower SDD than the least experienced observer, the bias of the least experienced observer was in the same range as for the other observers (compare *Table 3* and *Figure 6*).

On the Bland-Altman plots there was no relation between measurement error and degree of stenosis when visual estimation or caliper measurements using a predefined window setting were used. For caliper measurements using a wide window setting we found a tendency for the most experienced observer to overestimate lower degrees of stenosis (*Figure 6*), a trend that was less obvious for the least experienced observer.

Bland-Altman analysis of the three subgroups of stenoses revealed no significant dependence of bias or SDD on the severity of the stenosis, but for caliper measurements with wide window settings CTA tended to overestimate lower degrees of stenosis and slightly underestimated higher degrees of stenosis (see *Figure 7*).

Table 3 *Bland Altman analysis showing the agreement between DSA and CTA for four different observers and three measurement methods. The mean of two DSA readings was used as standard of reference.*

CTA method	Observer				Mean
	O1	O2	O3	O4	
Visual Estimation					
Bias	7.3	9.4	9.0	7.4	**8.3**
SDD	9.8	11.1	10.2	12.8	**11.0**
LoA	(-12.0, 26.6)	(12.3, 31.3)	(-11.0, 28.9)	(-17.7, 32.6)	(-13.3, 29.8)
Caliper measurements, wide window					
Bias	10.1	1.1	-1.0	4.1	**3.5**
SDD	11.8	15.9	15.8	17.8	**15.3**
LoA	(-13.2, 33.3)	(-30.0, 31.2)	(-32.1, 30.0)	(-30.8, 39.0)	(-26.5, 33.6)
No. of patients that were considered not evaluable					
	4	*5*	*3*	*7*	
Caliper measurements, predefined window					
Bias	-3.7	-5.8	-3.5	-2.4	**-2.0**
SDD	13.9	13.1	16.3	19.7	**15.9**
LoA	(-31.0, 23.7)	(-31.6, 20.0)	(-35.4, 28.4)	(-41.2, 36.1)	(-34.8, 27.4)
No. of patients that were considered not evaluable					
	9	*12*	*13*	*5*	

LoA = limits of agreement

SDD was significantly better for visual estimation compared to the other techniques for O1 and O3 ($p<0.05$, Levene's test).

Figure 6 *Bland Altman plots for comparison of DSA to CTA_{VE}, CTA_{WW} and CTA^{PW} for observer O1 with the longest experience in reading CTA (>15 years) and observer O4 who has the least experience (< 1 year). Note that independent of experience the best agreement with DSA was found for visual estimation*

Estimation

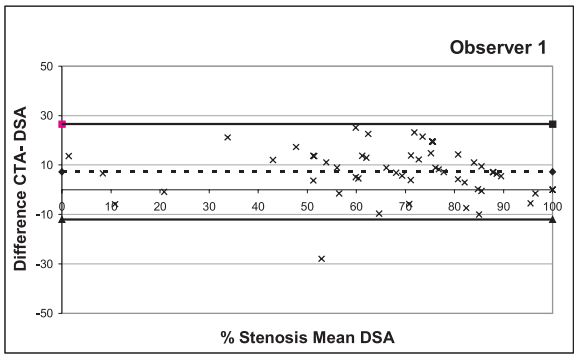

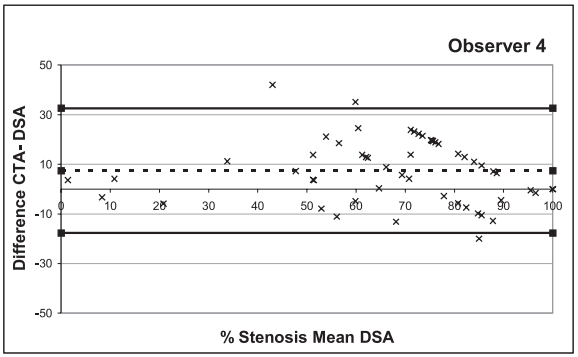

Caliper Wide Window

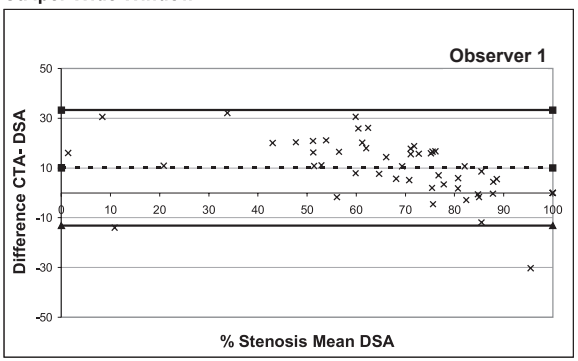

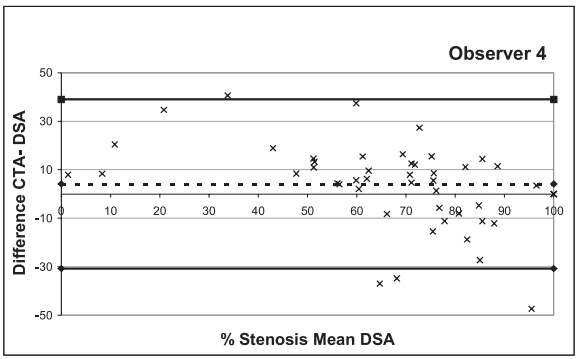

Caliper Preset Window

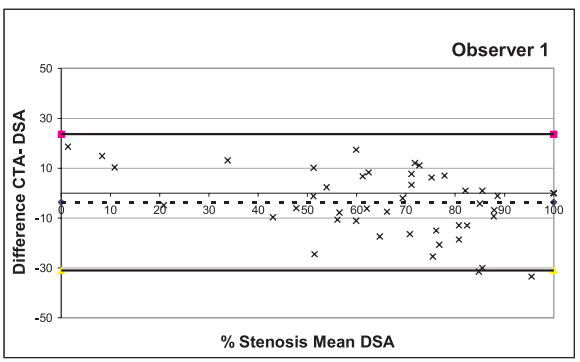

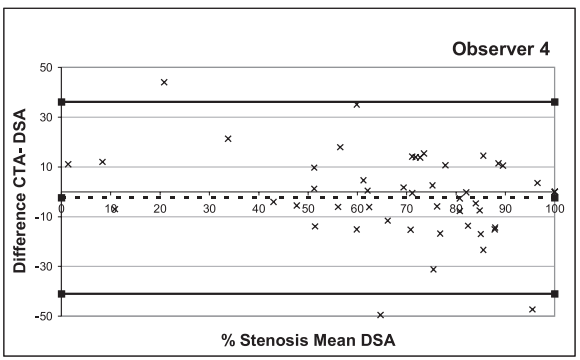

Figure 7 *Bland Altman plot split according to severity of stenosis degree. The mean of the four observations for caliper measurements on CTA using a wide window setting were used to illustrate the tendency to overestimate the degree of stenosis at lower degrees and underestimate it at higher degrees of stenosis. For 0-50% stenosis the bias was 18.5% (SDD 7.7%), for 51-70% stenosis the bias was 5.3% (SDD 9.6%), and for 71-100% stenosis or occlusion the bias was –3.1% (SDD 11.2%).*

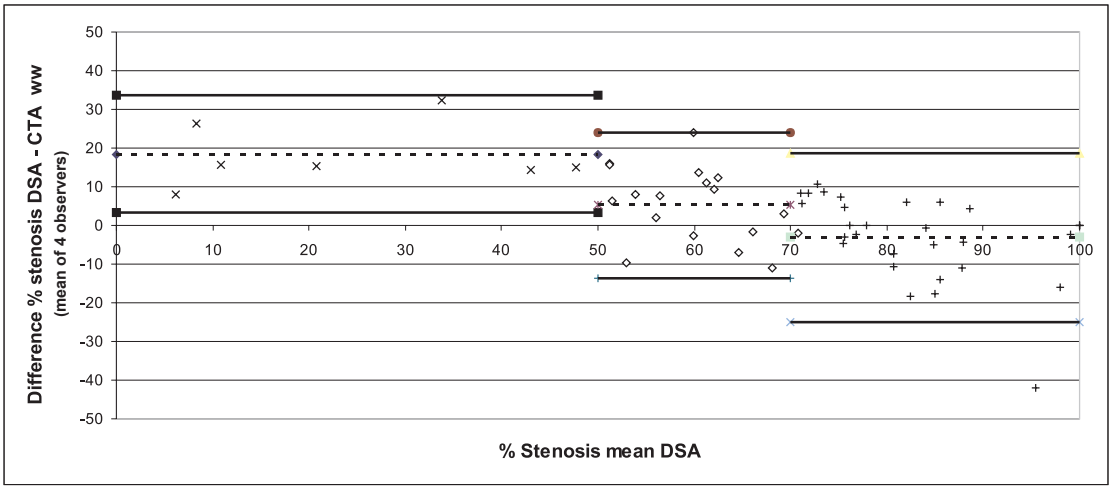

Discussion

To our knowledge, this is the first study showing that visual estimation outperforms the use of caliper measurements for determining the degree of carotid artery stenosis on CTA exams. Despite a mild overestimation with visual estimation (mean bias 8%), we could demonstrate good agreement between CTA and DSA with the best reproducibility (mean SDD 11%) and a correlation between CTA grading and DSA that was not significantly different from repeated measurements on DSA. In fact, the measurement variability between DSA and visual estimation on CTA (95% limits of agreement, -13% to 30%, SDD 11.0) is close to the inter-observer variability of repeated measurements on DSA that we found in this study (95% limits of agreement –28% to 18%, SDD 11.6). which is comparable to a previous study by Rothwell et al. (95% LoA -22 to 22%, SDD 11)[22,23] (*Figure 4*).

Non invasive imaging of the carotid arteries is essential for clinical decision making of treatment indication for surgery or stent placement. A recent meta-analysis in the Lancet reported moderate results for the use of CTA, especially in the category of 50-69% stenosis[24]. Although these analyses were mainly based on single slice scanners, it underlines the importance of knowledge of and improvement of accuracy of multislice CT technique. The main problem with quantifying vessel size with CTA is the limited spatial resolution of CT, which leads to blurring of vessel contours, both within the scan plane as well as along the z-axis. As a result, the border between vessel lumen and surrounding structures is not uniquely defined, which induces insecurities as to where precisely to put calipers for measurement of vessel diameter. This effect becomes more pronounced as the vessel diameter becomes smaller, such as in the region of a stenosis.

Many researchers have tried to find a solution to this problem with the aim of obtaining a sharper delineation of vascular edges and reducing uncertainty. One approach is to decrease the window width, which increases the image contrast and has therefore been suggested for better determination of stenosis degree. However, using a small window width makes the choice of the level extremely important.

Dix[19] and co-workers were the first to demonstrate that the use of binominal criteria (also called "full width at half maximum method") resulted in better reproducibility of carotid measurements compared to wider window settings. They selected a fixed level, set at halfway between the density within the vessel lumen and the surrounding tissue, combined with a window width of one, thus creating a black and white image with sharply delineated vessel edges. This technique showed high accuracy and precision in phantom experiments but was not tested on clinical data. Though clear boundaries are indeed achieved, this principle does not work in cases with a subtotal stenosis. In such a case the contrast enhancement within the lumen decreases due to partial volume effect, and the level for the binary window will be set too low, resulting in an overestimation of the residual lumen and an underestimation of the stenosis.

Another method to avoid blurring vessel edges was presented by Liu et al., not with a binary window but with preset narrow window settings that depend on the CT number in the carotid artery. These preset narrow window settings were based on phantom experiments in which the authors varied luminal contrast, degree of stenosis and window/level settings[18]. Depending on ranges of intra-luminal contrast enhancement, optimum window width and level were determined from these experiments. However, this study did not consider calcifications or high-grade stenosis. This method also suffers from shortcomings in the presence of subtotal stenoses: when intra-luminal contrast decreases in high-grade stenoses, the window level set according to the predefined criteria will be too high, and the lumen is no longer visualized (see *Figure 2*). Calcifications also constitute a limiting factor for this method: because they have a higher CT number than the vessel lumen, lumen and calcifications both appear 'white' at the predefined window settings and can therefore no longer be differentiated (see *Figure 3*). Even in the absence of intra-luminal contrast decrease or calcifications, the method was not as good as visual estimation, even for less-experienced observers.

The limitations of the above described narrow width techniques most apparent in the presence of calcifications and high-grade stenosis can be overcome if a window width is used. A wide window offers the observer the opportunity to correctly interpret misleading CT values caused by volume averaging, presenting as decreased intra-luminal contrast density in the region of a severe stenosis, and apparent narrowing of the lumen adjacent to calcifications due to blooming artifacts. At the level of the stenosis, however, blurring of vessel edges is almost inevitable and may hamper proper selection of the point where the caliper must be placed.

Visual estimation, in contrast to caliper measurements, is a simple and quick technique. As mentioned by two previous authors, visual estimation gives the observer the freedom to take decreasing luminal attenuation or calcifications into account when estimating the degree of a stenosis[25, 26]. Visual estimation is also dependent on the window width and level setting. If, however, the window is chosen just as wide as necessary to avoid the background to become completely black or the vessel lumen to become completely white, the technique appears quite robust. We found that such a technique for grading of carotid artery stenoses yielded the best correlation

with angiography and the least inter-observer variability (see *Figure 5*). Even in the presence of calcifications, the technique appears to work properly if the window width is chosen so that the calcification does not become completely white[27].

Our study suffered from the following limitations. We determined the degree of stenosis in a pre-selected group of patients with symptomatic high-grade stenosis. Contralateral arteries were selectively included and thus the study comprises an inhomogeneous group of symptomatic and asymptomatic carotids. Therefore we cannot say whether the results are also valid for other patient groups[28, 29]. Second, we analyzed variability by measuring the absolute differences instead of using categories and therefore could not determine sensitivity and specificity. However, our aim was to determine the exact measurement error for the four methods compared to angiography and for that purpose the Bland-Altman method is well suited.

The third shortcoming is that visual estimation was performed using 10% categories. Although it is less precise compared to caliper measurements, these 10% categories apply well to the recently suggested cut-off degrees in the group of >50% stenosis[4-6]. In addition, we did not further discriminate between near-occlusion and high-grade stenosis in the group of stenoses between 90 and 99%, which can be important in clinical practice since they imply different treatment strategies[4]. Despite this lower intrinsic precision of our visual grading system, however, results were best with visual estimation.

To our knowledge this is the first comparison of measurement techniques for determining carotid artery stenosis using multislice CTA in a clinical setting. Although several authors suggested the use of objective measurement criteria[15-19], most of these objective criteria have not gained a place in routine practice. Despite promising phantom studies, all techniques carry a certain subjectivity or shortcoming that seems inevitable when moving from phantom experiments to clinical application. The use of visual estimation and a wide window setting allows for identification of pitfalls like calcifications and decrease of contrast in high-grade stenosis.

In conclusion, visual estimation on CTA provides the best correlation with angiographic measurements of carotid artery stenosis and it outperforms caliper measurements in patients with symptomatic high-grade stenosis.

References

1. Rothwell PM, Coull AJ, Silver LE, Fairhead JF, Giles MF, Lovelock CE, Redgrave JN, Bull LM, Welch SJ, Cuthbertson FC, Binney LE, Gutnikov SA, Anslow P, Banning AP, Mant D, Mehta Z; Oxford Vascular Study. Population-based study of event-rate, incidence, case fatality, and mortality for all acute vascular events in all arterial territories (Oxford Vascular Study). Lancet 2005;366:1773-83.
2. Beneficial effect of carotid endarterectomy in symptomatic patients with high-grade carotid stenosis. North American Symptomatic Carotid Endarterectomy Trial Collaborators. N Engl J Med 1991; 325:445-53.
3. Roubin GS, Iyer S, Halkin A, Vitek J, Brennan C. Realizing the potential of carotid artery stenting: proposed paradigms for patient selection and procedural technique. Circulation. 2006; 113:2021-30.
4. Rothwell PM, Eliasziw M, Gutnikov SA, Fox AJ, Taylor DW, Mayberg MR et al. Analysis of poooled data from the randomised controlled trials of endarterectomy for symptomatic carotid stenosis. Lancet 2003; 361:107-16.
5. Halliday A, Mansfield A, Marro J, Peto C, Peto R, Potter J, Thomas D; MRC Asymptomatic Carotid Surgery Trial (ACST) Collaborative Group. Prevention of disabling and fatal strokes by successful carotid endarterectomy in patients without recent neurological symptoms: randomised controlled trial. Lancet 2004; 363:1491-502
6. Yadav JS, Wholey MH, Kuntz RE, Fayad P, Katzen BT, Mishkel GJ, Bajwa TK, Whitlow P, Strickman NE, Jaff MR, Popma JJ, Snead DB, Cutlip DE, Firth BG, Ouriel K. Protected carotid-artery stenting versus endarterectomy in high-risk patients. N Engl J Med. 2004; 351:1493-501.
7. Prokop M. Multislice CT angiography. Eur J Radiol. 2000;36:86-96.
8. Josephson SA, Bryant SO, Mak HK, Johnston SC, Dillon WP, Smith WS. Evaluation of carotid stenosis using CT angiography in the initial evaluation of stroke and TIA. Neurology. 2004; 63:457-60.
9. North American Symptomatic Carotid Endarterectomy Trial. Methods, patient characteristics, and progress. Stroke 1991; 22:711-20.
10. Dillon EH, van Leeuwen MS, Fernandez MA, Eikelboom BC, Mali WP. CT angiography: application to the evaluation of carotid artery stenosis. Radiology 1993;189:211-9.
11. Cumming MJ, Morrow IM. Carotid artery stenosis; a prospective comparison of CTA and conventional angiography. AJR 1994; 163:517-523.
12. Marks MP, Napel S, Jordan JE. Diagnosis of carotid artery disease: preliminary experience with MIP spiral CT angiography. AJR 1993; 160;1267-1271.
13. Anderson GB, Ashforth R, Steinke DE, Ferdinandy R, Findlay JM. CT angiography for the detection and characterization of carotid artery bifurcation disease. Stroke 2000; 31:2168-74.
14. Randoux B, Marro B, Koskas F. Carotid artery stenosis: prospective comparison of CT, 3D gadolinium enhanced MR and conventional angiography. Radiology 2001; 220:179-185.
15. Verhoek G, Costello P, Khoo EW. Carotid bifurcation CTA: assessment of interactive volume rendering. JCAT 1999; 23:590-596.
16. Leclerc X, Godefroy O, Pruvo JP. Computed tomographic angiography for the evaluationof carotid artery stenosis. Stroke 1995; 26:1577-1581.
17. Leclerc X, Godefroy O, Lucas C, Benhaim JF, Michel TS, Leys D, Pruvo JP. Internal carotid arterial stenosis: CT angiography with volume rendering. Radiology 1999; 210:673-82.
18. Yi Liu, MD, Kenneth D. Hopper, MD, David T. Mauger, PhD and Kimberly A. Addis, MD. CT Angiographic Measurement of the Carotid Artery: Optimizing Visualization by Manipulating Window and Level Settings and Contrast Material Attenuation. Radiology 2000; 217:494-500.
19. Dix JE, Evans AJ, Kallmes DF, Sobel AH, Phillips CD. Accuracy and precision of CT angiography in a model of carotid artery bifurcation stenosis. AJNR Am J Neuroradiol. 1997; 18:409-15.
20. Bland JM, Altman DG. Statistical methods for assessing agreement between two methods of clinical measurement. Lancet 1986; 1:307-10.
21. Jerrold H. Zar. Biostatistical Analysis, Prentice Hall College Div; 3rd edition (January 1996), page 386.
22. Rothwell PM, Gibson RJ, Slattery J, Warlow CP. Prognostic value and reproducibility of measurements of carotid stenosis. A comparison of

three methods on 1001 angiograms. European Carotid Surgery Trialists' Collaborative Group. Stroke 1994; 25:2440-4.

23. Young GR, Humphrey PR, Nixon TE, Smith ET. Variability in measurement of extracranial internal carotid artery stenosis as displayed by both digital subtraction and magnetic resonance angiography: an assessment of three caliper techniques and visual impression of stenosis. Stroke 1996 ; 27:467-73.
24. Wardlaw JM, Chappell FM, Best JJ, Wartolowska K, Berry E; NHS Research and Development Health Technology Assessment Carotid Stenosis Imaging Group. Non-invasive imaging compared with intra-arterial angiography in the diagnosis of symptomatic carotid stenosis: a meta-analysis. Lancet. 2006;367:1503-12.
25. Chen CJ, Lee TH, Hsu HL, Tseng YC, Lin SK, Wang LJ, Wong YC. Multi-Slice CT angiography in diagnosing total versus near occlusions of the internal carotid artery: comparison with catheter angiography. Stroke 2004; 35:83-5.
26. Zhang Z, Berg MH, Ikonen AE, Vanninen RL, Manninen HI. Carotid artery stenosis: reproducibility of automated 3D CT angiography analysis method. Eur Radiol 2004; 14:665-72.
27. Prokop M, Shin HO, Schanz A, Schaefer-Prokop CM. Use of maximum intensity projections in CT angiography: a basic review. Radiographics 1997; 17:433-51.
28. Rothwell PM. Analysis of agreement between measurements of continuous variables: general principles and lessons from studies of imaging of carotid stenosis. J Neurol 2000; 247:825-34.
29. Rothwell PM, Pendlebury ST, Wardlaw J, Warlow CP. Critical appraisal of the design and reporting of studies of imaging and measurement of carotid stenosis. Stroke 2000; 31:1444-50.

Reproducibility of Quantitative Measurements of Regional Brain Perfusion with Computed Tomography

Chapter Six

A Waaijer, IC van der Schaaf, BK Velthuis, M Quist, MJP van Osch, EPA Vonken, MS van Leeuwen, M Prokop. Reproducibility of Quantitative Measurements of Regional Brain Perfusion with Computed Tomography. In Revision for AJNR

Abstract

Purpose

To establish intra- and inter-observer variability for regional measurement of CT brain perfusion (CTP) and to determine whether reproducibility can be improved by calculating perfusion ratios.

Materials & Methods

CTP images were acquired in 20 patients with unilateral symptomatic carotid artery stenosis (CAS). We manually drew regions of interest (ROIs) in the cortical flow territories of the anterior (ACA), middle (MCA) and posterior cerebral artery (PCA) and the basal ganglia in each hemisphere recording cerebral blood volume (CBV), cerebral blood flow (CBF) and mean transit time (MTT), and calculated ratios of perfusion values between symptomatic and asymptomatic hemisphere. We assessed intra- and inter-observer variability by performing a Bland-Altman analysis of the relative differences between two observations and calculated standard deviations of relative differences (SDD_{rel}) as a measure of reproducibility. We used an F-test to assess significance of differences between SDD_{rel} of absolute CTP values and CTP ratios, and Levine's test to compare the four perfusion territories.

Results

MTT was the most reproducible parameter (SDD_{rel} ≤10%). Intra- and inter observer variability were higher for absolute CTP values compared to CTP ratios for CBV (16-17% versus 11-16%) and CBF (18% versus 10-13%) but not for MTT (5-9%). Reproducibility was best in the MCA territory: SDD_{rel} was ≤11% for perfusion ratios of all three parameters.

Conclusion

MTT is the most reproducible CTP parameter in patients with unilateral symptomatic CAS. Measurement variability in CBV and CBF can be improved if CTP ratios instead of CTP values are used. The MCA territory shows the least measurement variability.

Introduction

CT perfusion (CTP) is a widely available diagnostic tool that provides quick and minimally-invasive assessment of brain perfusion[1,2]. Currently, its main use is to identify patients with acute stroke who may benefit from thrombolysis by discriminating penumbra (tissue with reduced perfusion but potentially salvageable) from irreversible ischemia. CTP has also been used for other kinds of cerebrovascular disease: to predict delayed ischemia in patients with subarachnoid hemorrhage[3], to measure the reserve capacity in patients with carotid occlusive disease using acetozolamide[4], and to evaluate the effect of endovascular treatment[5].

Analysis of CT perfusion can be based on visual interpretation of perfusion maps or on quantitative perfusion measurements. Visual interpretation relies on the analysis of color-coded perfusion maps where regions with reduced perfusion can be detected by visual comparison with the surrounding tissue or the contra-lateral hemisphere[6,7].

Quantitative analysis can be performed by using a pixel-by-pixel analysis or by measuring average values in regions of interest (ROIs) in various anatomic perfusion territories of the brain. The pixel-based analysis is applied in acute stroke, where a threshold value has been suggested to distinguish between infarcted and potentially salvageable tissue[8]. Regional analysis using ROIs can rely on manual tracing of anatomic regions[9,10] or on placing circular ROIs[11,12]. ROIs can be mirrored to compare the affected to the non-affected hemisphere.

Quantitative measurements are complicated by the large variability of absolute perfusion values found in normal subjects and clinical patients[13]. This variability makes the discrimination between normal and reduced perfusion difficult. Several authors have therefore suggested using relative perfusion data based on the ratio between measurements in the symptomatic and asymptomatic hemisphere[14-16]. This method takes advantage of the basic symmetry of the brain and may correct for inter-patient variability of absolute perfusion values.

CT perfusion is becoming a widely used tool for analyzing brain perfusion[17,18], even though measurement variability (precision) is in the range of 15-30% when ROI-based techniques are used[12]. This is due to observer-dependent post-processing steps, which can strongly influence absolute perfusion values[19-21]. These observer-dependent steps are likely to affect both hemispheres equally. The goal of our study was to examine whether variability of ROI-based measurements could be reduced when perfusion ratios between the symptomatic and asymptomatic hemispheres are used instead of absolute perfusion values. A secondary goal was to study whether the measurement variability differed between the various cerebral flow territories in patients with symptomatic unilateral carotid artery stenosis.

Materials and Methods

Patient Group

Between September 2003 and May 2005 CT perfusion imaging was performed in 27 patients with symptomatic carotid artery stenosis. Patients were known to have a more than 50% stenosis from ultrasound and were referred to our department for endovascular treatment (carotid artery stent placement) or carotid endarterectomy (CEA)

as part of the International Carotid Stenting Study (ICSS) trial (www.cavatas.com). At our institution, CT perfusion measurements were added to the ICSS protocol to study the effect of the intervention on brain perfusion. The study was approved by our institutional review board and all patients had signed informed consent.
Exclusion criteria were the presence of a >50% contralateral stenosis (n=2), of motion artifacts (n=2) and the presence of a manifest large territorial infarct (n=3). Consequently we could evaluate 20 scans from 20 patients. Patient characteristics are shown in *Table 1*.

Table 1 Patient characteristics (n=20)

Patient demographics	
Mean age ± SD	68 ± 11.1 years (range, 48 to 84 years)
Male : female sex	14 : 6
Presenting event	
Amaurosis fugax	2
TIA	9
Stroke	9
Carotid arteries	
Symptomatic side, left : right	10 : 10
Mean stenosis ± SD, symptomatic side	88 ± 13 % (range, 60% to 99%)
Mean stenosis ± SD, asymptomatic side	11 ± 17 % (range, 0% to 50%)
Cerebral damage (non-contrast CT)	
No infarct	11
Small infarct (small branch area)*	5
Medium size infarct (major branch area)*	4

SD = standard deviation
**Infarct size was classified according to Lodder et al [35]*

CT Perfusion Scanning

The CTP scans were acquired on a 16-slice scanner (MX 8000 IDT or Brilliance-16, Philips Medical Systems, Cleveland, OH). The level of the scan was set at the basal ganglia, just above the level of the circle of Willis, with the scan angle parallel to the orbito-meatal line to prevent incorporation of the eye lenses. We used a collimation of 8 x 3 mm with a cycle time of 1s and acquired 40 data sets during 40 seconds of scanning. For a compromise between patient dose and signal-to-noise ratio a tube voltage of 90 kVp in combination with 150 mAs [22] was used. The $CTDI_{vol}$ for a single scan was 8.9 mGy, the DLP for the whole series of scans amounted to 854.4 mGy·cm. Using the dose

calculator provided by IMPACT website (www.impactscan.org), we estimated an effective dose of 1.8 mSv for the CTP examination. Reconstruction of two adjacent 12 mm slabs was performed using a slightly smoothing head filter (UB) and a field of view of 160 mm. Thus, a total of 2x40 images were available from each examination and were processed to obtain perfusion maps of two adjacent slabs.

For all perfusion scans we injected a bolus of 40 ml contrast (Ultravist 300, Schering, Berlin, Germany) with 300 mg iodine per ml at a flow rate of 5 ml/s followed by 40 ml of 0.9% saline using the same flow rate. Contrast material and saline chaser bolus were administered using a power injector with a dual head system (Stellant Dual CT injector, Medrad Europe BV, Beek, The Netherlands). To achieve non-enhanced baseline images, the scan was started 5 seconds after commencing the bolus injection in an antecubital vein.

Measurement of absolute CTP Values and relative CTP Ratios

CT perfusion maps were calculated using CTP prototype software (Philips Medical Systems, Best, the Netherlands). The software first performs a motion correction and then uses an anisotropic, edge-preserving spatial filter to reduce image noise. The resulting spatially aligned and noise-reduced data set is further processed to obtain CT perfusion vales for each voxel in the data set.

CT perfusion analysis is based on temporal changes in signal intensity during the first pass of a bolus of an iodinated contrast agent. Changes in CT numbers in a voxel over baseline (pre-contrast CT numbers) are linearly related to the concentration of the contrast agent in that voxel. Thus, a time concentration curve can be calculated for each voxel. The software used relies on the central volume principle to calculate perfusion values from the time concentration curve for each voxel[23].

The first step in the evaluation process is the manual selection of the arterial input function (AIF) and venous output function (VOF). For that purpose the user selects oval ROIs that incorporate the anterior cerebral artery (for AIF) and superior sagittal sinus (for VOF), after which the software then automatically identifies appropriate reference voxels for deriving AIF and VOF.

For each voxel the cerebral blood volume (CBV) is calculated as the ratio of the area under the time concentration curve (AUC) of this voxel to the AUC of the first passage through an artery. A correction factor H is applied to account for the difference in the hematocrit in small versus large vessels; $CBV = H \cdot AUC_{tissue}/AUC_{AIF}$. Therefore, the knowledge of optimum contrast enhancement is required, which should be provided by an arterial pixel devoid of partial volume effect. Since the AUC of the first passage of contrast agent through a vein is equal to the AUC of an artery when the blood-brain barrier is intact, usually the superior sagittal sinus is preferred as reference; $CBV = H \cdot AUC_{tissue}/AUC_{VOF}$. The mean transit time (MTT), the average time taken by the blood to cross the capillary network, is calculated by a deconvolution operation from the time concentration curve of a particular voxel and the AIF[24], whereby the MTT is related to the difference between the width of the tissue curve and the width of the AIF. Cerebral blood flow (CBF) for each voxel is finally calculated according to the formula: CBF = CBV / MTT[25]. A threshold value at 85 ml/100gr/min was set to remove vascular structures.

Subsequently, free-form ROIs were drawn to outline various cerebral flow territories on each of the two slabs, separately for each hemisphere. The territories were selected according to the maps of Damasio[26] assuring that

the ROIs were securely within the margin of the territory that belonged to a certain artery and excluded possible watershed areas (see *Figure 1*). We included the cortical flow territory of the anterior cerebral artery (ACA), middle cerebral artery (MCA), posterior cerebral artery (PCA) and the basal ganglia (BG), which contained both deep ACA and deep MCA territories. ROIs were chosen to include mainly grey matter and as little subcortical white matter as possible.

Given four territories per hemisphere and two slabs per patient, a total of 16 ROIs per patient were available. The average values for CBV, CBF and MTT within each ROI were recorded. We then calculated CTP ratios by dividing the CTP values in flow territories in the symptomatic hemisphere by the CTP values in the corresponding asymptomatic hemisphere.

Figure 1 *Analysis of manual outlined ROIs according to territorial division of Damasio[26].*

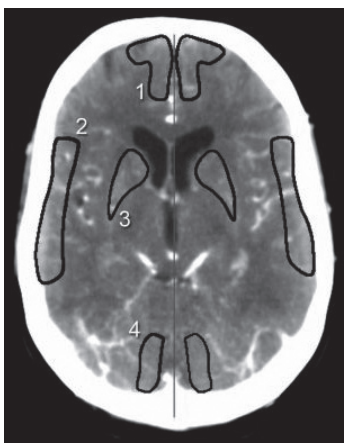

1 = ACA territory, 2 = MCA territory, 3 = basal ganglia, 4 = PCA territory.

Data Analysis

Measurements were acquired by two observers (A and B) and repeated after one week by observer A. For this purpose all steps from loading of the 2x40 slabs to drawing and evaluating the ROIs in the various perfusion territories were repeated.

For assessment of intra- and inter-observer variability we determined the relative differences between two observations and calculated the mean relative differences (mean bias) and the standard deviation of these differences (SDD_{rel}) according to the principle of Bland Altman. The relative difference indicates the difference for

each pair of observations divided by the mean of the two observations (e.g., [Δ CBV/mean CBV]*100%) and allows for comparing absolute CTP values and CTP ratios. For determination of inter-observer variability the first of the two observations of observer A was used.
In a first step we pooled the perfusion data from all territories to calculate global numbers for intra- and inter-observer variability. We performed an F-test to compare the intra- and inter-observer variability for absolute CTP values to that for CTP ratios. In a second step we separately analyzed intra- and inter-observer variability for each of the four flow territories and compared the variability for the various flow territories using Levine's test for homogeneity of variance. We also evaluated whether there was a difference in variability for absolute values between the symptomatic and a-symptomatic hemisphere using the t-test for independent samples. A test result with a p-value of less than 0.05 was considered statistically significant.

Results

Patient Characteristics

The mean and standard deviation for the absolute CT perfusion values (CBF, CBV and MTT) and relative CT perfusion ratios are shown in *Table 2*.

Intra- and Inter-Observer Variability

When evaluating the perfusion data from all territories together, analysis of intra-observer variability revealed a mean bias varying between -1.1 and 2.2%. This range was slightly larger, between -4.4 and 2.7%, for inter-observer variability. The relative standard deviations of the differences (SDD_{rel}) found for intra-observer and inter-observer variability are given in *Table 3*.
Intra- and inter-observer variability for absolute values separated for both hemispheres are shown in *Table 4*. Since no systematic difference was found, for further analysis data of both hemispheres were pooled together. Intra- and inter-observer variability was significantly lower for MTT than for CBV or CBF, independent of whether absolute CTP values or CTP ratios were considered. Intra- and inter-observer variability for MTT values and MTT ratios were not substantially different. However, intra-observer variability for CBF and CBV ratios was significantly lower than for absolute CBF and CBV values. Inter-observer variability for CBF ratios was also significantly lower than for absolute CBF values but no significant improvement of inter-observer variability could be shown if CBV ratios were used instead of absolute CBV values.
Bland-Altman plots that relate relative differences between observations to the various absolute perfusion parameters are given in *Figure 2* (inter-observer variability). The figures demonstrate that the relative differences were independent of the magnitude of the absolute perfusion values.

Table 2: Perfusion characteristics

Perfusion characteristics in our study group of 20 patients with symptomatic carotid artery stenosis. CT perfusion values and ratios (mean ± SD) are given for the various vascular flow territories. Note that numbers were calculated from mean values of three observations. For CT perfusion values, 80 data points (20 patients x 2 slabs x 2 hemispheres) were used for each territory. For CT perfusion ratios, 40 data points (20 patients x 2 slabs) were used for each territory.

CT perfusion values – symptomatic hemisphere			
Territory	**CBV (ml/100g)**	**CBF (ml/100g/min)**	**MTT (s)**
ACA	4.1 ± 1.4	50.4 ± 18.8	5.0 ± 0.7
MCA	5.3 ± 1.4	56.1 ± 17.8	5.9 ± 1.3
Basal ganglia	4.3 ± 1.3	49.3 ± 17.6	5.5 ± 1.2
PCA	4.9 ± 1.4	50.9 ± 15.4	5.8 ± 0.7
CT perfusion values – asymptomatic hemisphere			
Territory	**CBV (ml/100g)**	**CBF (ml/100g/min)**	**MTT (s)**
ACA	3.9 ± 1.3	50.9 ± 18.1	4.7 ± 0.7
MCA	5.3 ± 1.6	70.7 ± 22.3	4.5 ± 0.6
Basal ganglia	4.3 ± 1.3	57.2 ± 20.5	4.6 ± 0.9
PCA	5.0 ± 1.6	53.7 ± 16.9	5.6 ± 0.9
CT perfusion ratios (symptomatic / asymptomatic side)			
Territory	**CBV**	**CBF**	**MTT**
ACA	1.05 ± 0.14	1.01 ± 0.13	1.06 ± 0.10
MCA	1.01 ± 0.12	0.81 ± 0.14	1.28 ± 0.17
Basal ganglia	1.03 ± 0.09	0.88 ± 0.08	1.18 ± 0.12
PCA	1.05 ± 0.22	1.00 ± 0.17	1.06 ± 0.13

Table 3 Comparison of intra- and inter-observer variability for CT perfusion values and CT perfusion ratios.
Pooled data from all flow territories. Variability is expressed as the standard deviation of the relative differences for each pair of observations (SDD_{rel}) and is thus expressed as percentage (%). The range of relative differences is given in brackets. Note that both intra- and inter-observer variability are significantly lower for CBF ratios than for absolute CBF values, while for CBV this effect was only seen in intra-observer variability. For MTT the difference was small and significant for intra-observer variability only.

Intra-observer variability (SDD_{rel} [range of relative differences])			
	CBV	**CBF**	**MTT**
CT perfusion values	16% [-62%, 54%]	18% [-59%, 63%]	5% [-35%, 21%]
CT perfusion ratios	11% [-51%, 37%]	10% [-42%, 33%]	6% [-30%, 23%]
p-value*	*0.000*	*0.000*	*0.048*
Inter-observer variability (SDD_{rel} [range of relative differences])			
	CBV	**CBF**	**MTT**
CT perfusion values	17% [-78%, 63%]	18% [-67%, 55%]	9% [-30%, 34%]
CT perfusion ratios	16% [-44%, 71%]	13% [-49%, 51%]	9% [-36%, 30%]
p-value*	*0.135*	*0.000*	*0.295*

** F-test*

Table 4 *Comparison of intra- and inter-observer variability for CT perfusion values separately for the symptomatic and asymptomatic hemisphere*

Intra-observer variability (SDD_{rel})						
	Symptomatic side			**A-symptomatic side**		
	CBV	**CBF**	**MTT**	**CBV**	**CBF**	**MTT**
ACA	22%	22%	5%	20%	21%	5%
MCA	18%	20%	4%	19%	22%	5%
Basal Ganglia	18%	20%	4%	19%	20%	7%*
PCA	20%	22%	8%	20%	20%	4%
Inter-observer variability (SDD_{rel})						
	CBV	**CBF**	**MTT**	**CBV**	**CBF**	**MTT**
ACA	15%	19%	9%	20%*	22%	8%
MCA	12%	17%	6%	14%	19%	8%
Basal Ganglia	15%	15%	8%	21%	18%	9%
PCA	22%	16%	11%	14%	13%	6%

** Difference between asymptomatic and symptomatic hemisphere significantly different ($p<0.05$)*

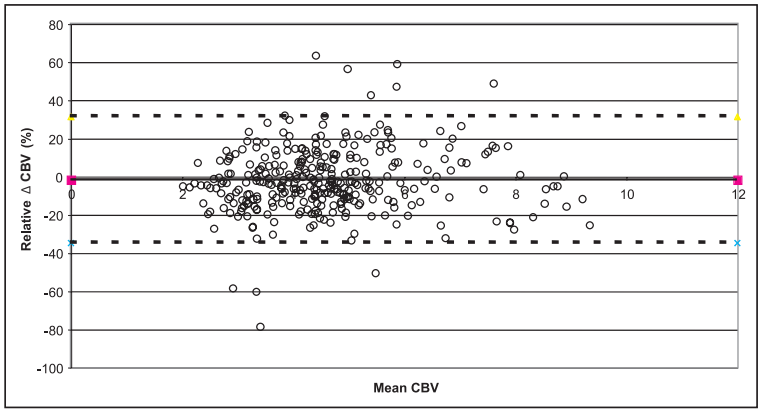

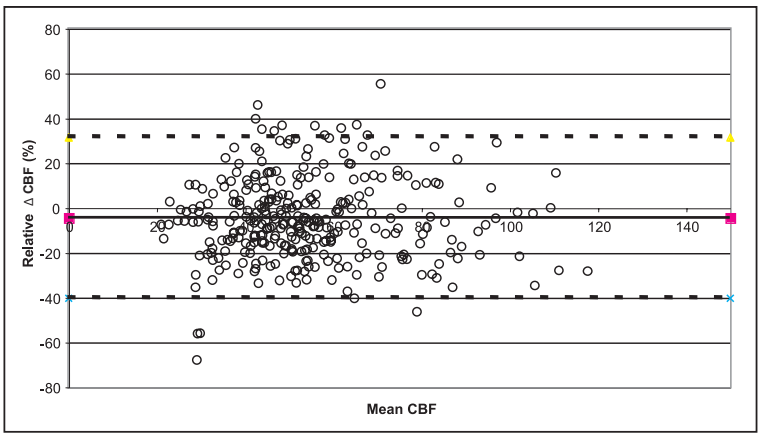

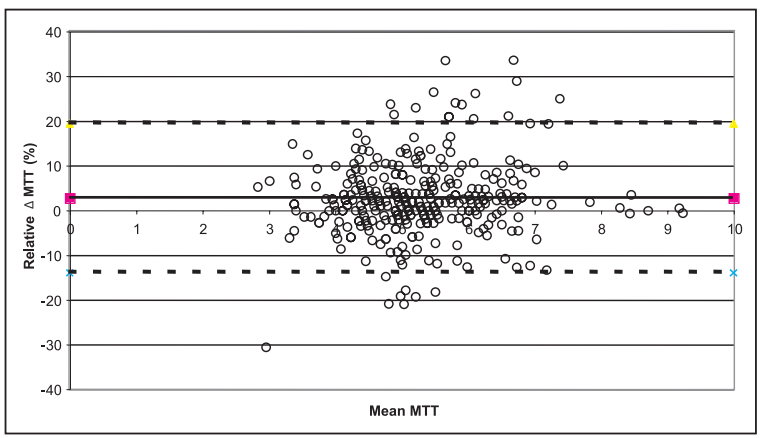

Figure 2 *Bland-Altman plots of the relative differences (inter-observer variability, pooled data) of absolute perfusion values against the mean absolute value for CBF (ml/ 100 gr/ min)*(**a**)*, CBV (ml/100 gr)* (**b**)*, and MTT (s)* (**c**)*. The relative ΔCBV, ΔCBF and ΔMTT indicates the difference between two observations divided by the mean of those two observations, given as percentage. The thick line represents the mean bias and the dotted lines indicate the upper and lower limits of agreement. These upper and lower limits of agreement for the relative differences were 37% and -37% for CBV, 38% and –43% for CBF, and 21% and –16% for MTT, respectively.*

Dependence of Observer Variability on Flow Territories

Intra- and inter observer variability for absolute MTT values was less than 10% for all territories and no significant difference between the different territories was seen (*Table 5*). Absolute perfusion values ranged from 11-18% for CBV and from 15-19% for CBF.

The introduction of ratios between CTP values in the symptomatic and asymptomatic hemisphere did not substantially change variability for MTT but mostly reduced variability for CBV and CBF. For intra-observer variability the use of ratios improved reproducibility in all territories, but the difference between the four flow territories was significant for CBF only ($p<0.05$). The variability was ≤8% for CBV, CBF and MTT in the MCA and BG territory. For inter-observer variability improvement was seen in all territories except the PCA territory. The difference between the four territories was significant for all parameters, being best in the MCA territory (≤11%).

Table 5 Comparison of intra-observer and inter-observer variability (SDD_{rel}) in the four flow territories.
The test of Levine for homogeneity of variance was used to check whether variability differed between flow territories. The least variability was commonly seen for the MCA territory. For CTP ratios the largest variability was usually found for the PCA territory.

Intra-observer variability (SDD_{rel})						
	CBV	**CBF**	**MTT**	**CBV ratio**	**CBF ratio**	**MTT ratio**
ACA	17%	18%	5%	12%	12%	4%
MCA	15%	17%	5%	5%	6%	5%
Basal Ganglia	16%	17%	6%	8%	8%	7%
PCA	18%	18%	6%	16%	12%	8%
p- value*	*0.730*	*0.884*	*0.210*	*0.249*	*0.029*	*0.090*
Inter-observer variability (SDD_{rel})						
	CBV	**CBF**	**MTT**	**CBV ratio**	**CBF ratio**	**MTT ratio**
ACA	16%	19%	8%	15%	16%	8%
MCA	11%	15%	6%	11%	9%	6%
Basal Ganglia	17%	15%	8%	13%	8%	8%
PCA	18%	15%	9%	23%	17%	10%
p-value*	*0.005*	*0.005*	*0.179*	*0.000*	*0.001*	*0.001*

** Test of Levine for homogeneity of variance*

Discussion

This study in patients with unilateral symptomatic carotid disease reveals three major findings; 1) the MTT is the most reproducible parameter for regional measurements CT perfusion, 2) the use of CBV and CBF ratios results in better reproducibility compared to absolute CBV and CBF values for this patient group and 3) when separate flow

territories are analyzed in such a patient group, the best reproducibility is observed in the MCA territory.

Our finding that MTT is the most reproducible parameter is in concordance with literature reports[12]. This may be explained by the fact that manual outlining of an ROI will inevitably introduce variability in the amount of included white matter. It is known that there is almost no difference in MTT between grey and white matter while there are major differences in CBV and CBF between these two tissue types[22, 27, 28]. The fact that MTT showed less than 10% variability for both absolute and relative values indicates that absolute and relative values are robust measures for use in clinical practice. This is confirmed by a recent publication by Wintermark et al.[29], who showed that both relative and absolute MTT can be used as threshold for discrimination between final infarct size and penumbra.

Perfusion techniques like PET and SPECT use CBF as main perfusion parameter. MTT, which is defined as CBV/CBF, can be measured using CT or MRI but is so far used as nonspecific indicator of a perfusion disturbance. However, the inverse of this ratio (namely CBF/CBV) was shown to be strongly related to cerebral perfusion pressure (CPP), and has even been suggested as a surrogate for CPP, a parameter that so far can only be measured invasively[30]. The CPP is responsible for maintenance of sufficient perfusion pressure in case of ischemia by means of the auto regulation mechanism. Although CBF is mostly used in clinical practice, the regional CBF is an insensitive indicator of the severity of occlusive cerebrovascular disease[31] because it does not change with small changes of CPP. Also clinical studies have shown that the ratio of CBF/CBV provides better information than either of these parameters alone[31, 32]. MTT is easily obtained from CT perfusion studies and has the lowest measurement variability. Given its close relation to CPP, it may become an important parameter for evaluating perfusion disturbances in clinical practice.

Our second result indicates that intra- and inter-observer variability for absolute CT perfusion values can be significantly improved when CTP ratios between measurements in the symptomatic and asymptomatic hemisphere are used in patients with unilateral stenoses. This can be explained by technical as well as physiological facts. Calculation of ratios eliminates variations caused by the choice of the AIF and VOF. In addition, it may also reduce the variability in the proportion of grey and white matter that is included in the regional analysis: if the ROIs drawn in both hemispheres are symmetrically placed, the relative amounts of grey and white matter should be similar. Calculating ratios will therefore eliminate part of the resulting measurement variability.

The third result indicated least variability in the MCA territory. Placement and size of ROIs may be a factor that can help explain these findings. The ROIs in the MCA territory tended to be larger than the ROIs in the other territories. This makes it likely that there is a larger overlap between ROIs drawn at repeated measurements or by different observers, which should positively influence reproducibility. The ROIs in the ACA and PCA territories were smaller, and while the medial extent of these territories is well defined by the interlobar fissure, the lateral extent is more difficult to define. This may result in variability in the amount of white matter that is included with resultant higher inter- and intra-observer variability (see *Figure 1*). Finally, intra-parenchymal vessels like distal ACA, MCA and PCA branches or venous structures can lead to very high measured cerebral blood volumes, when these are mistaken for parenchyma[10]. Although we set a threshold value for removing these structures, computerized removal can be insufficient or excessive and thus influence the measured perfusion values.

In summary, we found that in the most optimized situation; that is by using the relative perfusion values in the

MCA territory, a measurement variability of 5-10% can be achieved. Normal left-right differences are known to vary ±10%, while intra-patient differences for repeated measurements are in the range of 10-20%[13]. Therefore, measurement variability between two observers should not be more than 10%. This implies, that measurement of true perfusion abnormalities requires itself intra-patient comparison and that the use of absolute values introduces measurement errors. In our study population detection on perfusion values was not performed on a quantitative base, but further research will have to reveal whether the use of CTP ratios improves the detection of perfusion abnormalities.

Our study has some limitations. First, the presence of a carotid artery stenosis influences the AIF and thereby the measured absolute MTT and CBF[33]. However, since we used relative differences for further analysis, the absolute height of perfusion values is no longer influencing the intra and inter observer variability. A second difficulty in choice of AIF selection in the ACA is the assumption that this input function is equal over all brain voxels, which is in fact not known. However, the search for a method to define the localized AIF is still problematic and is at this moment subject of study[34]. Third, we have excluded patients with large territorial infarcts from further analysis. We have done so because perfusion measures are clinically more interesting for tissues with reduced perfusion and less so for manifest (chronic) infarcts. In the latter case, the abnormality is already immediately evident from non-contrast CT and CTP has little added value.

In conclusion, this study shows that when performing CT perfusion studies, MTT is the most reproducible parameter independent of flow territory or the use of absolute values or perfusion ratios. Substantial intra- and inter-observer variability in the range between 16 and 21% can be expected if regional measurements of absolute CBV and CBF values are performed. In clinical practice, such quantitative regional analysis of CBV and CBF values should therefore be interpreted with caution. Variability can be reduced by using the ratio between symptomatic and asymptomatic hemispheres. A variation in the order of 10% and lower can be expected for CBV and CBF ratios in the MCA territory, which make such ratios more suitable for clinical application. MTT measurements show a similar low variability, independent of flow territory or whether absolute or relative values are employed.

References

1. Klotz E, Konig M. Perfusion measurements of the brain: using dynamic CT for the quantitative assessment of cerebral ischemia in acute stroke. Eur J Radiol 1999; 30:170-84.
2. Wintermark M, Reichhart M, Thiran JPet al. Prognostic accuracy of cerebral blood flow measurement by perfusion computed tomography, at the time of emergency room admission, in acute stroke patients. Ann Neurol 2002; 51:417-32.
3. Nabavi DG, LeBlanc LM, Baxter B et al. Monitoring cerebral perfusion after subarachnoid hemorrhage using CT. Neuroradiol 2001; 43:7-16.
4. Jain R, Hoeffner EG, Deveikis JP, Harrigan MR et al.Carotid perfusion CT with balloon occlusion and acetazolamide challenge test: feasibility. Radiology 2004; 231:906-13.
5. Roberts HC, Dillon WP, Smith WS. Dynamic CT perfusion to assess the effect of carotid revascularization in chronic cerebral ischemia. AJNR 2000 ;21:421-5.
6. Eastwood JD, Lev MH, Wintermark M et al. Correlation of early dynamic CT perfusion imaging with whole-brain MR diffusion and perfusion imaging in acute hemispheric stroke. AJNR 2003; 24:1869-75.
7. Reichenbach JR, Rother J, Jonetz-Mentzel L et al. Acute stroke evaluated by time-to-peak mapping during initial and early follow-up perfusion CT studies. AJNR 1999; 20:1842-50.
8. Wintermark M, Reichhart M, Cuisenaire O et al. Comparison of admission perfusion computed tomography and qualitative diffusion- and perfusion-weighted magnetic resonance imaging in acute stroke patients. Stroke 2002; 33:2025-31.
9. Koenig M, Kra us M, Theek C et al. Quantitative assessment of the ischemic brain by means of perfusion-related parameters derived from perfusion CT. Stroke 2001; 32:431-7.
10. Sase S, Honda M, Machida Ket al. Comparison of cerebral blood flow between perfusion computed tomography and xenon-enhanced computed tomography for normal subjects: territorial analysis. J Comput Assist Tomogr 2005; 29:270-7.
11. Hoeffner EG, Case I, Jain R et al. Cerebral perfusion CT: technique and clinical applications. Radiology 2004; 231:632-44.
12. Fiorella D, Heiserman J, Prenger E et al. Assessment of the reproducibility of postprocessing dynamic CT perfusion data. AJNR 2004 ; 25:97-107.
13. Parkes LM, Rashid W, Chard DT et al. Normal cerebral perfusion measurements using arterial spin labeling: reproducibility, stability, and age and gender effects. Magn Reson Med 2004; 51:736-43.
14. Powers WJ, Press GA, Grubb RL Jr et al. The effect of hemodynamically significant carotid artery disease on the hemodynamic status of the cerebral circulation. Ann Intern Med 1987; 106:27-34.
15. Soinne L, Helenius J, Tatlisumak T et al. Cerebral hemodynamics in asymptomatic and symptomatic patients with high-grade carotid stenosis undergoing carotid endarterectomy. Stroke 2003; 34:1655-61.
16. Mayer TE, Hamann GF, Baranczyk J et al. Dynamic CT perfusion imaging of acute stroke. AJNR 2000; 21:1441-9.
17. Furukawa M, Kashiwagi S, Matsunaga N et al. Evaluation of cerebral perfusion parameters measured by perfusion CT in chronic cerebral ischemia: comparison with xenon CT. J Comput Assist Tomogr 2002; 26:272-8.
18. Wintermark M. Simultaneous measurement of regional cerebral blood flow by perfusion CT and stable xenon CT: a validation study. AJNR 2001; 22:905-14.
19. Kealey SM, Loving VA, Delong DM et al. User-defined vascular input function curves: influence on mean perfusion parameter values and signal-to-noise ratio. Radiology 2004 ;231:587-93.
20. Sanelli PC, Lev MH, Eastwood JD et al. The effect of varying user-selected input parameters on quantitative values in CT perfusion maps. Acad Radiol 2004; 11:1085-92.
21. van der Schaaf I, Vonken EJ, Waaijer A et al. Influence of partial volume on venous output and arterial input function. AJNR 2006;27:46-50.
22. Wintermark M. Using 80 kVp versus 120 kVp in perfusion CT measurement of regional cerebral blood flow. AJNR 2000; 21:1881-4.
23. Wintermark M, Maeder P, Thiran J-P et al. Quantitative assessment of cerebral blood flows by perfusion CT studies at low injection rates. Eur Radiol 2001; 11:1220-1230

24. Axel L. Cerebral blood flow determination by rapid-sequence computed tomography: theoretical analysis. Radiology 1980; 137:679-86.
25. Meier P. Zierler KL. On the theory of the indicator-dilution mehtod for measurement of cerebral blood flow and volume. J App Physiol 1954; 6:731-44.
26. Damasio H. A computed tomographic guide to the identification of cerebral vascular territories. Arch Neurol 1983; 40:138-42.
27. Nabavi DG, Cenic A, Dool J et al. Quantitative assessment of cerebral hemodynamics using CT: stability, accuracy, and precision studies in dogs. J Comput Assist Tomogr 1999; 23:506-15.
28. Kluytmans M, van der Grond J, Viergever MA. Gray matter and white matter perfusion imaging in patients with severe carotid artery lesions. Radiology 1998; 209:675-82.
29. Wintermark M, Flanders AE, Velthuis B et al. Perfusion-CT assessment of infarct core and penumbra: receiver operating characteristic curve analysis in 130 patients suspected of acute hemispheric stroke. Stroke. 2006 Apr;37(4):979-85.
30. Schumann P, Touzani O, Young AR,et al. Evaluation of the ratio of cerebral blood flow to cerebral blood volume as an index of local cerebral perfusion pressure. Brain 1998;121:1369-79
31. Powers WJ. Cerebral hemodynamics in ischemic cerebrovascular disease. Ann Neurol 1991;29:231-40
32. Gibbs JM, Wise RJ, Leenders KL,et al. Evaluation of cerebral perfusion reserve in patients with carotid-artery occlusion. Lancet 1984;1:310-4.
33. Yamada K, Wu O, Gonzalez RG et al. Magnetic resonance perfusion-weighted imaging of acute cerebral infarction: effect of the calculation methods and underlying vasculopathy. Stroke 2002; 33:87-94.
34. Defining a local arterial input function for perfusion MRI using independent component analysis.Calamante F, Morup M, Hansen LK. Magn Reson Med 2004;52:789-97.
35. Lodder J, Hupperts R, Boreas A et al. The size of territorial brain infarction on CT relates to the degree of internal carotid artery obstruction. J Neurol 1996; 243:345-9.

Hemodynamic effects of carotid revascularization in patients with symptomatic carotid artery stenosis: a CT perfusion study

Chapter Seven

A Waaijer, MS van Leeuwen, MJP van Osch, HB van der Worp, FL Moll, TH Lo, WPThM Mali, M Prokop. Hemodynamic effects of carotid revascularization in patients with symptomatic carotid artery stenosis; a CT perfusion study.
In revision for Radiology

Abstract

Purpose

To evaluate whether pre-treatment CT perfusion (CTP) analysis can be used in patients with unilateral symptomatic carotid artery stenosis to predict which patients will benefit most from treatment in terms of cerebral perfusion.

Materials and Methods

Thirty-six patients with unilateral symptomatic carotid artery stenosis underwent CTP on a multislice CT scanner before and after carotid revascularization. We calculated cerebral blood volume (CBV), mean transit time (MTT) and cerebral blood flow (CBF) values, and derived relative numbers that compared symptomatic to asymptomatic hemispheres: ratios of CBV (rCBV) and CBF (rCBF) and difference in MTT (dMTT). Patients were stratified in groups according to pre-treatment hemodynamic compromise indicated by dMTT: group 1, dMTT <1s, group 2, dMTT 1-2s and group 3, dMTT >2s. Changes between pre- and post-treatment dMTT, rCBV and rCBF were assessed in each group.

Results

On average, rCBV decreased from 1.09 to 0.97 ($p<0.001$), dMTT decreased from 1.30s before to 0.18s after treatment ($p<0.001$) and rCBF increased from 0.85 to 0.92 ($p<0.05$). In group 1 (n=16, 44%) no significant changes were seen; in group 2 (n=12, 33%) rCBV and dMTT changed significantly, and in group 3 (n=8, 22%) rCBV as well as dMTT and rCBF changed significantly.

Conclusion

Pre-treatment dMTT can be used to predict which patients will most improve after treatment in terms of cerebral perfusion. We found significant improvement in all three relative perfusion parameters (rCBV, rCBF and dMTT) in only a small group of patients. This might hold promise for selecting patients that benefit most from carotid intervention.

Introduction

In patients with recently symptomatic internal carotid artery stenosis of 70% or greater, carotid endarterectomy (CEA) is highly beneficial and leads to an absolute reduction in 5-year risk of ipsilateral ischemic stroke of 16%. Although the efficacy of CEA in patients with symptomatic internal carotid artery stenosis ≥70% is beyond doubt, six patients have to undergo surgery to prevent one stroke. Surgery may also be considered for patients with ≥ 50% stenosis, but in these patients the number needed to treat to prevent one stroke is more than three times as high[1]. To improve the selection of patients for CEA, better understanding of the risk factors for stroke in these patients is required. Although only 20% of patients with a transient ischemic attack (TIA) or stroke have a significant stenosis or occlusion of the extracranial internal carotid artery[2] and the majority of TIA's and ischemic strokes result from thrombosis and thrombo-embolism[3], it has been suggested that severe cerebral hemodynamic compromise is also associated with an increased risk of stroke and TIA[4-6]. To distinguish patients with and without hemodynamic impairment, a simple, widely available tool to measure cerebral perfusion is required. CT cerebral perfusion is now used in patients with acute stroke for the detection of the penumbra and irreversible ischemic damage[7, 8], to assess secondary cerebral ischemia in patients with subarachnoid hemorrhage[9,10], and in combination with acetazolamide, to test vasomotor reactivity in patients with cerebral occlusive disease[11].
We hypothesized that CT perfusion (CTP) analysis before carotid revascularization can be used to identify patients with impaired perfusion and allows assessment of changes in perfusion after stent placement or carotid endarterectomy.

Materials and Methods

Patients

All patients were participants of the International Carotid Stenting Study (ICSS), a randomized controlled trial in which CEA and stent placement are compared (www.cavatas.com, ISRCTN 25337470). Inclusion was based on the presence of a symptomatic internal carotid artery stenosis >50%, equally suitable for CEA or stenting. Between September 2003 and May 2005, a CT perfusion study was added to the ICSS imaging protocol in 53 patients.
For this study, we included only patients with unilateral carotid artery stenosis. Exclusion criteria for our study were therefore a contralateral stenosis >50%, as measured with duplex ultrasound, a modified Rankin Scale score ≤ 3, and the presence of contra-indication for CT angiography, such as renal failure or contrast allergy. Seventeen patients were thus excluded from analysis: two patients developed an occlusion between the time of pre-treatment CTP and the intervention, nine patients had a >50% contralateral carotid stenosis, and six patients were excluded due to technical problems with contrast administration or motion artifacts. Consequently, 36 of the 53 ICSS patients who underwent CT perfusion in the study period could be included in the current study. Patients were scanned within two weeks prior to treatment and one month after stent placement or CEA. Before revascularization and at one month follow-up the degree of stenosis in the treated carotid artery was assessed in all patients using duplex ultrasound.

The medical ethics committee of our hospital had given approval for this study and written informed consent was obtained from all patients.

CT Perfusion Scanning

Imaging Protocol

Dynamic CTP source images were acquired using a 16-slice scanner (MX8000 IDT, Philips Medical Systems, Cleveland, OH) or 40-slice scanner (Brilliance-40, Philips Medical Systems, Cleveland, OH). The scan was performed at the level of the basal ganglia, 3cm above the dorsum sellae, with the scan angle set parallel to the orbitomeatal line to avoid direct radiation exposure to the eye lenses. For the 16-slice scanner a collimation of 8 x 3mm was used and scans were reconstructed in two slabs of 12mm, yielding 2.4cm coverage. With the introduction of 40-slice technique, a collimation of 32 x 1.25mm was used and images were reconstructed in four adjacent slabs of 10mm, yielding 4.0cm coverage. The cycle time was 2s, resulting in 30 images acquired during 60s which has shown to result in accurate perfusion data[12]. For optimum signal-to-noise ratio, we used a low-kVp technique (90kVp on the 16-slice scanner, 80kVp on the 40-slice scanner) in combination with 150mAs[13]. Images were reconstructed using a slightly smoothing head filter ("UB") with a field of view of 160mm.
For all perfusion scans a bolus injection of 40ml contrast with an iodine concentration of 300mg I/ml (Ultravist 300, Schering AG, Berlin, Germany) was administered at 5ml/s followed by a 40ml-saline chaser bolus at 5ml/s using a power injector with a dual head system (Stellant Dual CT injector, Medrad Europe BV, Beek, The Netherlands).

Technique

CTP data were transferred to a post-processing workstation (Philips Medical Systems, Best, the Netherlands) on which cerebral blood volume (CBV), mean transit time (MTT), and cerebral blood flow (CBF) were calculated. Time-enhancement curves derived from contrast passage through the anterior cerebral artery and the superior sagittal sinus provided the arterial input function (AIF) and venous output function (VOF) respectively. For AIF, a region of interest (ROI) was placed over the both anterior cerebral arteries at each slab were after the computer depicted the optimum curve, based on height of the peak and the size of the area under the curve. The same was done for VOF within the superior sagittal sinus. Visual inspection by the operator was performed to assure that the complete AIF and at least seven points of the down slope of the VOF were shown. The CBV was calculated as the ratio of the area under the time concentration curve of the first bolus passage through the tissue to that of the area under the curve of the VOF. The MTT, the average time required by the blood to cross the capillary network, was calculated by a deconvolution operation[14]. According to the central volume principle, CBF was calculated from measured CBV and MTT values: CBF = CBV/ MTT[15]. This method has shown to be most accurate at lower injection rates[16, 17].

Postprocessing

To quantify changes in perfusion parameters before and after CEA or stenting, the two slabs closest to level of the basal ganglia of the pre-treatment CTP scan were matched to two corresponding slabs at the same level on the post-treatment CTP scan. On each slab an ROI was manually outlined corresponding to the cortical flow territory of the middle cerebral artery (MCA) on both hemispheres according to the maps of Damasio[18]. Automatic removal of bone, vessels and cerebrospinal fluid was always applied (*Figure 1*).

Data Analysis

CT perfusion analysis provides absolute perfusion data for each pixel in the symptomatic and asymptomatic hemispheres; CBV expressed asml/100 g tissue, MTT expressed in seconds and CBF expressed inml/100 g tissue/min. As brain perfusion measurements are subject to high inter-subject variation and influenced by physiologic stimuli[19, 20] we chose to include relative perfusion data in our analysis by normalizing measured values in the symptomatic hemisphere to those in the asymptomatic hemisphere. As a relative measure for MTT we chose the absolute difference in MTT values between the symptomatic and the asymptomatic hemisphere (dMTT) because MTT itself is derived from the difference between the width of the curves (AIF and voxel of interest). For relative CBF (rCBF) and relative CBV (rCBV) the ratios of the symptomatic to the asymptomatic hemisphere were calculated because these parameters are derived from the ratio of the areas under the attenuation curves (VOF and voxel of interest). For each CTP scan the mean of measurements in the two evaluated slabs was calculated for both absolute and relative data.

First we analyzed the total group of patients and compared absolute pre- and post treatment values and symptomatic versus asymptomatic hemispheres using a paired t-test. Subsequently, we analyzed the relative data and compared pre- and post treatment rCBV, dMTT and rCBF. Finally, we classified patients into three groups according to the baseline dMTT. MTT was chosen since this parameter has shown to be most reproducible[37,38]. In group 1 dMTT was <1s, in group 2 dMTT was 1-2s and in group 3 it was >2s, since this matched the recently reported values of Wintermark et al[34]. In each group, pre-treatment and post-treatment values for rCBV, dMTT and rCBF were compared using the Wilcoxon signed ranks test. Statistical analysis was performed using statistical package SPSS version 12.0. A p-value <0.05 was considered statistically significant.

Results

Patient characteristics are shown in *Table 1*. None of the included patients had symptoms between pre- and post-treatment CT and all but one patient had normalization of carotid duplex values after treatment. In groups 1 and 2 half of the patients had been randomized to stent placement and half of them to carotid endarterectomy while 75% of the patients in group 3 had been randomized to stent placement (difference not significant).

Figure 1 *Manual outlining of MCA territory. The green overlay shows the selected region without bone, vessels and cerebrospinal fluid that is used for calculation of perfusion values.*

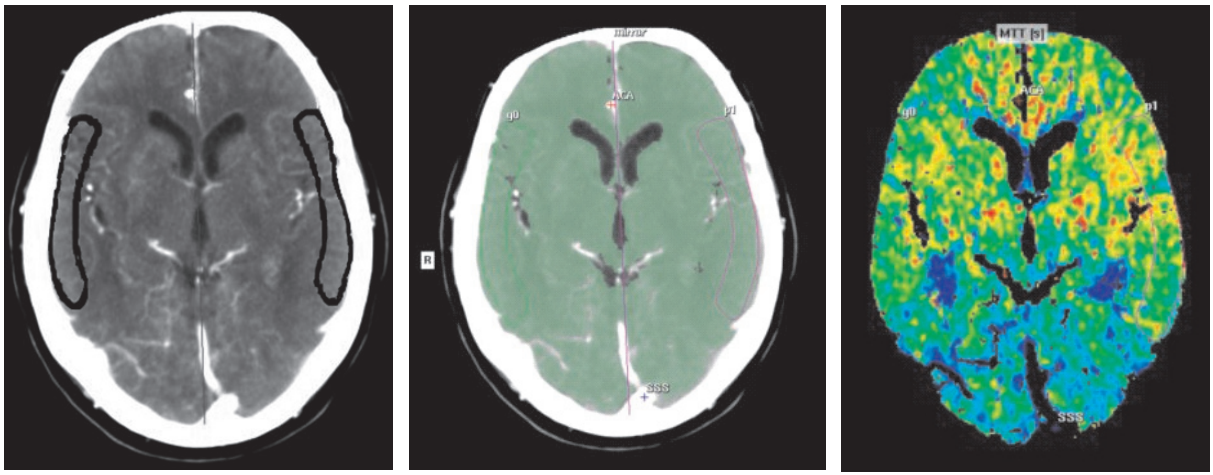

Absolute Perfusion Parameters

When comparing CT perfusion parameters before and after revascularization, we only found a significant decrease of MTT in the symptomatic hemisphere from to 5.7 ± 1.5 s before to 4.8 ± 1.2 s after treatment. No other perfusion parameter changed significantly (*Table 2*).

Relative Perfusion Parameters

Mean rCBV decreased from 1.09 ± 0.15 to 0.97 ± 0.12 ($p<0.001$), dMTT decreased from 1.30 ± 1.10s before to 0.18 ± 0.40s after carotid revascularization ($p<0.001$) and mean rCBF increased from 0.85 ± 0.18 to 0.92 ± 0.14 ($p=0.018$). *Table 2*

Subgroup Analysis based on dMTT

In 16 patients (44%) baseline dMTT was < 1s (group 1), in 12 patients (33%) baseline dMTT was 1-2s (group 2), and in eight patients (22%) baseline dMTT was > 2s (group 3).

The effect of carotid revascularization on cerebral perfusion parameters was highly dependent on the baseline dMTT (*Table 3*). In the 16 patients of group 1, no significant change in any of the relative CT perfusion values could be detected. In the 12 patients of group 2, mean rCBV decreased from 1.07 to 0.95 ($p<0.05$) and dMTT decreased by 1.30s ($p<0.05$) but no significant changes in rCBF occurred (from 0.82 to 0.90, $p=0.117$). In group 3 (22%), substantial improvement in cerebral perfusion parameters after treatment was found. Mean rCBV and dMTT decreased significantly (with 0.25 and 2.75s respectively), while rCBF increased significantly from 0.67 to 0.87 after treatment, a more than 30% increase (*Figure 2a-c* and *3*).

Table 1 *Patient characteristics (n=36)*

Patient demographics	
Age, years mean ± SD	67 ± 11
Males, n (%)	23 (64)
Presenting event	
Amaurosis fugax	13
TIA	19
Ischemic stroke	13
Treatment	
Carotid endarterectomy	15
Stenting	21
Carotid arteries	
Mean stenosis symptomatic side, ±SD (range)	86 ± 12% (55%, 99%)
Mean stenosis asymptomatic side, ±SD (range)	14 ± 15% (0%, 45%)
Left side symptomatic, n (%)	17 (47%)
Duplex ultrasound (peak systolic velocity, symptomatic side)*	
Before treatment (range)	388 cm/s (175 cm/s, 600 cm/s)
After treatment (range)	92 cm/s (20 cm/s, 210 cm/s)
Interval (days)	
Baseline CTP to post-treatment CTP (range)	42 d (27 d, 83 d)
Treatment to post-treatment CTP (range)	35 d (27 d, 54 d)
Medical history	
Hypertension, n (%)	19 (53%)
Diabetus Mellitus, n (%)	4 (11%)
Cardiac failure/ previous CABG/	
Atrial fibrillation/ previous MI, n (%)	8 (25%)

** 50% stenosis PSV>210 cm/s, 70% stenosis PSV>270 cm/s)*

Table 2 *Comparison of pre- and post-treatment CT perfusion data for the symptomatic and asymptomatic hemisphere (absolute perfusion values).*

ABSOLUTE DATA			
	CBV (ml / 100 g) mean ± SD	**CBF (ml / 100g / min) mean ± SD**	**MTT (s) mean ± SD**
Asymptomatic hemisphere, before treatment	5.0 ± 1.4	69.4 ± 27.5*	4.6 ± 1.1*
Asymptomatic hemisphere, after treatment	5.1 ± 1.7**	67.8 ± 23.9**	4.7 ± 1.3
Symptomatic hemisphere, before treatment	5.2 ± 1.2	57.9 ± 20.0*	5.7 ± 1.5*,†
Symptomatic hemisphere, after treatment	4.8 ± 1.5**	63.3 ± 21.9**	4.8 ± 1.2†

* *before treatment: significant difference between ipsilateral and contralateral hemisphere (p<0.01)*

** *after treatment: significant difference between ipsilateral and contralateral hemisphere (CBF, p<0.01; CBV, p<0.05)*

† *symptomatic hemisphere: significant difference before and after treatment (p<0.01)*

Table 3 *Comparison of relative CTP perfusion parameters for groups based on pre-treatment dMTT (group 1, dMTT <1s, group 2, dMTT 1-2s and group 3, dMTT >2s). Significance of difference between relative perfusion parameters before and after treatment was tested using the Wilcoxon signed ranks test. In addition, the mean degree of carotid stenosis on the symptomatic side measured by Duplex ultrasound is provided for comparison.*

	Group 1		**Group 2**		**Group 3**	
	n=16		**n=12**		**n=8**	
	mean ± SD	**p-value**	**mean ± SD**	**p-value**	**mean ± SD**	**p-value**
rCBV						
Pre-treatment	1.05 ± 0.2		1.07 ± 0.1		1.16 ± 0.14	
Post-treatment	1.00 ± 0.1	0.362	0.95 ± 0.2	**<0.05**	0.91 ± 0.12	**<0.05**
dMTT						
Pre-treatment	0.39 ± 0.5		1.40 ± 0.3		3.00 ± 0.6	
Post-treatment	0.23 ± 0.4	***0.346***	0.06 ± 0.5	***< 0.05***	0.25 ± 0.2	***< 0.05***
rCBF						
Pre-treatment	0.97 ± 0.2		0.82 ± 0.1		0.67 ± 0.2	
Post-treatment	0.96 ± 0.1	***0.730***	0.90 ± 0.2	***0.117***	0.87 ± 0.1	***<0.05***
Carotid stenosis						
Mean degree	78%		91%		93%	
(Range)	(55, 95)		(75, 99)		(85, 99)	

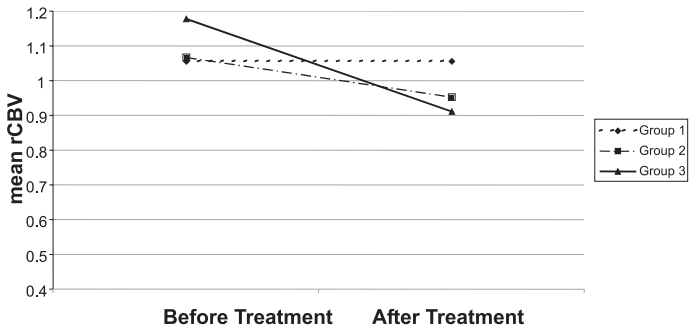

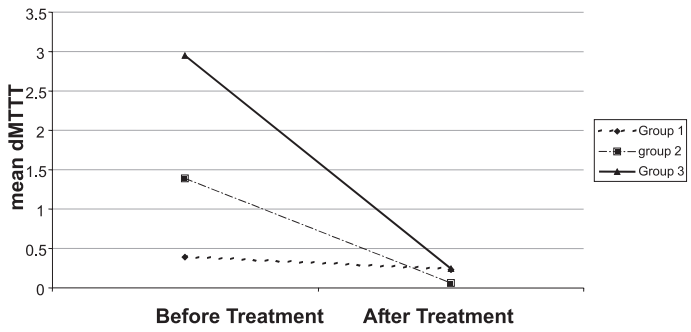

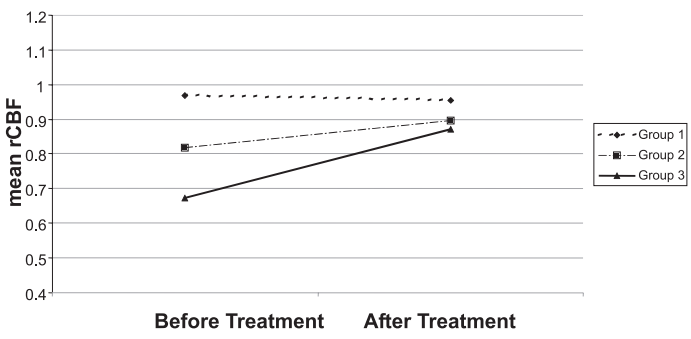

Figure 2a-c *Relative CT perfusion values measured before and after treatment for the three groups separately; Cerebral Blood Volume (2a) Mean Transit Time (2b) and Cerebral Blood Flow (2c).*

Figure 3 *Example of a patient from group 3 with a left sided carotid artery stenosis. The upper row shows the CT perfusion data and angiography before treatment while the lower row demonstrates the perfusion and angiography after treatment. Note the presence of prolonged MTT, slightly increased CBV and decreased CBF on the ipsilateral side before treatment, while after treatment there is symmetry of brain perfusion.*

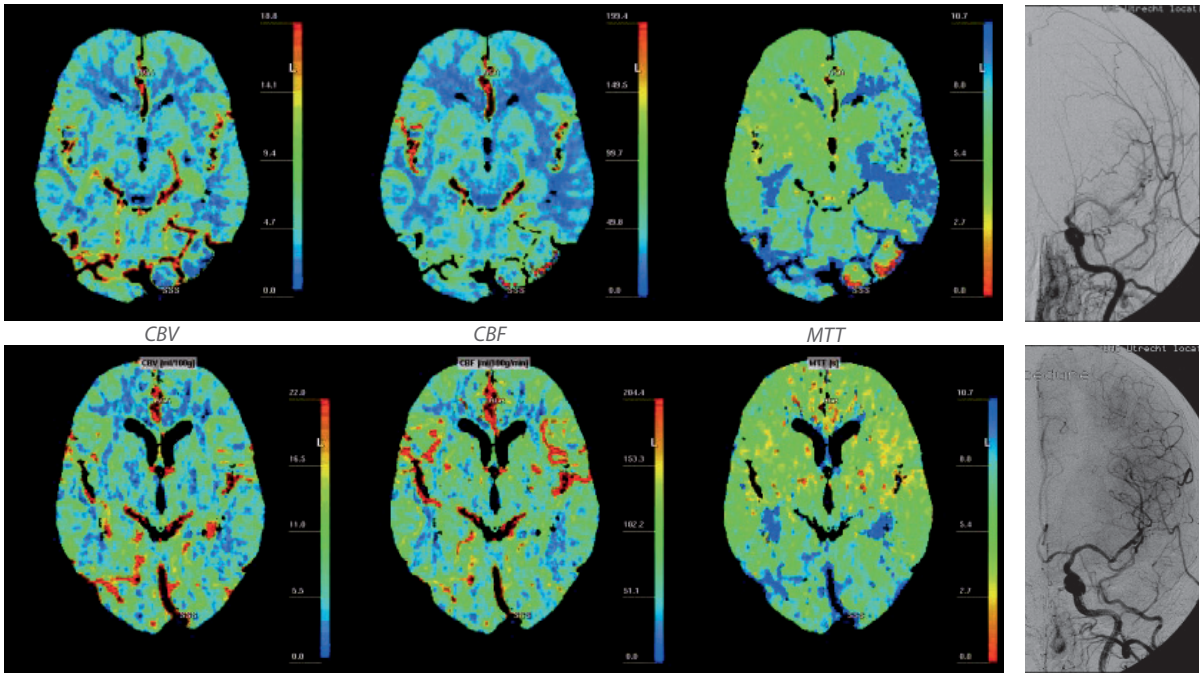

Discussion

Purpose of this CT perfusion study was to evaluate whether pre-treatment CT perfusion analysis in patients with unilateral symptomatic carotid artery stenosis can be used to distinguish between groups of patients that will respond differently to carotid revascularization. Using the inter-hemispheric difference in MTT at baseline, we could differentiate three groups of patients that differed in their subsequent response to treatment.

Our most important finding is that the group of patients with the largest inter-hemispheric MTT difference before treatment demonstrated significant changes in all examined perfusion parameters after treatment: the inter-hemispheric ratio of CBV (rCBV) decreased, the inter-hemispheric difference in MTT (dMTT) decreased and the inter-hemispheric ratio of CBF (rCBF) improved. However, this was the smallest group that contained only 22% of our patients. In the largest group of patients (44%) with an inter-hemispheric difference in MTT of less than 1s before revascularization no significant change in rCBV, dMTT or rCBF could be found after treatment. In 33% of our

patients the inter-hemispheric difference in MTT was 1-2s before treatment; in this group we found a significant improvement in rCBV and dMTT after carotid revascularization but no substantial change in rCBF.

Although only a minority of patients with a TIA or stroke have a significant stenosis or occlusion of the extracranial internal carotid artery[2], current patient selection for treatment of internal carotid artery stenosis is primarily based on the severity of the carotid stenosis but not on the presence or absence of ipsilateral hemodynamic compromise. Such an ipsilateral hemodynamic compromise is most likely the final result of a multitude of factors, including severity of the stenosis, the capacity for collateral compensation via the circle of Willis or leptomeningeal pathways. Risk of cerebrovascular events, however, is also related to other factors, such as plaque composition[21].

Patients with symptomatic carotid artery stenosis and ipsilateral hemodynamic compromise are at higher risk of disabling stroke than patients with normal cerebral perfusion[4]. Also, impaired cerebral perfusion is associated with watershed infarctions[22] and improvement of cerebral perfusion after carotid revascularization is associated with improvement in cognitive function[23, 24].

Early studies of cerebral perfusion after carotid endarterectomy reached conflicting conclusions[25], and improvement of imaging techniques has not resolved this controversy[26-29]. Part of these conflicting findings can be explained by the fact that most studies did not distinguish between patients with and patients without a baseline perfusion deficit. Further confusion has been caused by combining data from symptomatic and asymptomatic patients, carotid occlusions and carotid stenosis, and patients with unilateral and bilateral disease, despite the differences in response to treatment in these various groups[28, 30-32].

Thus, while earlier studies provided evidence for the presence of impaired perfusion in some patients with symptomatic carotid artery stenosis, it was not clear which individual patient would see a hemodynamic benefit from treatment, nor to what extent hemodynamic improvement could be expected, nor which technique or parameter provided the most useful information. Our results demonstrate that the MTT difference between symptomatic and asymptomatic hemispheres can be used to differentiate between groups of patients with unilateral symptomatic carotid artery stenosis with different response to treatment in terms of cerebral perfusion.

According to the formula CBF=CBV/ MTT, CBF is inversely related to MTT and proportional to CBV. In the first phase of hemodynamic compromise reduced arterial blood supply results in reduction of cerebral perfusion pressure (CPP) which results in prolongation of MTT. As a compensatory mechanism there is vasodilatation that results in an increased CBV. Consequently, CBF may remain within the normal range (Phase 1). As MTT increases further, compensatory vasodilatation reaches its maximum, and further hemodynamic compromise results in reduced CBF (Phase 2)[33]. This concept is in accordance with the finding that MTT has been shown to be sensitive to perfusion changes[32, 34].

In addition, the MTT is inversely correlated with CPP[35]. The extent of reduction of cerebral perfusion pressure has been called an important goal for cerebral perfusion analysis in patients suspected of hemodynamic impairment[33]. We therefore chose MTT as a selection parameter and differentiated three groups depending on the inter-hemispheric difference in dMTT at baseline. However, while the MTT normalized after treatment, rCBF remained <1.0 for all three groups (*Figure 2c*), indicating a reduced CBF in the hemisphere ipsilateral to the carotid stenosis. The cause of this lack of normalization is unclear but it may be related to the presence of irreversible changes of the intracranial vasculature.

To our knowledge this is the first study that shows impairment of cerebral perfusion in a subgroup of patients with symptomatic carotid artery stenosis using CT perfusion. Unlike PET or SPECT techniques CTP allows direct measurement of MTT, and in contrast to transcranial Doppler, CTP allows territorial analysis. Although the patients with dMTT> 2s had on average the highest degree of stenosis, severity of stenosis in group 1 (dMTT<1s) ranged from 55-95%, indicating that the degree of stenosis is not the only factor that determines the severity of perfusion impairment, which has been shown previously[36].

Our study has some limitations. Although CT perfusion analysis yields absolute quantitative data, several studies have shown that values obtained with this technique are subject to physiological variations and are influenced by post-processing steps[37, 38]. Some of these limitations, intrinsic to absolute perfusion values, are overcome by using relative perfusion parameters, relating the absolute perfusion data in the symptomatic hemisphere to the contralateral, asymptomatic hemisphere. The advantage of this approach is the elimination of physiological variations and inter-patient differences in total cerebral perfusion but the disadvantage is that results will be more difficult to interpret when significant stenoses are present in both carotid arteries. Also, the presence of a carotid stenosis has shown to influence the AIF and may result in overestimation of absolute MTT and underestimation of absolute CBF using MRI perfusion[39]. Despite discussion about the placement of AIF, recent investigations have shown that there is no significant difference in CTP values based on the ipsi- or contra-lateral AIF in patients with a severe carotid artery stenosis[40].

Secondly, we did not compare CT perfusion values to a reference standard such as PET or Xe-CT. However, previous studies have already shown that CBF measured with CT perfusion correlates well to these established techniques[16,39].

Third, we did not evaluate the effects of the configuration of the circle of Willis on perfusion because for such a multi-factorial analysis much more patients are needed and the purpose of this study was to evaluate whether it is possible to discriminate patients with different response to carotid intervention based on cerebral perfusion at baseline.

Fourth, we included patients treated by carotid endarterectomy and stent placement. In our opinion this is acceptable because patients had been randomized to either treatment strategy and no major differences in terms of success of carotid revascularization were expected. We also confirmed this with duplex measurements that demonstrated normalization of peak systolic velocities in all but one patient (treated with stent placement). The fact that group 3 contained more stent patients was not statistically significant and potentially related to the relatively small size of the study population.

Fifth, the included patients all had Rankin <3, but could still have cerebral infarction. We have included these patients since they consist a relevant part of all patients that may benefit from treatment. However, in case of cerebral infarction, we have always avoided inclusion of damaged brain to achieve representative perfusion values.

Conclusion

Knowledge of individual cerebral perfusion parameters may help to predict the improvement in cerebral perfusion after treatment of carotid artery stenosis. Using the inter-hemispheric difference in MTT before treatment as a discriminator between groups of patients we found that the effect of carotid revascularization on cerebral perfusion is highly dependent on the severity of the MTT difference before treatment. Only a subgroup of the patients (22%) with symptomatic carotid artery stenosis showed a significant improvement in rCBV, dMTT and rCBF after treatment while more than 40% of patients did not have any significant change in perfusion parameters. This may indicate that only a subgroup of patients with symptomatic carotid artery stenosis suffers from hemodynamic impairment. Since CT perfusion is a widely available tool it may help increase our insight in the hemodynamic mechanisms in patients with symptomatic carotid artery stenosis.

References

1. Rothwell PM, Eliasziw M, Gutnikov SA et al. Analysis of poooled data from the randomised controlled trials of endarterectomy for symptomatic carotid stenosis. Lancet 2003;361:107-16
2. Hankey GJ, Slattery JM, Warlow CP. The prognosis of hospital-referred transient ischaemic attacks. J Neurol Neurosurg Psychiatry 1991;54:793-802
3. Barnett HJ. Hemodynamic cerebral ischemia. An appeal for systematic data gathering prior to a new EC/IC trial. Stroke 1997;28:1857-60
4. Blaser T, Hofmann K, Buerger T, Effenberger O, Wallesch CW, Goertler M. Risk of stroke, transient ischemic attack, and vessel occlusion before endarterectomy in patients with symptomatic severe carotid stenosis. Stroke 2002;33:1057-62
5. Caplan LR, Hennerici M. Impaired clearance of emboli (washout) is an important link between hypoperfusion, embolism, and ischemic stroke. Arch Neurol 1998;55:1475-82
6. Markus H, Cullinane M. Severely impaired cerebrovascular reactivity predicts stroke and TIA risk in patients with carotid artery stenosis and occlusion. Brain 2001;124:457-467
7. Wintermark M, Reichhart M, Cuisenaire O et al. Comparison of admission perfusion computed tomography and qualitative diffusion- and perfusion-weighted magnetic resonance imaging in acute stroke patients. Stroke 2002;33:2025-31
8. Klotz E, Konig M. Perfusion measurements of the brain: using dynamic CT for the quantitative assessment of cerebral ischemia in acute stroke. Eur J Radiol 1999;30:170-84
9. Nabavi DG, LeBlanc LM, Baxter B et al. Monitoring cerebral perfusion after subarachnoid hemorrhage using CT. Neuroradiol 2001;43:7-16
10. van der Schaaf I, Wermer MJ, van der Graaf Y, Velthuis BK, van de Kraats CI, Rinkel GJ. Prognostic value of cerebral perfusion-computed tomography in the acute stage after subarachnoid hemorrhage for the development of delayed cerebral ischemia. Stroke 2006;37:409-13
11. Jain R, Hoeffner EG, Deveikis JP, Harrigan MR, Thompson BG, Mukherji SK. Carotid perfusion CT with balloon occlusion and acetazolamide challenge test: feasibility. Radiology 2004;231:906-13
12. Wintermark M, Smith WS, Ko NU, Quist M, Schnyder P, Dillon WP. Dynamic perfusion CT: optimizing the temporal resolution and contrast volume for calculation of perfusion CT parameters in stroke patients. AJNR 2004 ;25:720-9.
13. Wintermark M. Using 80kVp versus 120kVp in perfusion CT measurement of regional cerebral blood flow. AJNR 2000; 21:1881-4.
14. Axel L. Cerebral blood flow determination by rapid-sequence computed tomography: theoretical analysis. Radiology 1980;137:679-86
15. Meier P. Zierler KL. On the theory of the indicator-dilution mehtod for measurement of cerebral blood flow and volume. J App Physiol 1954; 6:731-44.
16. Wintermark M, Thiran JP, Maeder P, Schnyder P, Meuli R. Simultaneous measurement of regional cerebral blood flow by perfusion CT and stable xenon CT: a validation study. AJNR 2001;22:905-14
17. Wintermark M, Maeder P, Thiran JP, Schnyder P, Meuli R. Quantitative assessment of regional cerebral blood flows by perfusion CT studies at low injection rates: a critical review of the underlying theoretical models. Eur Radiol. 2001;11:1220-30.
18. Damasio H. A computed tomographic guide to the identification of cerebral vascular territories. Arch Neurol 1983;40:138-42
19. Parkes LM, Rashid W, Chard DT, Tofts PS. Normal cerebral perfusion measurements using arterial spin labeling: reproducibility, stability, and age and gender effects. Magn Reson Med 2004;51:736-43
20. Field AS, Laurienti PJ, Yen YF, Burdette JH, Moody DM. Dietary caffeine consumption and withdrawal: confounding variables in quantitative cerebral perfusion studies? Radiology 2003;227:129-35
21. Takaya N, Yuan C, Chu B et al. Association between carotid plaque characteristics and subsequent ischemic cerebrovascular events: a prospective assessment with MRI--initial results. Stroke 2006; 37:818-23.
22. Ringelstein EB, Weiller C, Weckesser M, Weckesser S. Cerebral vasomotor reactivity is significantly reduced in low-flow as compared to thromboembolic infarctions: the key role of the circle of Willis. J Neurol Sci 1994 ;121:103-9
23. Kishikawa K, Kamouchi M, Okada Y, Inoue T, Ibayashi S, Iida M. Effects of carotid endarterectomy on cerebral blood flow and neuropsychological test performance in patients with high-grade carotid stenosis. J Neurol Sci 2003;213:19-24
24. Moftakhar R, Turk AS, Niemann DB et al. Effects of carotid or vertebrobasilar stent placement on cerebral perfusion and cognition. AJNR 2005;26:1772-80

25. Schroeder T. Hemodynamic significance of internal carotid artery disease. Acta Neurol Scand 1988;77:353-72
26. Wilkinson ID, Griffiths PD, Hoggard N et al. Short-term changes in cerebral microhemodynamics after carotid stenting. AJNR 2003;24:1501-7
27. Gauvrit JY, Delmaire C, Henon H et al Diffusion/perfusion-weighted magnetic resonance imaging after carotid angioplasty and stenting. J Neurol 2004;251:1060-7
28. Kluytmans M, van der Grond J, Viergever MA. Gray matter and white matter perfusion imaging in patients with severe carotid artery lesions. Radiology 1998;209:675-82
29. Ances BM, McGarveyml, Abrahams JM et al. Continuous arterial spin labeled perfusion magnetic resonance imaging in patients before and after carotid endarterectomy. J Neuroimaging 2004;14:133-8
30. Sacca A, Pedrini L, Vitacchiano G et al. Cerebral SPECT with 99mTc-HMPAO in extracranial carotid pathology: evaluation of changes in the ischemic area after carotid endarterectomy. Int Angiol 1992;11:117-21
31. Cikrit DF, Dalsing MC, Harting PS et al. Cerebral vascular reactivity assessed with acetazolamide single photon emission computer tomography scans before and after carotid endarterectomy. Am J Surg 1997;174:193-7
32. Soinne L, Helenius J, Tatlisumak T et al. Cerebral hemodynamics in asymptomatic and symptomatic patients with high-grade carotid stenosis undergoing carotid endarterectomy. Stroke 2003;34:1655-61
33. Derdeyn CP, Grubb RL Jr, Powers WJ. Cerebral hemodynamic impairment: methods of measurement and association with stroke risk. Neurology 1999;53:251-9
34. Wintermark M, Flanders AE, Velthuis B et al. Perfusion-CT assessment of infarct core and penumbra: receiver operating characteristic curve analysis in 130 patients suspected of acute hemispheric stroke. Stroke 2006;37:979-85
35. Schumann P, Touzani O, Young AR, Morello R, Baron JC, MacKenzie ET. Evaluation of the ratio of cerebral blood flow to cerebral blood volume as an index of local cerebral perfusion pressure. Brain 1998;121:1369-79
36. Powers WJ, Press GA, Grubb RL Jr et al. The effect of hemodynamically significant carotid artery disease on the hemodynamic status of the cerebral circulation. Ann Intern Med 1987; 106:27-34.
37. Sanelli PC, Lev MH, Eastwood JD, Gonzalez RG, Lee TY. The effect of varying user-selected input parameters on quantitative values in CT perfusion maps. Acad Radiol. 2004;11:1085-92
38. Fiorella D, Heiserman J, Prenger E, Partovi S. Assessment of the reproducibility of postprocessing dynamic CT perfusion data. AJNR 2004;25:97-107
39. Yamada K, Wu O, Gonzalez RG, Bakker D, Ostergaard L, Copen WA, Weisskoff RM, Rosen BR, Yagi K, Nishimura T, Sorensen AG. Magnetic resonance perfusion-weighted imaging of acute cerebral infarction: effect of the calculation methods and underlying vasculopathy. Stroke. 2002;33:87-94.
40. Bisdas S, Nemitz O, Berding G, Weissenborn K, Ahl B, Becker H, Donnerstag F. Correlative assessment of cerebral blood flow obtained with perfusion CT and positron emission tomography in symptomatic stenotic carotid disease.Eur Radiol 2006 Apr 1; [Epub ahead of print]

Summary, conclusions, discussion and future perspectives

Chapter Eight

Summary

Chapter 1 provides an introduction to this thesis. In the Netherlands about 40.000 patients yearly suffer from stroke or TIA. In 20-30% of these cases a stenosis in the carotid artery is found. This stenosis is caused by atherosclerotic plaque formation. Symptoms are thought to be the result of cerebral embolism by formation of thrombi at the plaque and the luminal obstruction which causes reduced blood flow to the brain. Endarterectomy has proven beneficial in the prevention of stroke by removal of this stenosis, but carries a risk for complications. However, a new treatment option has been proposed: carotid artery stenting. Although this is a very promising less-invasive treatment, it has not yet proven to be as effective as surgery. Therefore the UMCU participates in an international randomized controlled trial, the ICSS. We studied participants of the ICSS using multislice CT technique, offering a unique population of patients with symptomatic carotid artery stenosis to study pathophysiologic mechanisms of stroke.

Chapter 2 describes the possibilities of the multislice CT for neurovascular applications. The main improvement of this technique, compared to single-slice technique, is that multislice CT angiography results in near-isotropic imaging and fast rotation times that allow imaging of the whole range from the aortic arch to the intra-cranial vasculature within 15 seconds. This gives good images for evaluation of the carotid stenosis and thereby makes this technique competitive with MRA. It can be used to determine the degree of carotid stenosis, to analyze the patency of intracranial arteries (the circle of Willis) and to measure brain perfusion. The combination of non-contrast enhanced CT, CTP and CTA result in a complete work-up in patients with cerebrovascular disease and can easily be performed in the acute situation. Techniques to measure the degree of stenosis and to display the vasculature are discussed and scan parameters for both 16, 40 and 64 slice CT are provided.

In *Chapter 3* the effect of lowering kVp and varying mAs on image quality on CTA of the Circle of Willis was assessed by phantom experiments as well as clinical evaluation. The goal was to see whether improvement of image quality could be achieved in combination with dose reduction.
Dose is mainly determined by two factors: mAs and Kilovoltage (kVp). If one or both is increased this results in higher dose and less noise. Principally increase of dose results in improvement of image quality. However, the iodine in contrast material that is used for CTA, has the property that it gives more attenuation (signal) at lower kVp. Phantom experiments showed that at identical dose, the use of 90kVp with adaptation of mAs, resulted in a better signal-to-noise ratio compared to the conventionally used 120kVp. In patients, mean CT attenuation was significantly higher with 90kVp than with 120kVp. Also, in patients that were scanned with 90kVp resulting in 30% lower total dose in stead of 120kVp and regular dose, the arterial enhancement and visualization of small arterial detail improved significantly, resulting in better overall image quality. It was thus concluded that the use of lower kilovoltage settings can improve image quality at lower total patient dose.

Chapter 4 describes the anatomical variations in the circle of Willis in 91 ICSS patients. The circle of Willis consists of 5 arterial segments at the base of the brain that are all connected if the circle is complete. It can thereby provide collateral flow via the contralateral carotid artery or the vertebro-basilar system in patients with carotid stenosis. However, autopsy studies have shown that the circle has many configurations including missing segments, asymmetry or hypoplasia of segments, thereby hampering potential routes for collateral flow. We compared the ICSS population to 91 patients without cerebrovascular disease, and assessed the presence and size of the segments of the circle both in patients and controls. In ICSS patients we found significantly more absent or hypoplastic segments in the anterior part of the circle. This suggests that incompleteness of the circle may be a risk factor for the development of symptoms in case of carotid stenosis by preventing collateral supply.

In *Chapter 5* we compared various techniques to measure the degree of stenosis using Multislice CT and compared this to DSA as standard of reference. DSA was performed in all patients that were randomized to carotid artery stenting. Since CTA has lower resolution compared to DSA, use of reconstructions, calipers and preset windowing criteria have been proposed. Two experienced observers, one 5 year resident and one first year resident performed visual estimation and measurement using calipers on multiplanar reconstructions with wide window settings and with preset window settings, for 55 carotid arteries. The use of visual estimation outperformed the other techniques for all four observers and resulted in comparable inter-observer variability as repeated DSA measurements.

To evaluate the potentials of CT perfusion, first the reproducibility of CT perfusion measurements was determined. *Chapter 6* describes the results of two observers who determined perfusion values in 20 patients with unilateral symptomatic carotid artery stenosis. We established intra- and inter-observer variability for regional measurement of CT perfusion in four cerebral territories and evaluated whether reproducibility can be improved by calculating relative perfusion values.
We concluded that MTT is the most reproducible CTP parameter in patients with unilateral symptomatic CAS. Measurement variability in CBV and CBF can be improved if CTP ratios instead of CTP values are used. The MCA territory shows the least measurement variability.

In *Chapter 7* we determined whether pre-treatment CT perfusion analysis in patients with unilateral symptomatic carotid artery stenosis can be used to distinguish between groups of patients that will respond differently to carotid revascularization, in terms of changes in cerebral perfusion.
Based on the previous study we used relative MTT defined as difference in MTT between two hemispheres, to distinguish three groups of patients (group 1; <1s, group 2; 1-2s and group 3; >2s inter hemispheric difference in MTT). Sixteen patients (44%) were classified in group 1, 12 patients (33%) in group 2, and eight patients (22%) in group 3. Only patients with the largest MTT difference (group 3) showed significant improvement of CBF, CBV and MTT. This indicates that the relative MTT before treatment may be used as parameter that can predict hemodynamic response to treatment.

Conclusions and discussion

Stroke and TIA are common causes of death and long-term disability in the Netherlands, frequently being caused by carotid artery stenosis. At this moment, screening of patients with symptomatic carotid artery stenosis consists of duplex in combination with MRA. In case of disagreement DSA is performed. Treatment decision is mainly based on the severity of stenosis degree, as a beneficial effect of endarterectomy dependent on the degree of stenosis, was shown in large trials. However, numbers on risk reduction acquired from trials should be interpreted with care, since they do not necessarily provide the evidence for treatment of the individual patient[1]. Increasingly attention is paid to the multi-factorial determination of benefit from treatment.

In such perspective, the advantage of MSCT is twofold. First is the wide accessibility of CT scanners that are mostly 24/7 available, also for patients that are in worse condition and require monitoring etc. This is an important property in patients with symptomatic carotid stenosis where a quick intervention results in a substantial increase of benefit of surgical treatment[2, 3]. Second, CT angiography of the carotids gives not only information about stenosis but in one scan session also about the circle of Willis and brain perfusion.

We concluded that if multislice CTA is used to determine the degree of stenosis, visual estimation is the most reproducible and accurate way to measure the degree of stenosis. Although generally measurement on the axial source images is recommended, visual estimation outperformed measurement using calipers, both for experienced and non-experienced observers. This implies that it is not required to make difficult and time-consuming reconstructions to measure the degree of stenosis. On the contrary, we revealed that simple estimation provides a quick and robust method to assess the stenosis.
Beside the stenosis degree, other factors have also shown to influence the risk of recurrent stroke and TIA, such as the presence of collaterals and the hemodynamic status[4,5]. Using CTA the additional information of the intracranial circulation (the circle of Willis) can be achieved within short time and minor dose increase. The anterior part of the circle was found to be significantly more often incomplete in ICSS patients, which is in agreement with previous studies[6] and suggests that the anterior pathway may function for collateral supply in the presence of a carotid stenosis[7]. However, the posterior part of the circle showed less hypoplastic but more absent segments in patients compared to controls. It remains uncertain to what degree these hypoplastic segments do have the potential for collateral supply.
Although we have near-isotropic imaging, further improvement of image quality of the circle is still required, since partial volume effect, splay artefacts around the skull base, and noise, may hamper optimal visualization. MRA techniques are improving as well and are competitive with CTA technique for imaging of both extra- and intra-cranial arteries. Also radiation dose and the use of potentially nephrotoxic contrast agent obligate careful use of CTA; especially the eye lenses are at risk when more CT imaging of the brain is performed within a short time. Our study in which we prospectively assessed the effect of lower kVp for CTA of the circle of Willis, showed that improvement of image quality can be achieved with lower dose compared to conventional technique. This has now been implemented in clinical practice.

For further insight in hemodynamics, we evaluated the brain perfusion in ICSS patients before and after treatment. Measurement of brain perfusion by using CT has been introduced several years ago, but has gained renewed interest with the introduction of multislice scanners. In this theses we aimed to improve insight in the methodological aspects of perfusion scanning; the use of ratios showed to improve the reproducibility and differences between flow territories were revealed. However, quantitative analysis is still difficult. First because the selection of the arterial input function is debatable; whether this should be the ipsilateral or contralateral ACA or MCA. Second, both selection of AIF and VOF are dependent on density measurement in the horizontal plane which is strongly influenced by the size of the selected vessel and slice thickness[8]. Use of relative values avoids these problems, but impairs for example evaluation of patients with bilateral disease. Therefore we used relative MTT measured in the MCA territory and found that the effect of carotid revascularization on cerebral perfusion is highly dependent on the severity of the MTT difference before treatment. Only a small group of patients (22%) showed significant improvement in all three perfusion parameters, suggesting that these patients have most benefit from treatment. Further studies will have to define whether this is in concordance with response in terms of functional improvement and stroke reduction.

Future perspectives

The results of this thesis show that multislice CT has the potential to fulfill an important role in the diagnosis of symptomatic carotid artery stenosis and is increasingly being applied in clinical practice. However, there are other issues that are not yet revealed. For example, plaque morphology which has also shown to be related to stroke risk, can be evaluated by multislice CT as well[9]. This requires more detailed study of the carotid wall and comparison with the histological specimen and will perhaps become clear in further studies on the ICSS patients.
Further study on the relation between the configuration of the circle of Willis, brain perfusion, plaque characteristics and long-term outcome will provide us more insight in cerebral hemodynamics of patients with carotid disease. Also, comparison of CT to recently introduced MR techniques like selective arterial spin labeling, may give insight in the property of hypoplastic segments of the circle and the mechanism of collateral supply.
Another potential use of the CTA is selection of patients for surgical or endovascular treatment; the presence of kinkings and coilings in the carotid as well as tandem stenosis may hamper endovascular approach and hard calcifications may prevent full expansion of the stent[10], while for endarterectomy these characteristics do not play a role.
In conclusion, multislice CT has shown to be capable of providing essential information of the carotid artery, intracranial circulation and brain perfusion in patients with symptomatic carotid artery stenosis. The results of this thesis may, in combination with ongoing studies on ICSS patients, help to achieve a more individualized approach for selection of treatment.

References

1. Rothwell PM, Mehta Z, Howard SC, Gutnikov SA, Warlow CP. Treating individuals 3: from subgroups to individuals: general principles and the example of carotid endarterectomy. Lancet 2005;365:256-65.
2. Fairhead JF, Mehta Z, Rothwell PM. Population-based study of delays in carotid imaging and surgery and the risk of recurrent stroke. Neurology 2005;65:371-5.
3. Giles MF, Rothwell PM. The need for emergency treatment of transient ischemic attack and minor stroke. Expert Rev Neurother. 2005:203-10.
4. Henderson RD, Eliasziw M, Fox AJ, Rothwell PM, Barnett HJ. Angiographically defined collateral circulation and risk of stroke in patients with severe carotid artery stenosis. North American Symptomatic Carotid Endarterectomy Trial [NASCET] Group. Stroke 2000;31:128-32.
5. Blaser T, Hofmann K, Buerger T, Effenberger O, Wallesch CW, Goertler M. Risk of stroke, transient ischemic attack, and vessel occlusion before endarterectomy in patients with symptomatic severe carotid stenosis. Stroke 2002;33:1057-62.
6. Kameyama M, Okinaka SH. Collateral circulation of the brain with special reference to atherosclerosis of the major cervial and cerebral arteries. Neurology 1963; 13:279-86.
7. Hendrikse J, Eikelboom BC, van der Grond J. Magnetic resonance angiography of collateral compensation in asymptomatic and symptomatic internal carotid artery stenosis. J Vasc Surg 2002; 36:799-805.
8. Latchaw RE, Yonas H, Hunter GJ, Yuh WT, Ueda T, Sorensen AG, Sunshine JL, Biller J, Wechsler L, Higashida R, Hademenos G; Council on Cardiovascular Radiology of the American Heart Association. Guidelines and recommendations for perfusion imaging in cerebral ischemia: A scientific statement for healthcare professionals by the writing group on perfusion imaging, from the Council on Cardiovascular Radiology of the American Heart Association. Stroke 2003 ;34:1084-104.
9. Eliasziw M, Streifler JY, Fox AJ et al. Significance of plaque ulceration in symptomatic patients with high grade carotid stenosis. NASCET. Stroke 1994; 25:304-308.
10. Roubin GS, Iyer S, Halkin A, Vitek J, Brennan C. Realizing the potential of carotid artery stenting: proposed paradigms for patient selection and procedural technique. Circulation 2006; 113:2021-30.

Samenvatting in het Nederlands

Introductie

In Nederland krijgen ongeveer 40.000 mensen per jaar een (tijdelijke) beroerte. Bij 20-30% van deze personen wordt er een vernauwing in de halsslagader (in medische termen: de arteria carotis interna), gevonden.
Deze vernauwing wordt veroorzaakt door slagaderverkalking (atherosclerose) in de wand van de slagader. Het idee is dat bloedstolsels kunnen losschieten van de vernauwing en ergens vast blijven zitten in de kleine bloedvaatjes van de hersenen waardoor dat deel van de hersenen te weinig bloed krijgt. Ook kan de vernauwing een verstoring van de doorbloeding (hemodynamiek) in de hersenen veroorzaken. Eerder onderzoek heeft aan getoond dat behandeling van zo'n vernauwing middels een operatie, waarbij de vernauwing wordt opgeheven, het risico op herhaling van een beroerte sterk vermindert. Echter, in hoeverre dit risico wordt verminderd hangt af van de ernst van de vernauwing (stenose graad) en daarbij geeft operatie ook een risico op complicaties. Inmiddels is er een nieuwe behandelmogelijkheid, namelijk stent plaatsing. Hierbij wordt via de lies een buisje in halsslagader geplaatst waardoor de vernauwing wordt opgerekt. Dit is minder belastend voor de patiënt en een veelbelovende methode, maar er is nog niet aangetoond dat dit een zelfde risicoreductie geeft als de operatie. Daarom doet het UMCU mee aan een internationale studie, de ICSS, waarbij geloot wordt tussen beide behandelmethoden. Om meer inzicht te krijgen in risicofactoren voor het krijgen van een beroerte of complicaties, bestudeerden wij de deelnemers aan de ICSS studie middels een nieuwe scan techniek: de multislice CT. In dit proefschrift worden de eerste resultaten van deze onderzoeken beschreven.

Hoofdstuk 2 beschrijft de mogelijkheden van de multislice scanner. Voor het afbeelden van bloedvaten en doorbloeding in de hersenen, is het grote voordeel van deze techniek dat het veel sneller gaat en een hogere resolutie heeft in vergelijking met de eerdere singleslice scanners. De bloedvaten kunnen vanaf de aortaboog tot en met de schedel binnen 15 sec worden afgebeeld, wat goede beelden van de halsslagader geeft en de techniek vergelijkbaar met MRA maakt. Multislice CT kan daarom worden gebruikt om de ernst van de vernauwing te bepalen, de bloedvaten in de hersenen af te beelden (o.a. de cirkel van Willis) en om hersendoorbloeding (perfusie) te meten. De combinatie van deze technieken resulteert in een complete work-up bij patiënten met stoornissen in de doorbloeding van de hersenen en kan ook goed worden uitgevoerd in de acute situatie. Verschillende technieken worden in dit hoofdstuk besproken en de scanparameters staan vermeld.

In *Hoofdstuk 3* wordt gekeken naar mogelijkheden om de stralingsdosis van de CT te verminderen met optimalisering van de beeldkwaliteit. Daarvoor wordt gebruikt gemaakt van de eigenschappen van de rontgenstraling van de CT en het jodiumhoudende contrast middel wat wordt gegeven om bloedvaten zichtbaar te maken. Het verhogen van de kilovoltage van de scanner geeft in principe meer dosis en minder ruis, en dus een betere beeldkwaliteit. Echter, het jodium wordt beter zichtbaar bij lager kilovoltage. Daarom werd bestudeerd of met verlaging van de kilovoltage met enige aanpassing van de stroom (ampere, mAs) de bloedvaten in de hersenen beter zichtbaar kunnen worden gemaakt. Dit werd met behulp van fantoom experimenten en later ook bij patiënten onderzocht. Zowel uit de experimenten als de patiënt studies bleek dat middels verlaging van het kilovoltage en aanpassing van de mAs, betere beeld kwaliteit bij minder dosis kon worden bereikt.

Hoofdstuk 4 beschrijft anatomische variaties in de cirkel van Willis bij patiënten die deelnemen aan de ICSS studie. De cirkel van Willis ligt onderin de hersenen en bestaat uit 5 bloedvaten die als een cirkel met elkaar in verbinding staan. Als er een vernauwing of afsluiting van een halsslagader is, kan bloed naar de hersenen via deze cirkel vanuit de andere (contralaterale) halsslagader of vanuit de achterste circulatie. Bij studies van overleden personen is echter gezien dat deze cirkel vaak niet compleet is aangelegd, en sommige vaten ontbreken of onderontwikkeld zijn, waardoor bloedstroom vanaf de andere hersengebieden (collaterale bloedstroom) belemmerd wordt. Wij vergeleken de anatomie van de cirkel van Willis van ICSS patiënten met patiënten die om andere redenen een CT scan van de hersenen kregen, maar geen hersenschade hadden. Bij de ICSS patiënten vonden we significant vaker afwezige of onderwikkelde bloedvaten dan bij de controle groep. Dit wijst erop, dat het incompleet zijn van deze cirkel mogelijk een risicofactor is voor het krijgen van symptomen wanneer er een vernauwing in de halsslagader aanwezig is.

In *Hoofdstuk 5* vergeleken we drie verschillende meetmethoden van multislice CT techniek om de ernst van de vernauwing te meten. Daarbij diende de DSA als gouden standaard ter vergelijking. Digitale Subtractie Angiografie (DSA) maakt bloedvaten zichtbaar door direct contrast in de arterie in de lies te spuiten, waardoor de vaten heel scherp afgebeeld worden. Het direct in de lies prikken is echter belastend en heeft een bepaald risico voor de patiënt. Omdat bekend is van CT dat het een minder goede resolutie heeft dan DSA, worden verschillende meettechnieken aanbevolen in de literatuur om de accuratesse en reproduceerbaarheid van CT metingen te verbeteren. Deze zijn echter nauwelijks getest in een klinische situatie. Wij lieten daarom 4 waarnemers (2 ervaren radiologen, een ervaren arts-assistent en een niet-ervaren arts-assistent radiologie), bij 55 halsslagaders de ernst van de vernauwing bepalen. Dit werd gedaan middels een schatting, middels meten op de dwarse doorsnede met een meetlat op de computer en met eenzelfde meetlat maar dan met een beperkte grijsschaal op de computer. Schatten was voor alle waarnemers echter de meest betrouwbare methode in vergelijking met DSA en had ook de minste variatie tussen de metingen van verschillende waarnemers.

Om de mogelijkheden van perfusie CT beter te bestuderen, werd eerst de reproduceerbaarheid van CT perfusiemetingen bepaald. *Hoofdstuk 6* beschrijft de resultaten van twee waarnemers die in 20 patiënten met een eenzijdige vernauwing van de halsslagader de perfusie bepaalden. Drie parameters werden gemeten; bloed volume in de hersenen (cerebral blood volume (CBV)), gemiddelde reistijd door het hersenweefsel (mean transit time (MTT)) en bloedstroom (cerebrale bloed flow (CBF)). Zowel variatie binnen twee metingen van 1 waarnemer alsook tussen metingen van de 2 verschillende waarnemers werden vastgesteld. Hiertoe werden 4 gebieden in de hersenen afzonderlijk geselecteerd en er werd bestudeerd of reproduceerbaarheid beter werd als de ratio van twee hersenhelften werd gebruikt in plaats van de absolute waarden. De MTT was de meest reproduceerbare parameter in alle hersengebieden. De meetvariatie werd minder voor CBV en CBF als de verhouding (ratio) werd gebruikt en voor alle parameters gold dat de meetvariatie het minste was in het middengebied.

In *Hoofdstuk 7* wordt de CT perfusie gebruikt om vast te stellen of de MTT waarde voorafgaand aan de behandeling, een voorspellende waarde heeft voor de mate van verbetering in perfusie na de behandeling. Daartoe werden drie groepen onderscheiden op basis van de grootte van het verschil in MTT tussen de aangedane en niet-aangedane hersenhelft. Bij zestien patiënten was er een klein verschil (<1 sec), bij 12 patiënten een matig verschil (1-2sec) en bij 8 patiënten was er een verschil van > 2 sec in MTT tussen beide hersenhelften. Alleen in deze laatste en kleinste groep, trad er een significante verbetering op van alle drie de perfusie parameters na de behandeling. Hieruit kan worden geconcludeerd, dat MTT mogelijk een geschikte parameter is om patiënten met verschillende mate van perfusie vermindering voorafgaand aan de behandeling te onderscheiden, en daarmee te voorspellen in hoeverre verbetering te verwachten is.

Conclusie en Discussie

Een beroerte is een veelvoorkomende oorzaak van overlijden en blijvende invaliditeit in Nederland, en wordt vaak veroorzaakt door een vernauwing in de halsslagader. Op dit moment bestaat diagnostiek van een dergelijke vernauwing uit onderzoek met echo en magnetische resonantie techniek (MRA). Als deze niet overeenstemmen word een intra-arteriele angiografie (DSA) gedaan, wat een meer risicovolle en belastende procedure is. Het criterium voor behandeling is de ernst van de vernauwing: uit grote studies is gebleken dat naar mate de ernst van de vernauwing toeneemt, behandeling resulteerd in een sterkere afname van het risico op een nieuwe beroerte.
Echter, hierbij moet men zich realiseren dat de getallen uit grote studies geldig zijn voor een groep, maar daarmee niet per definitie ook voor de individuele patiënt[1]. Daarom wordt er steeds meer aandacht besteedt aan de factoren die voor het individu het te behalen voordeel voorspellen. De multislice CT scanner kan een belangrijke rol spelen omdat deze in bijna ieder ziekenhuis beschikbaar is en gedurende 24 uur per dag, ook voor patiënten die in een matige conditie zijn, waardoor snel de benodigde informatie kan worden verkregen. Omdat een behandeling kort na het ontstaan van de eerste symptomen een sterke afname op de kans op herhaling van symptomen geeft is snelle diagnostiek belangrijk[2,3].
Het tweede voordeel van CT is dat het ook informatie over de collaterale bloedvaten (waaronder de cirkel van Willis) en doorbloeding van de hersenen zelf geeft. Deze informatie zou kunnen bijdragen aan betere individuele risico-inschatting van de patiënt[4,5]. Hoewel op dit moment een goede scankwaliteit wordt bereikt, streven we naar nog scherpere afbeeldingen met minder stralenbelasting. Zowel binnen de CTA als MRA techniek wordt gezocht naar mogelijkheden voor verbetering van het afbeelden van bloedvaten naar en in de hersenen. Het grote nadeel van de CT is dat er schadelijke stralen worden gebruikt (waar bijvoorbeeld de ooglens relatief gevoelig voor is) en contrastmiddel wat belastend is voor de nieren. In dit proefschrift werd aangetoond dat een lagere dosis door scannen met lager kilovoltage betere scankwaliteit oplevert, hetgeen ook nu al in de praktijk wordt toegepast.
De informatie over de cirkel van Willis kan in enkele seconden extra worden verkregen zonder dat extra contrastmiddel nodig is en met een weinig extra stralingsbelasting voor de patiënt. Uit ons onderzoek blijkt dat patiënten uit de ICSS studie veel vaker een niet volledig functionele cirkel hebben, hetgeen overeenkomt met eerdere studies, en suggereert dat deze manier van bloedvoorziening belangrijk is als de halsslagader vernauwd is.
Om beter inzicht te krijgen in de hemodynamiek bij patiënten met een symptomatische vernauwing van de

halsslagader, onderzochten we de hersendoorbloeding (perfusie) met CT voor en de behandeling. Hoewel deze techniek al langer bestaat, is het pas echt toepasbaar geworden met de komst van multislice scanners. Onderzoek naar hoe perfusiemetingen het meest betrouwbaar kunnen worden verricht liet zien dat er verschillen zijn tussen de verschillende hersengebieden en dat relatieve waarden beter reproduceerbaar zijn dan absolute waarden. Dit kan worden verklaard door verschillende methodologische aspecten van de techniek[8]. Het nadeel van relatieve waarden is dat het moeilijker toepasbaar wordt als patiënten in beide hersenhelften verstoorde doorbloeding hebben. Wij gebruikten daarom de meest reproduceerbare perfusiemaat (MTT) om verder te analyseren. Op basis van de relatieve MTT voor de behandeling konden er drie groepen worden onderscheiden. Daarbij zagen wij dat er slechts een kleine groep patiënten was (22%) die een significante verbetering vertoonden van de hersendoorbloeding na de behandeling. Verdere studie is echter nodig om aan te tonen of deze verbetering ook samengaat met een klinische verbetering, dwz. een afname in het aantal beroertes.

Toekomst

De beschreven resultaten tonen aan dat de multislice CT de potentie heeft om een belangrijke rol in diagnostiek bij patiënten met een beroerte en een vernauwing in de halsslagader te vervullen. Er zijn echter meer factoren dan beschreven in dit onderzoek welke ook invloed hebben op het ontwikkelen van symptomen en complicaties rondom behandeling. Dit zijn bijvoorbeeld de aard en de vorm van de vernauwing[9], en ook deze kunnen mogelijk met CT goed in beeld worden gebracht. Voor precies onderzoek hiernaar is echter een goede vergelijking met het microscopische aspect van de vernauwing noodzakelijk en dit wordt mogelijk duidelijk in de volgende studies van de ICSS patiënten. Daarnaast is het belangrijk om te weten of de combinatie van factoren en de prognose van patiënten op de langere termijn een relatie laten zien, zodat beter kan worden ingeschat welk individu de meeste baat heeft bij behandeling. Nieuwe MRI technieken (zoals selectieve arteriele spinlabeling (ASL)) gaan hier naar verwachting ook een belangrijke bijgrage aan leveren.
Een andere potentiële rol voor de CT is het selecteren van patiënten voor ofwel een operatie of stent plaatsing; een ongewoon beloop van de halsslagader kan het plaatsen van een stent soms bemoeilijken of harde verkalkingen goede ontplooiing van de stent tegenhouden, hetgeen met de CT vaak in een oogopslag kan worden vastgesteld[10].
Concluderend kan met de multislice CT in korte tijd essentiële informatie worden verkregen over de halsslagader, de bloedvaten in de hersenen en de doorbloeding van de hersenen bij patiënten met een symptomatische vernauwing van de halsslagader. De resultaten van dit proefschrift zullen, in combinatie met verdere studies bij de ICSS patiënten, mogelijk gaan bijdragen aan een meer individualistisch gerichte aanpak van behandeling van een symptomatische vernauwing in de halsslagader.

References

1. Rothwell PM, Mehta Z, Howard SC, Gutnikov SA, Warlow CP. Treating individuals 3: from subgroups to individuals: general principles and the example of carotid endarterectomy. Lancet 2005;365:256-65.
2. Fairhead JF, Mehta Z, Rothwell PM. Population-based study of delays in carotid imaging and surgery and the risk of recurrent stroke. Neurology 2005;65:371-5.
3. Giles MF, Rothwell PM. The need for emergency treatment of transient ischemic attack and minor stroke. Expert Rev Neurother. 2005:203-10.
4. Henderson RD, Eliasziw M, Fox AJ, Rothwell PM, Barnett HJ. Angiographically defined collateral circulation and risk of stroke in patients with severe carotid artery stenosis. North American Symptomatic Carotid Endarterectomy Trial [NASCET] Group. Stroke 2000;31:128-32.
5. Blaser T, Hofmann K, Buerger T, Effenberger O, Wallesch CW, Goertler M. Risk of stroke, transient ischemic attack, and vessel occlusion before endarterectomy in patients with symptomatic severe carotid stenosis. Stroke 2002;33:1057-62.
6. Kameyama M, Okinaka SH. Collateral circulation of the brain with special reference to atherosclerosis of the major cervial and cerebral arteries. Neurology 1963; 13:279-86.
7. Hendrikse J, Eikelboom BC, van der Grond J. Magnetic resonance angiography of collateral compensation in asymptomatic and symptomatic internal carotid artery stenosis. J Vasc Surg 2002; 36:799-805.
8. Latchaw RE, Yonas H, Hunter GJ, Yuh WT, Ueda T, Sorensen AG, Sunshine JL, Biller J, Wechsler L, Higashida R, Hademenos G; Council on Cardiovascular Radiology of the American Heart Association. Guidelines and recommendations for perfusion imaging in cerebral ischemia: A scientific statement for healthcare professionals by the writing group on perfusion imaging, from the Council on Cardiovascular Radiology of the American Heart Association. Stroke 2003; 34:1084-104.
9. Eliasziw M, Streifler JY, Fox AJ et al. Significance of plaque ulceration in symptomatic patients with high grade carotid stenosis. NASCET. Stroke 1994; 25:304-308.
10. Roubin GS, Iyer S, Halkin A, Vitek J, Brennan C. Realizing the potential of carotid artery stenting: proposed paradigms for patient selection and procedural technique. Circulation 2006; 113:2021-30.

Dankwoord, List of Publications and Curriculum Vitae

Dankwoord

Dit proefschrift is het resultaat van een samenwerking tussen de afdeling radiologie, neurologie en chirurgie. Bij deze wil ik een ieder die hieraan heeft bijgedragen bedanken voor alle hulp en de plezierige tijd. Een aantal wil ik graag speciaal noemen.

Dr. M.S. van Leeuwen, beste Maarten, zonder jouw enthousiasme was dit proefschrift er niet geweest. Het onderzoek naar oropharynxtumoren leidde via de bolustechnieken naar de breinperfusie, toch mooi. Ik heb veel van je geleerd, niet alleen op het gebied van onderzoek doen, maar ook in breder perspectief. Ik ben je veel dank verschuldigd daarvoor.
Prof. dr. M. Prokop, beste Mathias, het was even wennen aan jouw manier van werken, maar ik heb er zeer veel plezier aan beleefd! Hoe jij altijd maximaal de mogelijkheden weet te benutten is bewonderenswaardig, ookal duurde het vaak even voor je tijd had...Je gevleugelde uitspraak "less is more!" deed soms even pijn, maar leidde zonder uitzondering tot een beter resultaat. Veel dank voor je tijd en geduld.
Prof. dr. W.P.Th.M. Mali, beste professor, onze wekelijkse ontmoeting werd uiteindelijk de rode draad door mijn onderzoekstraject. Ik prijs me nog altijd gelukkig met het feit dat ik bij de ICSS studie betrokken raakte, welke ik kon initiëren en die mij de kans gaf datgene te doen waarvan ook ikzelf overtuigd was. Veel dank voor de ruimte die u mij daarbij gaf.
Dr. B.K. Velthuis, beste Birgitta, je hebt me met vele kleine en grote zaken geholpen en je perfectionisme werkte aanstekelijk. Samenwerken met jou was een grote stimulans en ik hoop dat we dat ook in de toekomst blijven doen.

Prof. dr. L.J. Kappelle en dr. H.B. van der Worp, jullie betrokkenheid bij de ICSS trial vanuit de neurologie was een flinke stimulans om patiënten te includeren en Bart, ik heb het nooit vervelend gevonden met enige regelmaat naar je poli te komen om op de CT te beoordelen of een potentiële kandidaat misschien geschikt was. Dank ook voor al die patiënten die je includeerde en enthousiasmeerde voor alle onderzoeken die ze te wachten stonden.

Prof. dr. F.L. Moll, dr. H.J.M. Verhagen en dr. R.W.H. van Reedt Dortland; als vaatchirurgen was een discussie met jullie tijdens de wekelijkse vaatbespreking altijd buitengewoon leerzaam voor mij, daar de meningen binnen een vakgroep toch wel eens uiteen blijken te kunnen lopen. Zonder jullie inzet was de ICSS trial niet zo'n succes geworden en ik waardeer dit zeer.

Prof. dr. A.C. van Huffelen, Prof. dr. Y. van der Graaf, bedankt voor het beoordelen van mijn manuscript.

De interventie-radiologen: drs. T.H. Lo en drs. G.A.P. de Kort, beste Rob en Gerard, jullie hebben in korte tijd veel succesvolle carotis stentplaatsingen verricht, zeer bewonderenswaardig hoe vaardig en soepel dit telkens gaat. Ook dit heeft de ICSS tot een goed lopende studie gemaakt.

Dr. F.J.A. Beek, drs. Th.D. Witkamp, Joost Kardux en Wouter Velthuis; jullie hebben enorm veel werk voor mij verricht met eindeloze metingen en scoringen. Onmisbaar voor het carotis-meetstuk, super! Thijs van Osch en Evert-Jan Voncken; dank voor jullie geduldige uitleg telkens weer over technische aspecten van de perfusie CT!

Vanuit Philips: Hanny Wilmsen en Marcel Quist; jullie wil ik graag bedanken voor de ondersteuning bij de CTA en CT perfusie studies.

Irene van der Schaaf, ik vond (en vind) het geweldig om jou als collega te hebben! Je optimisme was een grote steun bij al die moeilijke momenten in het begin, waarin nog niet alle plannen helder waren en we ons door blauwe hoofden en fantoom experimenten worstelden. Je wordt vast en zeker een geweldig neuro-interventie radioloog!
Annemarieke Rutten, Hester Gietema en Nicky Peters, wat was het gezellig op onze kamer, eerst zonder en later met daglicht! Altijd een luisterend oor en met jullie doorzettingsvermogen zijn drie grote studies gestart, super. Hester, nog even doorbijten, het wordt zeker een prachtig proefschrift! Anne, altijd helder commentaar, misschien kan die tas de volgende keer ietsje minder vol na het shoppen in Chicago?! Nicky, knap hoe jij de vertaalslag tussen techniek en kliniek weet te maken!
Jeroen Hendrikse, je scherpzinnige opmerkingen en optimistische visie waren altijd bemoedigend, ik wens je veel succes met de voortzetting van je onderzoek. Peter-Jan van Laar, goedgemutst en nooit last van stress... Bob, Fleur, Liesbeth, Auke, Matthijs, Sander, Niek, Audrey, Stephanie, de dames van het Julius en alle anderen van epirad, mooie discussies, veel succes met jullie carrières! Lisa, ik had me geen beter opvolger kunnen wensen. Met je rustige en gedegen aanpak gaat het zeker goed komen met de ICSS en ik verheug me op onze verdere samenwerking. Veel succes!

Cees en Anneke, onafscheidelijk duo van het trialbureau! Anneke, enorm veel dank voor het maken van de vele follow-up afspraken, het zorgvuldig bijhouden van de database en al die andere kleine dingen die je stilzwijgend regelde. Cees, zonder jouw rust en excel kennis was er geen ordening van mijn perfusie waarden gekomen. Anouk, op jouw SPSS kennis ik kon terug altijd terug vallen. Dank!

De stafleden en arts-assistenten van de radiologie; over de ICSS patienten: "is het nu een scan voor wetenschap of kliniek?!" Dank voor jullie hulp en interesse bij het klinische deel van de studie.
De secretaresses: Vanessa, Gabrielle en Desiree; heel veel dank voor het regelen van allerlei lastige afspraken die vaak op laatste moment weer verzet moesten worden, jullie bleven altijd vrolijk. Technici: Sven en Karel; altijd gereed om niet werkende systemen weer op gang te helpen….super!
De laboranten van de CT: Karin, Angelique, Bob, Yannick; jullie moesten iedere keer weer de protocollen aanpassen en waren nooit te beroerd om mee te denken over mogelijke veranderingen; dank voor al jullie hulp. Annelies en Judith; dank voor de altijd secure post-processing. De laboranten van de MR: Niels, Greet, Marja, Simone, Brandon; dank voor jullie flexibiliteit als het gaat om de ICSS patiënten...Mourad; altijd bereid een duplex'je te regelen....

Michel; dank voor je gezellige hulp bij de experimenten en veel succes met je bezigheden in het onderwijs en verdere studie. Wilma en Mathilde; op de angiokamer een onlosmakelijk duo waardoor het op rolletjes loopt! Jullie enthousiasme en interesse voor de ICSS maakte veel mogelijk, dank daarvoor.
De fotografie: Karin, Eugene, Jan en Roy; enorm bedankt voor alle hulp op digitaal en photoshop-gebied, jullie vormen een goed team!

De radiologen in Amersfoort: opleider dr. Henk-Jan Baarslag, vice-opleider dr. Lorentz Quekel; bedankt voor de ruimte die jullie mij gaven om een en ander af te ronden. Nu met de neuro-CT (of MRI?) in Amersfoort aan de wetenschap!

Vriendinnen-collegae: Jet & Marieke; koffietjes & rose'tjes, heerlijk om mijn hart te luchten en altijd veel plezier, de andere dames: Leven En Feesten!

Mijn roeiteam; de ideale uitlaatklep voor onderzoeksperikelen! Een paar mooie halen door het Hilversumskanaal maakte altijd veel goed...Ik hoop dat we dit nog lang blijven doen.

Mijn paranimfen, lieve zus en lieve Ellen, jullie houden mij met beide benen op de grond, klaar om alle tegenslagen te relativeren, en zijn gelukkig altijd beschikbaar om ook kleine successen met een goed glas te vieren...heerlijk! Ellen, ook jij heel veel succes met jouw wetenschappelijk werk wat zonder twijfel tot een mooi resultaat gaat leiden.

Lieve papa en mama, jullie hebben me altijd gestimuleerd om de kansen die ik kreeg te benutten en onvoorwaardelijk vertrouwen in mijn plannen gehad. Zonder dat had ik hier niet gestaan. Broer en zus, Pieter en Corina, ik ben blij dat we niet meer zo ver uit elkaar wonen, fijn dat jullie er zijn.

Lieve Antoine, never a dull moment, en dat hele grote hart...

Manuscripts based on the studies presented in this thesis

A Waaijer, TH Lo, LJ Kappelle, FL Moll, WPThM Mali. Nieuwe inzichten in behandelmogelijkheden voor patiënten met een symptomatische carotis stenose. Ned Tijdschr Geneeskd. 2005; 149:1261-6

A Waaijer, IC van der Schaaf, BK Velthuis, M Prokop. 40 slice Neuro-CT Angiography. Diagnostic Imaging Europe, December 2005/ January 2006

Prokop M, Waaijer A, Kreuzer S. CT angiography of the carotid arteries. JBR-BTR. 2004;87:23-9

A Waaijer, MS van Leeuwen, BK Velthuis, CJG Bakker, GAP de Kort, M Prokop. Dose Reduction and Image Quality: Reducing kVp and Increasing mAs Settings for CT Angiography of the Circle of Willis. Accepted for Radiology

A Waaijer, MS van Leeuwen, TH Lo, FJ Beek, J Kardux, WB Velthuis, M Prokop. Grading of Carotid Artery Stenosis with Multidetector CT Angiography: Visual Estimation or Measurements? In revision for Radiology

A Waaijer, MS van Leeuwen, HB van der Worp, HJM Verhagen, WPThM Mali, BK Velthuis. Anatomic variations in the circle of Willis in patients with symptomatic carotid artery stenosis assessed with multislice CT angiography. Accepted for Cerebrovascular Disease

A Waaijer, IC van der Schaaf, BK Velthuis, M Quist, MJP van Osch, EPA Vonken, MS van Leeuwen, M Prokop. Reproducibility of Quantitative Measurements of Regional Brain Perfusion with Computed Tomography. In revision for AJNR

A Waaijer, MS van Leeuwen, MJP van Osch, HB van der Worp, FL Moll, TH Lo, WPThM Mali, M Prokop. Hemodynamic effects of carotid revascularization in patients with symptomatic carotid artery stenosis; a CT perfusion study. In revision for Radiology

Not in this thesis:

van der Schaaf I, Vonken EJ, Waaijer A, Velthuis B, Quist M, van Osch T. Influence of partial volume on venous output and arterial input function. AJNR 2006; 27:46-50

Wintermark M, Flanders AE, Velthuis B, Meuli R, van Leeuwen M, Goldsher D, Pineda C, Serena J, van der Schaaf I, Waaijer A, Anderson J, Nesbit G, Gabriely I, Medina V, Quiles A, Pohlman S, Quist M, Schnyder P, Bogousslavsky J, Dillon WP, Pedraza S. Perfusion-CT assessment of infarct core and penumbra: receiver operating characteristic curve analysis in 130 patients suspected of acute hemispheric stroke. Stroke 2006; 37:979-85

Westermeyer J, Thuras P, Waaijer A. Size and complexity of social networks among substance abusers: childhood and current correlates. Am J Addict. 2004;13:372-80

Waaijer A, Terhaard CH, Dehnad H, Hordijk GJ, van Leeuwen MS. Tumor growth during the waiting period for radiotherapy in patients with oropharyngeal carcinoma. Ned Tijdschr Geneeskd. 2003;147:1277-82

Waaijer A, Terhaard CH, Dehnad H, Hordijk GJ, van Leeuwen MS, Raaymakers CP, Lagendijk JJ. Waiting times for radiotherapy: consequences of volume increase for the TCP in oropharyngeal carcinoma. Radiother Oncol. 2003;66:271-6

Conference Proceedings

ICSS Meeting 2004, London;

Oral presentation: The ICSS trial: Inclusion Procedure and Follow-Up; A Waaijer, HB van der Worp, FL Moll, LJ Kappelle, WPThM Mali

Nederlandse Radiologendagen 2004, Noordwijk;

Oral presentation: Measuring Carotid Artery Stenosis on MS-CTA: Objective or Subjective; A. Waaijer, MS van Leeuwen, M Olree, M Prokop

Oral presentation: CTA of the Circle of Willis: Improvement with 90 kV? A Waaijer, BK Velthuis, CJG Bakker, GAP de Kort, MS van Leeuwen, M Prokop

Philips User Meeting 2004, Barcelona;

Oral presentation: Optimization of Contrast Using Multislice CT; A Waaijer, BK Velthuis, CJG Bakker, GAP de Kort, MS van Leeuwen, M Prokop

RSNA 2004, Chicago;

Electronic poster: 40-Slice CT Perfusion; A. Waaijer, IC van der Schaaf, MS van Leeuwen, S Pohlman, M Prokop, BK Velthuis

American Society of Therapeutic and Interventional Neuroradiology 2004, New Orleans;

Oral presentation: DW-MRI after Carotid Stenting: New Lesions Without Using a Protection Device; A Waaijer, R Lo, TD Witkamp, M Prokop

Poster Presentation: Changes in Cerebral Perfusion Before and After Carotid Artery Stenting; A Waaijer, MS van Leeuwen, BK Velthuis, HB van der Worp, FL Moll, M Prokop, WPThM Mali

American Stroke Association 2004, New Orleans;

Poster Presentation: Diffusion Weighted MR Imaging After Carotid Artery Stenting Without Using Protection Device; A Waaijer, R Lo, TD Witkamp, M Prokop

European Congres of Radiology 2005, Vienna;

Oral presentation: Measuring Carotid Artery Stenosis; A. Waaijer, MS van Leeuwen, M Olree, M Prokop
(First price for best scientific presentation in the topic vascular)

Oral presentation: CTA of the Circle of Willis: Improvement with 90 kV? A Waaijer, BK Velthuis, CJG Bakker, GAP de Kort, MS van Leeuwen, M Prokop

Oral presentation: DW-MRI after Carotid Stenting Without using a Protection Device; A Waaijer, R Lo, TD Witkamp, M Prokop

Nederlandse Radiologendagen 2005, Noordwijk:

Oral Presentation: Changes in Cerebral Perfusion in patients with symptomatic carotid artery stenosis; A Waaijer, MS van Leeuwen, BK Velthuis, HB van der Worp, FL Moll, M Prokop, WPThM Mali

RSNA 2005, Chicago;

Oral Presentation: CT perfusion for analysing the hemodynamic effects of carotid desobstruction in patients with symptomatic carotid artery stenosis; A Waaijer, MS van Leeuwen, BK Velthuis, HB van der Worp, FL Moll, M Prokop, WPThM Mali

ECR 2006, Vienna;

Oral Presentation: Anatomic variations in the circle of Willis in patients with symptomatic carotid artery stenosis assessed with multislice CT Angiography; A Waaijer, BK Velthuis, HB van der Worp, HJ Verhagen, M Prokop, WPThM Mali, MS van Leeuwen

Oral Presentation: Hemodynamic effects of carotid revascularization in patients with symptomatic carotid artery stenosis. A CT perfusion study; A Waaijer, MS van Leeuwen, BK Velthuis, HB van der Worp, FL Moll, M Prokop, WPThM Mali

Curriculum Vitae

De auteur van dit proefschrift werd geboren op 11 juli 1976 in De Bilt. Haar middelbare schooltijd bracht zij door op College Blaucapel te Utrecht. Na aanvankelijk te zijn uitgeloot begon zij in 1994 aan de studie Geneeskunde te Leuven, maar werd in datzelfde jaar nageplaatst en stapte over naar Maastricht. Tijdens het derde studiejaar participeerde ze in een uitwisselingsprogramma waarbij drie studiemaanden in Linköping, Zweden, werden gevolgd. In 1998 werd het doctoraaldiploma behaald. Voor het co-schap psychiatrie maakte ze een uitstap naar Minneapolis, USA, om tevens te werken aan een onderzoek naar de sociale netwerken van drugsgebruikers. De overige co-schappen werden afgelegd aan de Universiteit van Groningen, alwaar in 2001 de artsenbul behaald werd. Hierna startte zij als arts-assistent Kinderheelkunde in het Wilhelmina Kinderziekenhuis (UMCU), wat ze combineerde met onderzoek naar de groei van oropharynxtumoren in de wachttijd voor radiotherapie, onder begeleiding van dr. M.S. van Leeuwen en Prof. dr. G.J. Hordijk. Na een korte periode als poortarts in het UMCU begon zij in maart 2003 op de afdeling radiologie als arts-onderzoeker. Onder supervisie van Prof. dr. W.P.Th.M. Mali coördineerde zij de ICSS trial en onder begeleiding van Prof. dr. M. Prokop werden de mogelijkheden van de nieuwe multislice scanner onderzocht, hetgeen resulteerde in dit proefschrift. Vanaf september 2005 werkt zij als arts-assistent in opleiding tot radioloog in het Meander Medisch Centrum te Amersfoort, eerst onder supervisie van Prof. dr. P.F.G.M. van Waes en na zijn afscheid onder supervisie van dr. H.J. Baarslag. In 2007 zal zij terugkeren naar het UMCU om daar de opleiding af te ronden.